	Country		Italy				
	Vehicle make		**Fiat** (continued)				
	Model		Barchetta 1.7i	Bravo 1.8i	Brava 1.9 JTD	Marea 2.4 TDI	Multipla 1.6i Bipower
1	Body style	–	2 Ca 2	3 Li 5	5 Li 5	4 Li 5	5 Gli 6
2	Useful power at engine speed	kW (bhp) rpm	96 (131) 6300	83 (113) 5800	77 (105) 4000	91 (124) 4000	76/68 (103/92) 5750
3	Max. torque at engine speed	Nm rpm	164 4300	154 4400	200 1500	265 2000	144 (Gas 130) 4000
4	Maximum speed	km/h	200	193	185	195	168 (Gas 157)
5	Acceleration from 0 to 100 km/h	s	8.9	10	10.6	10.5	13.5 (Gas 16)
6	Curb weight	kg	1060	1100	1180	1280	1300
7	Gross vehicle weight	kg	1260	1600	1570	1870	1870
8	Weight-to-power ratio	kg/kW	11	14.8	14.9	14.1	17.1
9	Fuel consumption	l/100 km	EU 6.5/11.6	EU 6.5/11.3	EU 4.5/7.3	EU 6/10.2	EU 7.2/11.1
10	Fuel octane number	RON	95	95	Diesel	Diesel	95 + gas
11	Tank capacity	l	50	50	50	63	38 (Gas 164)
12	Engine swept volume	cm^3	1747	1747	1910	2387	1581
13	Bore/stroke	mm	82/82.7	82/82.7	82/90.4	82/90.4	86.4/67.4
14	Compression ratio	–	10.3	10.3	18.45	20.7	10.5
15	Specific power output	kW/l	54.9	47.5	40.3	38.1	48.1
16	Engine type	–	q 4 R 4Ve	q 4 R 4Ve	q 4 R	5 R	q 4 R 4Ve
17	Fuel management	–	EI	EI	EP/CR-T-Ic	EP/eV-T-Ic	EI
18	Alternator (14 V)	A	75/85	75/85	75	75/85	80/90
19	Battery (12 V)	Ah	50	50	60	70	50
20	(Engine pos.)/drive config.	–	v	v	v	v	v
21	Transmission ratio	1st/2nd gear 3rd/4th gear 5th/6th gear	3.91/2.24 1.52/1.16 0.95	3.91/2.24 1.52/1.16 0.97	3.91/2.24 1.44/1.03 0.77	3.8/2.24 1.36/0.97 0.77	3.91/2.24 1.52/1.16 0.97
22	Final drive ratio	–	3.56	3.35	3.05	3.18	4.07
23	Gearshift	H (A)	5	5	5	5	5
24	Cooling	l	6.9	6.7	6.1	7.6	7
25	Vehicle length	mm	3915	4025	4190	4390	3995
26	Vehicle width	mm	1640	1755	1740	1740	1870
27	Vehicle height	mm	1270	1420	1410	1420	1700
28	Wheelbase	mm	2275	2540	2540	2540	2665
29	Track, front/rear	mm	1410/1410	1440/1440	1460/1460	1470/1440	1510/1520
30	Turning circle diameter	m	10.5	10.4	10.4	10.7.	11.0
31	Ground clearance	mm	120	150	150	120	120
32	Suspension, front	–	DQl-F-Ku-Td	DQl-F-Ku-Td	DQl-F-Ku-Td	DQl-F-Ku-Td	DQl-F-Ku-Td
33	Suspension, rear	–	Ll-Sf-Ku-Td	Ll-Sf-Ku-Td	Ll-Sf-Ku-Td	Ll-Sf-Ku-Tc	Ll-Sf-Ku-Td
34	Tires	–	195/55 R 15	175/65 R 14	175/65 R 14	175/70 R 14	185/65 R 15
35	Braking system		4Sb	Sb-Tb	Sb-Tb	4Sb-ABS	Sb-Tb

See PP. 898 for abbreviations and explanations.

PETITIONER'S EXHIBIT 1002
US PATENT NO. 6,557,540

	Lamborghini	Lancia					
Ulysse 2.1 TD	Diabolo SV 5.7i	Y 1.2 i.e.	Delta 2.0 i.e. Turbo HPE	Dedra 1.9 TD	Kappa 2.4 JTD	Z 2.0 i.e.	
5 Gli 5-7	2 Co 2	3 Li 5	3 Li 5	5 Ko 5	4 Li 5	5 Gli 5-8	1
80 (109) 4300	390 (530) 7100	63 (86) 6000	142 (193) 5500	66 (90) 4200	100 (136) 4000	97 (132) 5500	2
250 2000	605 5500	113 4500	290 3400	186 2500	304 2000	180 4200	3
175	320	177	225	174	202	186	4
							5
13.3	3.85	10.9	7.5	13.9	10	10.1	
1615	1530	910	1330	1285	1510	1555	6
2385	–	1390	1830	1765	2000	2360	7
20.2	3.9	14.4	9.4	18.9	15.1	16	8
EU 6.7/10.8	EU 17.3/37.9	EU 5.1/9.2	EU 8/14.6	EU 5.9/8.8	EU 6.2/10.2	EU 8.5/13.5	9
Diesel	95	95	95	Diesel	Diesel	95	10
80	100	47	61	60	70	80	11
2088	5707	1242	1995	1929	2387	1998	12
85/92	87/80	70.8/78.9	84/90	82.6/90	82/90.4	86/86	13
21.5	10	10.2	8	19.2	18.45	10.4	14
38.3	68.3	50.7	71.2	34.2	41.9	48.5	15
q 4 R 3Ve	12 V 4Ve	q 4 R 4Ve	4 R 4Ve	4 R	5 R	4 R 4Ve	16
EP/eV-T-Ic	EI	EI	EI	EP/V	EP/CR-T-Ic	Motronic	17
90	85	65/75	70	70	100/120	90	18
50/60	55	40	55	60	70	70	19
v	Mm-h	v	v	v	v	v	20
3.42/1.78 1.12/0.8 0.61	2.31/1.52 1.12/0.88 0.68	3.91/2.16 1.48/1.12 0.9	3.8/2.24 1.52/1.16 0.81	3.91/2.24 1.44/1.03 0.79	3.8/2.24 1.36/0.97 0.71	3.25/1.78 1.19/0.9 0.73	21
4.79	4.1	3.73	3.56	3.17	3.56	4.64	22
5	5	5	5	5	5	5	23
9	15	4.5	8.5	8.8	8.3	8.5	24
4455	4470	3725	4010	4345	4685	4470	25
1830	2040	1690	1760	1700	1825	1835	26
1710	1110	1440	1760	1450	1460	1710-1810	27
2825	2650	2380	2540	2540	2700	2825	28
1535/1540	1540/1640	1385/1370	1485/1415	1435/1415	1545/1535	1535/1540	29
11.8	13.0	9.6	11.6	11.4	10.9	11.8	30
130	140	150	150	150	140	–	31
DQI-F-Ku-Td	DQI-Db-Sf-Ku	DQI-F-Ku-Td	DQI-F-Ku-Td	DQI-F-Ku-Td	DQI-F-Sf-Ku-Td	DQI-F-Sf-Td	32
Vla-Sf-Ku-Td	DQI-Db-Sf-Ku	LI-Sf-Ku-Td	LI-Sf-Ku-Td	LI-Sf-Ku-Td	DQu-Sf-Ku-Td	Vla-P-LI-Sf-Ku-Td	33
195/70 R 14	1)	195/50 R 15	215/45 R 16	185/60 R 14	195/65 R 15	205/65 R 15	34
Sb-Tb	4Sb-ABS	Sb-Tb	4Sb-ABS	4Sb-ABS	4Sb-ABS	Sb-Tb	35

1) Front 235/35 ZR 18; Rear 335/30 ZR 18

PETITIONER'S EXHIBIT 1002
US PATENT NO. 6,557,540

Country			Italy	Japan			
Vehicle make			Maserati	Daihatsu	Honda		
Model			3200 GT BiTurbo	Charade 1.3i	Z 0.7 Ti	Logo 1.3	Civic Aerodeck 1.5i
1	Body style	–	2 Co 2+2	5/3/4 Li 5	3 Mv 4	5/3 Li 5	5 Ko 5
2	Useful power	kW (bhp)	271 (368)	62 (84)	47 (64)	48 (65)	84 (114)
	at engine speed	rpm	6250	6500	6000	5000	6500
3	Max. torque	Nm	491	105	93	108	134
	at engine speed	rpm	4500	5000	3700	2500	5200
4	Maximum speed	km/h	280	170	> 130	152	190
5	Acceleration from 0 to 100 km/h	s	5.1	11	–	14.5	11.5
6	Curb weight	kg	1590	830	960	940	1135
7	Gross vehicle weight	kg	1940	1350	–	1365	1610
8	Weight-to-power ratio	kg/kW	5.9	13.2	25.3	19.2	13.1
9	Fuel consumption	//100 km	(Ed.) 11/26	EU 5.6/8.9	(Ed.) 6/10	EU 5.5/7 8	EU 5.7/8.8
10	Fuel octane number	RON	95	91	–	95	95
11	Fuel tank capacity	l	90	50	35	40	55
12	Engine swept volume	cm^3	3217	1296	657	1343	1493
13	Bore/stroke	mm	80/80	76/71.4	66/64	75/76	75/84.5
14	Compression ratio	–	8	9.5	8.5	9.2	9.6
15	Specific power output	kW//	84.2	47.8	57.8	35.7	56.2
16	Engine type	–	8 V 4Ve	q 4 R 4Ve	Mm 3 R 4Ve	q 4 R	q 4 R 4Ve
17	Fuel management	–	El-2Tlc	El	El-T-lc	El	El
18	Alternator (14 V)	A	105	60	35	70	70/75
19	Battery (12 V)	Ah	60	36	32	36	36/55
20	(Engine pos.)/drive config.	–	h-ASR	v	aa	v	v
21	Transmission ratio	1st/2nd gear	4.22/2.51	3.18/1.84	2.7/1.55	3.23/1.78	3.25/1.78
		3rd/4th gear	1.67/1.23	1.25/0.86	1.03/0.74	1.25/0.94	1.25/0.94
		5th/6th gear	1/0.83	0.71		0.77	0.7
22	Final drive ratio	–	3.23	4.27	3.04	4.06	3.89
23	Gearshift	H (A)	6 (4)	5 (4)	(4)	5 (3+St)	5 (4+St)
24	Cooling	l	14	4.5	–	4.8	4.8
25	Vehicle length	mm	4510	3780	3395	3785	4425
26	Vehicle width	mm	1820	1620	1475	1645	1695
27	Vehicle height	mm	1310	1390	1680	1520	1440
28	Wheelbase	mm	2660	2395	2360	2360	2620
29	Track, front/rear	mm	1525/1540	1385/1390	1280/1290	1425/1400	1480/1490
30	Turning circle diameter	m	11.5	9.6	9.2	10.2	11.0
31	Ground clearance	mm	120	160	200	140	150
32	Suspension, front	–	DDQl-Sf-Ku-Td	DQl-F-Sf-Ku-Td	DQl-F-Sf-Ku-Td	Ql-F	DDQl-Sf
33	Suspension, rear	–	DDQl-Sf-Ku-Td	Ql-Ll-Sf-Ku-Td	De-P-Ll-Sf-Td	Vla-Sf-Ku-Td	Ql-Ll-Sf
34	Tires	–	1)	145 R 13	175 R 15	175/70 R13	175/70 R 13
35	Braking system		4Sb-ABS	Sb-Tb	Sb-Tb	Sb-Tb	Sb-Tb

1) Front 235/40 ZR 18; Rear 265/35 ZR 18

See P. 898 for abbreviations and explanations.

PETITIONER'S EXHIBIT 1002
US PATENT NO. 6,557,540

Accord Coupé 2.0i	Capa 1.5i	Odyssey 3.5i	HR-V 1.6i	**Lexus** IS 200 2.0i	GS 300 3.0i	**Mazda** AZ Wagon 0.7 Ti	
2 Co 5	5 Mv 5	5 Gli 7	3 Ge 4	4 Li 5	4 Li 5	3/5 Mv 4	1
108 (147) 6000	72 (98) 6300	157 (213) 5200	77 (105) 6200	114 (155) 6200	163 (222) 5800	44 (60) 6000	2
184 5000	133 3500	310 4300	135 3400	195 4400	298 3800	83 4000	3
208	170	> 190	165	215	230	135	4
							5
10.1	–	–	11.2	9.5	8.2	–	
1355	1110	1910	1125	1300	1665	750	6
–	–	–	1530	–	2120	–	7
12.5	15.4	12.2	14.6	11.4	10.2	19.7	8
EU 7.1/12.2	(Ed.) 4.5/9	(Ed.) 9/13.1	EU 7.2/9.9	(Ed.) 7/13	EU 8.8/16	(Ed.) 4/8	9
95	95	95	95	95	–	95	10
65	40	75	55	70	75	30	11
1997	1493	3471	1590	1988	2997	657	12
85/88	75/84.5	89/93	75/90	75/75	86/86	65/66	13
10	9.4	9.4	9.6	9.6	10.5	10.5	14
54.1	48.2	45.2	48.4	57.3	56.1	57.8	15
4 R 4Ve	4 R 4Ve	6 V 4Ve	q 4 R 4Ve	6 R 4Ve	6 R 4Ve	3 R 4Ve	16
EI	EI	EI	EI	EI	EI	EI-T-Ic	17
90	75	95	75	–	60	300 W	18
52	36	52	20/45	–	60	36	19
v	v	v	aa (v)	h-ASR	h-ASR	v (aa)	20
3.29/1.96 1.34/1.03 0.81	2.47-0.45	2.43/1.37 0.88/0.58	3.5/1.96 1.34/1.07 0.87	– – –	3.36/2.18 1.43/1 0.75	3.38/2.06 1.28/0.89 0.72	21
4.26	5.81	3.94	4.56	–	3.62	5.94	22
5	(St)	(4)	5 (St)	6 (4)	(5)	5 (4/3)	23
–	4.8	7	4.8	–	8.4	4	24
4765	3775	5110	4010	4400	4810	3395	25
1785	1640	1920	1695	1720	1800	1475	26
1400	1650	1730	1590	1410	1450	1690	27
2670	2360	3000	2350	2670	2800	2360	28
1555/1535	1425/1420	1680/1680	1470/1455	1495/1485	1535/1510	1290/1290	29
11.1	9.6	11.5	10.8	–	11.0	8.4	30
150	150	160	190	150	150	–	31
DQI-QI-LI-Sf-Ku-Td	DQI-F-Sf-Ku-Td	DQI-QI-Sf-Ku-Td	DQI-F-Sf-Ku-Td	DQI-QI-LI-Sf-Ku-Td	DDQI-Sf-Ku-Td	QI-F-Ku	32
QI-LI-Sf-Ku-Td	VIa-LI-Sf-Ku-Td	QI-LI-Sf-Ku-Td	De-P-Sf-Ku-Td	DQI-DQu-LI-Sf-Ku-Td	DQI-QI-SI-Sf-Ku-Td	Sa-LI-P-Sf-Td	33
195/65 R 15	175/70 R 13	215/65 R 16	195/70 R 15	215/45 R 17	225/55 R 16	135 R 12	34
4Sb-ABS	Sb-Tb-ABS	Sb-Tb-ABS	Sb-Tb-ABS	4Sb-ABS	4Sb-ABS	Sb-Tb	35

PETITIONER'S EXHIBIT 1002
US PATENT NO. 6,557,540

Country			Japan				
Vehicle make			Mazda (continued)			Mitsubishi	
Model			Demio 1.3i	323P 1.5i	626 Wagon 2.0i	Colt 1.6i	Carisma 1.8 GDI
1	Body style	–	5 Ko 5	3 Li 5	5 Ko 5	4/3 Li 5	4/5 Li 5
2	Useful power at engine speed	kW (bhp) rpm	53 (72) 5500	65 (88) 5500	100 (136) 5800	129 (175) 7500	92 (125) 5500
3	Max. torque at engine speed	Nm rpm	105 3500	132 4000	181 4500	167 7000	174 3750
4	Maximum speed	km/h	158	173	202	> 210	200
5	Acceleration from 0 to 100 km/h	s	13.2	11.8	10.5	7.5	10
6	Curb weight	kg	950	1010	1305	1020	1215
7	Gross vehicle weight	kg	1450	1540	1850	1445	1685
8	Weight-to-power ratio	kg/kW	17.9	16.5	11.8	7.9	13.2
9	Fuel consumption	l/100 km	EU 6/8.7	EU 6.3/9.7	EU 6.7/10.9	(Ed.) 8/14	EU 5/8.4
10	Fuel octane number	RON	95	95	95	91	95
11	Fuel tank capacity	l	43	50	64	50	60
12	Engine swept volume	cm^3	1324	1498	1991	1597	1834
13	Bore/stroke	mm	71/83.6	78/78.4	83/92	81/77.5	81/99
14	Compression ratio	–	9.4	9.4	9.7	11	12.5
15	Specific power output	kW/l	40	43.4	50.2	80.8	50.2
16	Engine type	–	q 4 R 4Ve	q 4 R 4Ve	q 4 R 4Ve	4 R 4Ve	4 R 4Ve
17	Fuel managment	–	EI	EI	L-Jetronic	EI	EId
18	Alternator (14 V)	A	70	70	80	50/70	75
19	Battery (12 V)	Ah	50	40	55/75	45/60	50
20	(Engine pos.)/drive config.	–	v	v	v	v	v
21	Transmission ratio	1st/2nd gear 3rd/4th gear 5th/6th gear	3.42/1.84 1.29/0.97 0.82	3.42/1.84 1.29/0.97 0.78	3.31/1.83 1.31/0.97 0.76	3.07/1.95 1.38/1.03 0.77	3.58/1.95 1.27/0.97 0.77
22	Final drive ratio	–	3.85	4.11	4.11	4.63	3.72
23	Gearshift	H (A)	5 (3)	5 (4)	5 (4)	5 (4)	5 (4)
24	Cooling	l	6	6	7	5	6
25	Vehicle length	mm	3810	4035	4660	4290	4435
26	Vehicle width	mm	1670	1695	1710	1690	1695
27	Vehicle height	mm	1540	1410	1520	1390	1400
28	Wheelbase	mm	2390	2505	2670	2500	2550
29	Track, front/rear	mm	1420/1420	1460/1460	1480/1470	1450/1460	1455/1475
30	Turning circle diameter	m	9.4	9.8	10.8	10.6	11.2
31	Ground clearance	mm	150	140	160	120	150
32	Suspension, front	–	QI-F-Ku-Td	DQI-F-Ku-Td	DQI-F-Ku	DQI-F-Ku	DQI-F-Ku
33	Suspension, rear	–	VIa-Sf-Td	QI-LI-F-Ku-Td	QI-LI-Sf-Ku	QI-LI-Sf	QI-LI-Sf
34	Tires	–	165/70 R 13	175/65 R 14	185/65 R 14	185/65 R 14	175/65 R 14
35	Braking system		Sb-Tb	Sb-Tb	4Sb-ABS	Sb-Tb	4Sb

See PP. 898 for abbreviations and explanations.

PETITIONER'S EXHIBIT 1002
US PATENT NO. 6,557,540

	Nissan		Subaru	Suzuki		Toyota	
Space Star 1.3i	Almera 1.4i	Terrano II 2.4i	Legacy 2.0i	Wagon R 1.0i	X-90 1.6i	Yaris 1.0i	
5 Gli 5	3/4/5 Li 5	3/5 Ge 5	4 Li 5	5 Mv 4	2 Ge 2	5 Li 5	1
63 (86) 6000	64 (87) 6000	85 (116) 4800	92 (125) 5600	48 (65) 6500	71 (97) 5600	50 (68) 6000	2
117 3000	116 4000	191 3200	184 3600	181 3500	132 4000	90 4100	3
170	172	160	188	140	150	156	4
							5
13.4	12.6	13.7	10.8	–	–	12	
1120	1035	1630	1370	845	1100	820	6
1655	1545	2510	1815	1330	1360	–	7
17.8	16.2	18.7	15.7	15.9	15.6	16.4	8
EU 5.6/9	EU 5.8/9.2	EU 10.3/15.8	EU 7.7/12.3	EU 5/7.6	EU 6.7/9.8	(Ed.) 5/8	9
95	95	95	95	95	95	95	10
55	50	72	64	42	42	45	11
1299	1392	2389	1994	997	1590	998	12
71/82	73,6/81,8	89/96	92/75	68/68.6	75/90	69/66.7	13
10	9.5	8.6	10	10	9.5	10	14
48.5	46	35.6	46.1	48.2	44.7	50.1	15
q 4 R 4Ve	q 4 R 4Ve	4 R 3Ve	4 Bx 4Ve	4 R 4Ve	4 R 4Ve	q 4 R 4Ve	16
EI	EI	EI	EI	EI	EI	EI	17
50/70	70	50	90	300 W	70	70	18
45/60	55	60	48	26	48	50	19
v .	v	aa	aa	v	aa	v	20
3.73/2.05 1.32/0.97 0.79	3.33/1.96 1.29/0.9 0.73	3.59/2.25 1.42/1 0.82	3.55/2.11 1.45/1.09 0.87	3.42/1.89 1.28/0.91 0.76	3.65/1.95 1.38/1 0.8	3.55/1.91 1.31/0.97 0.8	21
4.21	4.17	4.63	3.9	4.39	4.3	3.94	22
5	5	5	5 (4)	5 (4/3)	5 (4)	5 (4)	23
5	4	8	6	5	5.3	5	24
4030	4120	4185	4600	3410	3710	3610	25
1700	1690	1755	1700	1575	1695	1660	26
1520	1390	1830	1410	1700	1560	1500	27
2500	2535	2450	2650	2335	2200	2370	28
1475/1470	1470/1435	1455/1430	1460/1455	1360/1355	1425/1430	1450/1430	29
9.6	10.4	10.8	11.1	9.6	9.8	9.8	30
150	140	121	160	150	170	–	31
DQI-F-Ku-Td	DQI-F-Sf-Td	DDQI-Tf-Ku-Td	DQI-F-Sf-Ku-Td	QI-F-Sf-Ku-Td	DQI-Db-Sf-Ku-Td	DQI-F-Sf-Td	32
QI-LI-F-Ku-Td	Ta-LI-QI-Sf-Ku-Td	Sa-LI-P-Sf-Ku-Td	Ma-Sf-Ku-Td	Ta-P-Sf-Td	Sa-LI-Sf-Td	Vla-Sf-Td	33
175/65 R 14	175/70 R 13	235/75 R 15	195/60 R 15	155/65 R 13	195/65 R 15	175/65 R 14	34
Sb-Tb	Sb-Tb	Sb-Tb-ABS	4Sb-ABS	Sb-Tb	Sb-Tb-ABS	Sb-Tb	35

PETITIONER'S EXHIBIT 1002
US PATENT NO. 6,557,540

	Country		Japan		Korea		
	Vehicle make		Toyota (Continued)		Daewoo		
	Model		Avensis 2.0 TD-CR	Picnic 2.0i	Matiz 0.8i	Lanos 1.5i	Nubira 2.0i
1	Body style	–	4/5 Li 5	5 Gli 6	5 Li 5	4/3/5 Li 5	5 Ko 5
2	Useful power at engine speed	kW (bhp) rpm	82 (112) 4000	94 (128) 5400	38 (52) 5900	55 (75) 5400	100 (136) 5600
3	Max. torque at engine speed	Nm rpm	250 2500	178 4400	69 4600	113 3400	184 4000
4	Maximum speed	km/h	180	180	144	170	195
5	Acceleration from 0 to 100 km/h	s	12	10.8	17	15	9
6	Curb weight	kg	1280	1335	725	1005	1285
7	Gross vehicle weight	kg	1830	2010	1210	1595	1860
8	Weight-to-power ratio	kg/kW	18.1	14.2	19.1	18.3	11
9	Fuel consumption	l/100 km	EU 5.2/8.5	EU 7.4/12.3	EU 5.2/8.4	EU 5.9/11.4	EU 7.4/15.1
10	Fuel octane number	RON	Diesel	95	95	91	–
11	Fuel tank capacity	l	62	60	35	48	62
12	Engine swept volume	cm^3	1975	1998	796	1349	1998
13	Bore/stroke	mm	86/85	86/86	86.5/72	76.5/73.4	86/86
14	Compression ratio	–	23	9.5	9.3	9.5	9.5
15	Specific power output	kW/l	33.4	47	47.7	40.8	50.1
16	Engine type	–	4 R	4 R 4Ve	q 3 R	q 4 R	q 4 R 4Ve
17	Fuel managment	–	EP/CR-T-Ic	EI	EI	EI	EI
18	Alternator (14 V)	A	70	80	65	75/100	75/85
19	Battery (12 V)	Ah	80	60	35	46/55	55
20	(Engine pos.)/drive config.	–	v	v	v	v	v
21	Transmission ratio	1st/2nd gear 3rd/4th gear 5th/6th gear	3.54/2.04 1.32/0.95 0.73	3.54/2.04 1.32/1.03 0.82	3.82/2.21 1.42/1.03 0.84	3.55/2.05 1.35/0.97 0.76	3.55/2.16 1.48/1.13 0.87
22	Final drive ratio	–	3.74	3.94	4.44	4.18	3.55
23	Gearshift	H (A)	5	5 (4)	5	5	5 (4)
24	Cooling	l	6.9	6.7	3.8	7	7
25	Vehicle length	mm	4490	4530	3595	4235	4515
26	Vehicle width	mm	1710	1695	1495	1680	1700
27	Vehicle height	mm	1430	1620	1480	1430	1430
28	Wheelbase	mm	2630	2735	2340	2520	2570
29	Track, front/rear	mm	1480/1450	1470/1450	1315/1280	1405/1425	1465/1455
30	Turning circle diameter	m	11.6	11.0	9.0	9.8	10.6
31	Ground clearance	mm	140	150	140	160	140
32	Suspension, front	–	DQl-F-Ku-Td	DQl-F-Sf-Ku-Td	Ql-F-Sf-Td	Ql-Ll-F-Sf-Ku-Td	DQl-F-Sf-Ku-Td
33	Suspension, rear	–	DQu-Ll-Ku-Td	Vla-Ll-Sf-Ku-Td	Vla-Ll-Sf-Td	Vla-Ll-Sf-Ku-Td	Vla-Sf-Ku-Td
34	Tires	–	185/65 HR 14	195/65 R 14	145/70 R 13	155 R 13	185/65 R 14
35	Braking system		Sb-Tb-ABS	Sb-Tb-ABS	Sb-Tb	Sb-Tb	4Sb-ABS

See PP. 898 for abbreviations and explanations.

PETITIONER'S EXHIBIT 1002
US PATENT NO. 6,557,540

			Sweden				
Hyundai		**Kia**	**Saab**				
Atos 1.0i	Coupé 2.0i	Carnival 2.5i	9-3 2.0i	9-3 2.2 TD	9-5 2.0i Turbc	9-5 3.0i Turbo	
5 Mv 5	3 Co 4/5	5 Gli 5-7	5/3 Li 5	3/5 Li 5	4 Li 5	5 Ko 5	1
41 (56) 5500	102 (139) 6000	121 (165) 6500	96 (131) 6100	85 (116) 4300	110 (150) 5500	147 (200) 5000	2
82 3100	182 4900	222 4100	177 4300	260 1900	215 2500	310 2500	3
142	201	185	200	200	215	230	4
							5
15.1	8.6	–	11	10.9	9.8	8.7	
820	1250	1735	1295	1350	1485	1650	6
1220	1600	2425	1860	1910	–	2180	7
20	12.2	14.3	13.5	15.9	13.5	10.9	8
EU 5.4/8	EU 7.3/11.4	EU 8.9/15.3	EU 6.8/13.1	EU 4.6/8.9	EU 7.2/13.5	EU 8.5/17.2	9
95	95	95	95	Diesel	95	95	10
35	55	75	68	68	75	75	11
999	1975	2497	1985	2172	1985	2962	12
76/73	82/93.5	80/82.8	90/78	84/98	90/78	86/85	13
9.5	10.3	10.5	10.1	19.5	9.3	9.5	14
41	51.6	48.5	48.4	39.1	55.4	49.6	15
q 4 R 3Ve	q 4 R 4Ve	q 6 V 4Ve	4 R 4Ve	4 R 4Ve	q 4 R 4Ve	q 6 V 4Ve	16
EI	EI	EI	Motronic	EP/eV-T-Ic	Ze-T	Ze-T-Ic	17
60	75/90	80	70/130	120	90/130	90/130	18
40/45	68	54	60	85	60	60	19
v	v	v	v	v	v	v	20
3.54/1.95 1.31/0.92 0.78	3.31/1.95 1.39/1.06 0.84	3.75/1.95 1.3/0.94 0.75	3.38/1.76 1.12/0.89 0.7	3.38/1.76 1.12/0.89 0.7	3.38/1.76 1.18/0.89 0.66	2.58/1.41 1/0.74	21
4.53	3.84	4.31	4.45	4.45	4.05	4.28	22
5 (3)	5 (4)	5 (4)	5 (4)	5 (4)	5 (4)	(4)	23
6	6	8	10	10	9	9.7	24
3495	4340	4890	4630	4630	4810	4810	25
1495	1730	1895	1710	1710	1790	1790	26
1610	1300	1730	1430	1430	1450	1450	27
2380	2480	2905	2600	2600	2705	2705	28
1315/1300	1470/1450	1625/1600	1450/1440	1450/1440	1520/1520	1520/1520	29
9.1	10.0	13.0	11.1	11.1	10.8	10.8	30
160	150	170	140	140	–	–	31
QI-F-Sf-Ku-Td	DQI-F-Sf-Ku-Td	QI-F-Ku-Td	DQI-F-Ku	DQI-F-Ku	DQI-F-Sf-Ku-Td	DQI-F-Sf-Ku-Td	32
Ta-QI-LI-Sf-Td	DQu-Sf-Td	Sa-P-LI-Sf-Ku-Td	VIa-Sf-Ku-Td	VIa-Sf-Ku-Td	DQu-LI-Sf-Ku-Td	DQu-LI-Sf-Ku-Td	33
155/70 R 13	205/50 R 15	205/70 R 15	185/65 HR 15	185/65 HR 15	205/65 R 15	205/60 R 15	34
Sb-Tb-ABS	4Sb-ABS	Sb-Tb	4Sb-ABS	4Sb-ABS	4Sb-ABS	4Sb-ABS	35

PETITIONER'S EXHIBIT 1002
US PATENT NO. 6,557,540

	Country		Sweden				
	Vehicle make		Volvo				
	Model		S40 1.8i	V40 1.9 TDI	S70 2.0i	V70 2.4i	S80 2.8 T6
1	Body style	–	4 Li 5	5 Ko 5	4 Li 5	5 Ko 5	4 Li 5
2	Useful power at engine speed	kW (bhp) rpm	92 (125) 5500	70 (95) 5000	93 (126) 6250	125 (170) 6100	200 (272) 5400
3	Max. torque at engine speed	Nm rpm	174 3750	190 2000	170 4800	220 4700	380 2000
4	Maximum speed	km/h	200	180	195	210	250
5	Acceleration from 0 to 100 km/h	s	10.5	12.5	11.7	9.2	7.2
6	Curb weight	kg	1230	1250	1430	1470	1590
7	Gross vehicle weight	kg	1750	1790	1890	1970	2100
8	Weight-to-power ratio	kg/kW	13.4	14.4	15.4	11.4	8
9	Fuel consumption	l/100 km	5.7/6.9/9.1	5.2/6.3/8.3	EU 8.1/13.4	EU 7.8/15	EU 8/16.4
10	Fuel octane number	RON	95	Diesel	95	95	98
11	Fuel tank capacity	l	60	60	70	70	80
12	Engine swept volume	cm^3	1834	1870	1984	2435	2783
13	Bore/stroke	mm	81/89	80/93	81/77	83/90	81/90
14	Compression ratio	–	12.5	20.5	10	10.3	8.5
15	Specific power output	kW/l	50.2	35.3	46.9	51.3	71.9
16	Engine type	–	4 R 4Ve	4 R	q 5 R	q 5 R 4Ve	q 6 R 4Ve
17	Fuel management	–	Eld	EP/V-T	El	El	Motronic-2Tlc
18	Alternator (14 V)	A	80	80	100	100	120
19	Battery (12 V)	Ah	62	72	520 A	520 A	600 A
20	(Engine pos.)/drive config.	–	v	v	v	v	v
21	Transmission ratio	1st/2nd gear 3rd/4th gear 5th/6th gear	3.58/1.94 1.26/0.97 0.76	3.61/1.86 1.32/0.97 0.76	3.07/1.77 1.19/0.87 0.7	3.07/1.77 1.19/0.87 0.7	2.92/1.57 1/0.7
22	Final drive ratio	–	3.72	3.44	4.45	4.00	3.29
23	Gearshift	H (A)	5 (4)	5 (4)	5 (4)	5 (4)	(4)
24	Cooling	l	5	7.4	7.2	7.2	10.7
25	Vehicle length	mm	4480	4480	4720	4720	4820
26	Vehicle width	mm	1720	1720	1760	1760	1830
27	Vehicle height	mm	1390	1390	1400	1430	1450
28	Wheelbase	mm	2550	2550	2660	2660	2790
29	Track, front/rear	mm	1450/1470	1450/1470	1520/1470	1520/1470	1580/1560
30	Turning circle diameter	m	10.6	10.6	10.2	10.2	10.9
31	Ground clearance	mm	150	150	140	140	150
32	Suspension, front	–	DQl-F-Sf-Ku-Td	DQl-F-Sf-Ku-Td	DQl-F-Ku	DQl-F-Ku	DQl-F
33	Suspension, rear	–	Ql-Ll-Zl-Sf-Ku-Td	Ql-Ll-Zl-Sf-Ku-Td	Ma-Sf-Ku-Td	Ma-Sf-Ku-Td	Ma-Sf-Ku-Td
34	Tires	–	195/55 VR 15	195/55 VR 15	185/65 R 15	185/65 R 15	205/65 R 15
35	Braking system		4Sb-ABS	4Sb-ABS	4Sb-ABS	4Sb-ABS	4Sb-ABS

See PP. 898 for abbreviations and explanations.

PETITIONER'S EXHIBIT 1002
US PATENT NO. 6,557,540

	Spain				Czech. Rep.	USA	
	Seat				Skoda	Buick	
C70 2.3i	Arosa 1.0i	Arosa 1.7 SDI	Ibiza 1.9 TDI	Cordoba 2.0i	Octavia 1.8 T	Le Sabre 3.8i	
2 Ca 4	3 Li 5	3 Li 5	5/3 Li 5	4 Li 5	5 Ko 5	4 Li 5-6	1
176 (239) 5100	37 (50) 5000	44 (60) 4200	81 (110) 4000	110 (150) 6000	110 (150) 5700	153 (208) 5200	2
330 2700	86 3000	115 2200	235 1900	180 4500	210 1750	312 3700	3
250	151	157	193	216	216	200	4
							5
6.9	17.4	16.8	10.2	8.5	9.1	--	
1560	865	960	1060	1120	1315	1620	6
1970	1265	1360	1520	1580	1830	--	7
–	23.4	21.8	13	10.2	11.8	10.6	8
8.4/11.3/16.3	EU 4.7/7.5	EU 3.6/5.9	EU 3.9/6.4	EU 6.4/11.9	EU 6.2/10.9	EPA 7.8/12.4	9
95	95	Diesel	Diesel	95	95	91	10
68	34	34	45	45	55	36	11
2319	999	1716	1896	1984	1781	3791	12
81/90	67.1/70.6	79.5/86.4	79.5/95.5	82.5/92.8	81/86.4	96.52/86.36	13
8.5	10.5	19.5	19.5	10.5	9.5	9.4	14
75.9	37	25.6	42.7	55.4	61.7	40.4	15
q 5 R 4Ve	4 R	4 R	q 4 R	4 R 4Ve	q 4 R 5Ve	q 6 V	16
EI-T	Motronic	EP/eV	EP/eV-T-Ic	Motronic	Motronic-T-Ic	EI	17
100	70	70	90	70/90	70/90	120	18
520 A	36	61	61	44/60	44/60	54	19
v-ASR	v	v	v	v-EDS	v	v-ASR	20
3.07/1.77 1.19/0.87 0.7	3.46/2.1 1.45/1.1 0.89	3.46/1.96 1.25/0.93 0.74	3.78/2.06 1.35/0.97 0.74	3.3/1.94 1.31/1.03 0.84	3.3/1.94 1.31/1.03 0.84	2.92/1.57 1/0.7	21
4.00	4.06	3.33	3.3	3.68	3.68	2.86	22
5 (4)	5	5	5	5	5	(4)	23
7	6	6	6.5	6.3	6.3	11	24
4720	3535	3535	3855	4145	4510	5080	25
1820	1640	1640	1640	1640	1730	1865	26
1410	1460	1460	1420	1420	1430	1450	27
2660	2325	2325	2445	2445	2510	2850	28
1520/1520	1370/1400	1370/1400	1430/1395	1430/1395	1515/1490	1580/1580	29
11.7	9.8	9.8	10.4	10.4	10.8	12.3	30
120	110	110	150	130	140	140	31
DQI-F-Sf-Ku-Td	DQI-F-Td	DQI-F-Td	DQI-F-Td	DQI-F-Ku-Td	DQI-F-Sf-Ku-Td	DQI-F-Sf-Ku-Td	32
Vla-QI-LI-Sf-Ku-Td	Vla-Sf-Td	Vla-Sf-Td	Vla-Sf-Td	Vla-Sf-Ku-Td	Vla-LI-Sf-Ku-Td	Ea-QI-SI-Sf-Ku-Td	33
225/45 ZR 17	155/70 R 13	155/70 R 13	185/55 R 15	195/45 R 16	175 R 14	215/70 R 15	34
4Sb-ABS	Sb-Tb	Sb-Tb	4Sb	4Sb-ABS	4Sb-ABS	4Sb-ABS	35

PETITIONER'S EXHIBIT 1002
US PATENT NO. 6,557,540

	Country		USA				
	Vehicle make		**Cadillac**	**Chevrolet**	**Chrysler**		
	Model		Catera 3.0i	Impala 3.4i	Stratus 2.5i	Sebring 2.0i	300 M 2.7i
1	Body style	–	4 Li 5	4 Li 5-6	4 Li 5	2 Co 5	4 Li 5
2	Useful power at engine speed	kW (bhp) rpm	149 (203) 6000	134 (182) 6000	120 (163) 5850	104 (141) 6000	149 (203) 5800
3	Max. torque at engine speed	Nm rpm	260 3600	279 4000	214 4400	177 4800	258 4850
4	Maximum speed	km/h	200	> 180	210	200	210
5	Acceleration from 0 to 100 km/h	(0-97 km/h) s	8.5	10	10.5	11	10.2
6	Curb weight	kg	1710	1540	1435	1335	1610
7	Gross vehicle weight	kg	–	–	1930	–	2120
8	Weight-to-power ratio	kg/kW	11.5	11.5	12.2	12.8	10.8
9	Fuel consumption	l/100 km	EPA 9.4/13.1	(Ed.) 9/15	EU 7.1/15.1	(Ed.) 8/12	EPA 9/11.2
10	Fuel octane number	RON	95	91	95	91	92
11	Fuel tank capacity	l	60	64.5	60	64	64
12	Engine swept volume	cm^3	2962	3350	2497	1996	2736
13	Bore/stroke	mm	86/85	92/84	83.5/76	87.5/83	86/78.5
14	Compression ratio	–	10	9.5	9.4	9.6	9.7
15	Specific power output	kW/l	50.3	40	48.1	52.1	54.5
16	Engine type	–	6 V 4Ve	q 6 V	q 6 V 4Ve	q 4 R 4Ve	6 V 4Ve
17	Fuel management	–	Motronic	EI	EI	EI	EI
18	Alternator (14 V)	A	120	105/140	90	90	125
19	Battery (12 V)	Ah	300 A	54	60	430 A	60
20	(Engine pos.)/drive config.	–	h-ASR	v-ASR	v	v	v
21	Transmission ratio	1st/2nd gear 3rd/4th gear 5th/6th gear	2.86/1.62 1/0.72	2.92/1.57 1/0.71	2.84/1.57 1/0.69	3.54/2.13 1.36/1.03 0.81	2.84/1.57 1/0.69
22	Final drive ratio	–	3.9	3.29	3.91	3.94	3.89
23	Gearshift	H (A)	(4)	(4)	(4)	5 (4)	(4)
24	Cooling	l	10	11.2	10	7	8.2
25	Vehicle length	mm	4930	5080	4750	4850	5000
26	Vehicle width	mm	1790	1855	1820	1770	1920
27	Vehicle height	mm	1430	1460	1380	1340	1420
28	Wheelbase	mm	2730	2805	2740	2635	2870
29	Track, front/rear	mm	1505/1520	1575/1555	1530/1530	1510/1505	1575/1565
30	Turning circle diameter	m	11.0	11.5	11.8	12.2	12.3
31	Ground clearance	mm	130	120	140	140	130
32	Suspension, front	–	DQl-F-Ku-Td	DQl-F-Sf-Ku-Td	DDQl-Sf-Ku-Td	DDQl-Sf-Ku-Td	Ql-Ll-F-Sf-Ku-Td
33	Suspension, rear	–	Ql-Sl-Sf-Ku-Td	Ql-Ll-F-Sf-Ku-Td	Ea-DQl-Ql-Ll-Sf-Ku-Td	Ea-DQl-Ql-Ll-Sf-Ku-Td	Ea-Ql-Ll-F-Sf-Ku-Td
34	Tires	–	225/55 R 16	225/60 R 16	185/65 R 15	195/70 HR 14	225/55 R 17
35	Braking system		4Sb-ABS	4Sb-ABS	4Sb	Sb-Tb	4Sb-ABS

See PP. 898 for abbreviations and explanations.

PETITIONER'S EXHIBIT 1002
US PATENT NO. 6,557,540

Dodge Caravan 2.4i	**Ford** Windstar 3.8i	**Lincoln** Continental 4.6i	**Mercury** Cougar 2.5i	**Oldsmobile** Alero 2.4i	**Plymouth** Voyager 3.0i	**Pontiac** Sunfire 2.2i	
5 Gli 5-8	4 Gli 5-7	4 Li 5-6	3 Co 4	2 Co 5	5 Gli 7	2 Ca 5	1
112 (152) 5200	149 (203) 4900	205 (279) 5750	127 (173) 6250	112 (152) 5600	112 (152) 5200	86 (117) 5000	2
226 4000	326 3600	373 4750	224 4250	210 4400	239 4000	183 3600	3
170	> 175	215	225	200	175	175	4
							5
–	–	–	8.5	10.5	–	–	
1595	1690	1760	1375	1340	1605	1300	6
–	2440	–	–	–	–	–	7
14.2	11.3	8.6	11	12	14.3	14	8
EPA 9.4/11.8	EPA 10.2/13.8	EPA 9.8/13.8	EPA 8.4/12.4	EPA 7.8/11.2	EPA 9.8/12.4	EPA 6.4/10	9
–	91	–	91	91	87	91	10
75	95	76	60	57	75	57.5	11
2429	3797	4601	2544	2392	2972	2190	12
87.5/101	96.8/86	90.2/90	82.4/79.5	90/94	91.1/76	89/88	13
9.4	9.3	9.85	9.7	9.5	8.9	9	14
46.1	39.2	44.6	49.9	46.8	37.7	39.3	15
q 4 R 4Ve	6 V	8 V 4Ve	q 6 V 4Ve	q 4 R 4Ve	q 6 V	q 4 R	16
EI	EI	EI	EI	EI	EI	EI	17
90/120	130	130	130	105	90/120	105	18
600 A	58	84	68	52	600 A	54	19
v	v-ASR	v	v	v-ASR	v	v	20
2.84/1.57 1/0.69	2.77/1.54 1/0.69	2.77/1.54 1/0.69	3.42/2.14 1.45/1.03 0.77	2.96/1.63 1/0.68	2.69/1.55 1	3.91/2.18 1.45/1.03 0.74	21
3.91	3.89	3.56	4.06	3.42	3.19	3.58	22
(4/3)	(4)	(4)	5 (4)	(4)	(3/4)	5 (3/4)	23
10.6	11.9	12.8	7.5	9.8	10.6	9.1	24
4740	5125	5260	4700	4740	4730	4620	25
1950	1915	1870	1770	1780	1920	1710	26
1740	1790	1420	1320	1390	1740	1360	27
2880	3065	2770	2700	2720	2880	2645	28
1600/1630	1640/1600	1600/1560	1505/1490	1500/1505	1600/1630	1465/1435	29
11.5	12.3	12.5	10.9	11.3	11.5	10.9	30
140	150	150	–	120	140	150	31
DQI-F-Td	DQI-F-Sf-Ku-Td	QI-F-Ku-Lue	DQI-F-Ku-Td	DQI-F-Sf-Ku-Td	DQI-F-Ku-Td	DQI-F-Sf-Ku-Td	32
Sa-P-Td	Vla-Sf-Ku-Td	QI-LI-Ku-Lue	QI-LI-F-Sf-Ku-Td	DQu-LI-Sf-Ku-Td	Sa-P-Td	Vla-LI-Sf-Ku-Td	33
205/75 R 14	205/75 R 15	225/60 R 16	205/60 R 15	215/60 R 15	205/75 R 14	195/70 R 14	34
Sb-Tb	Sb-Tb-ABS	4Sb-ABS	4Sb	4Sb-ABS	Sb-Tb	Sb-Tb-ABS	35

PETITIONER'S EXHIBIT 1002
US PATENT NO. 6,557,540

Index of headings

A

A pillar (body structure) 722
A/D converters 92
A/F mixture adjustment 519
A/F mixture formation 367, 372, 452, 458, 509, 515, 517, 518, 560
A/F mixture ignition 477
A-arm (suspension linkage) 622
Abrasion (wear) 331
ABS for commercial vehicles 644, 649, 693
ABS for passenger cars 644, 649, 659, 708, 803
Absorption method (exhaust soot) 566
Absorption silencer 450
AC firing 809
ACC, see Adaptive Cruise Control 714
Acceleration 34, 342, 345
Acceleration and braking diagram 344
Acceleration due to gravity 13
Acceleration power 345
Acceleration resistance 337
Acceleration sensors 107, 808
Accelerator pump (carburetors) 461
Accelerator-pedal module 501
Accelerator-pedal travel sensors 501
Accident hazard (ignition systems) 492
Accident record (tachograph) 795
Accidents (body stresses) 722
Accidents (classification into collision types) 728
Accumulators, see Batteries 866
ACEA specifications for mineral oils 235
Acoustic impedance 50
Acoustic quality control 55
Acoustic tuning devices (exhaust systems) 451
Acoustics (terminology, units, symbols) 50
Action limits (statistics) 160
Active power and conductance 65
Active safety (vehicle bodies) 726
Active suspension 615
Actuating force, braking system 647
Actuating force, steering system (regulations) 638
Actuation device, braking systems 644, 656, 688
Actuators 124
Actuators, characteristic data, features 130
Actuators, electromechanical 124
Actuators, fluid-mechanical 129
ADA, see Auto-Directional Antenna 786
Adaptation equipment, mechanical (diesel-engine management) 540
Adaptive Cruise Control (ACC) 714
Addendum modification (gears) 296
Additional spark (ignition) 496
Additives (engine coolant) 249
Additives (fuel) 240, 243
Additives (lubricants) 230
Adhesion to road surface 343
Adhesion/slip curves 606, 659, 697
Adhesive technology 322
Adhesives, single or dual-component 322
Adjustment (brakes) 681
Adjustment (steering wheel and seats) 814
Admittance 65
Advance or retard mechanisms (ignition timing) 489
Advanced ignition 478
Aerodynamic drag in kW 339
Aerodynamic/fast-back body designs (wind resistance) 350
Aerodynamics (passenger cars) 721
Afterburning 521
Agricultural tractors (requirements) 362
Air bags 691, 757, 803
Air bypass actuator (ME-Motronic) 501
Air compressors 687
Air conditioners, automotive 777
Air cooling (direct cooling) 410, 430
Air driers (air brakes) 688
Air filters 438
Air requirements (A/F mixture) 458
Air suspension 616, 618
Airbags 730, 803
Air-flow angle (crosswind) 350
Air-flow sensors (K-/L-Jetronic) 468, 473
Air-fuel (A/F) mixture 414, 458
Air-fuel (A/F) ratio 458
Air-mass flow sensors 116, 475
Alarm systems 767
ALB, see Automatic Load-sensitive Braking-force metering 678, 689
Alcohols (alternative fuels) 246
All-wheel drive 605
Alphabets and numbers 897
Alternating current 65
Alternating-current (AC) machines 72, 135
Alternative fuels 243
Alternator drive system 880
Alternator output 862
Alternator-current curve 875
Alternators 874, 899
Altitude compensation (KE-Jetronic) 470
Aluminum bodywork 723
Aluminum casting alloys 199

PETITIONER'S EXHIBIT 1002
US PATENT NO. 6,557,540

American gears 301
American units 19
Ampere (definition) 12
Ampere turns 71
Amplifier (car radio) 787
Amplitude 29
Analog circuits (integrated) 83
Analog-digital converters 92, 498
Analysis (exhaust-gas emissions) 526
Analysis (reliability) 165
Angle of impact (crosswind) 350
Angle sensors 99
Ångström (unit) 14
Angular frequency 15, 29
Annealing 273
Announcement ID (car radio) 786
Anodic corrosion protection 264
Anodizing 264
Antenna diversity receivers 786
Antennas for motor vehicles 788
Antennas, automatic 788
Anti-Corrosion Code 724
Anti-foaming agent (diesel fuels) 243
Antifreeze 249, 430
Anti-judder function 506
Anti-knock properties (octane number) 238
Anti-knock quality (octane rating) 238
Antilock braking systems (ABS) for commercial vehicles 644, 649, 693
Antilock braking systems (ABS) for passenger cars 644, 649, 659, 708, 803
API classifications (mineral oils) 235
Apparent power 65
Application forces (braking systems) 647
Application-specific IC (ASIC) 86
Aquaplaning, see Wet road surfaces 343
Arc discharge (spark plugs) 477
Arc pressure welding 321
Architecture rules (CARTRONIC®) 888
Arcing voltage (ignition) 477
Area 148
ARI, see Radio information for the driver 786
Arithmetic series 147
Articulated bus (definition) 716
Articulated road trains (definition) 716
Articulated vehicles (definition) 716
Artificial networks (EMC) 895
ASIC, see Application-Specific IC 86
Aspect (height-width) ratio (tires) 630
Assembled-representation diagrams (automotive electrical systems) 854
ASU, see Automatic FM interference suppression 786
Asynchronous drive 580
Asynchronous machines 133
ATF oil 236
ATF, see Automatic Transmission Fluids 230
Atmospheric humidity (vehicle stress) 364
Atmospheric pollutants 364
Atmospheric-pressure-dependent full-throttle stop (ADA) (diesel fuel injection) 540
Austenitizing (hardening) 268
Auto directional antenna (ADA) 786
Auto-ignition 367
Automatic adjustment (brakes) 681
Automatic braking systems 644
Automatic clutches 590
Automatic gear shift (automotive transmissions) 597
Automatic headlight level adjustment 754
Automatic load-sensitive braking-force metering (ALB) 675, 678, 689
Automatic seat belts 729, 803
Automatic transmission 342, 597
Automatic Transmission Fluids (ATF) 236
Automatic UHF interference suppression (ASU) 786
Automotive alarm systems 767
Automotive comfort and convenience systems 812
Automotive electrical systems 862
Automotive hydraulics 816
Automotive paints (properties) 228
Automotive pneumatics 832
Automotive windshield and window glass 774
Auxiliary drives (automotive hydraulics) 827
Auxiliary driving lamps 756
Auxiliary-air valves (K-Jetronic) 468
Axial-piston pumps/motors (automotive hydraulics) 818
Axle oscillation 613

B

B pillar (body structure) 722
Backlash (gears) 299
Backup (reversing) lamps 763
Bainitizing (hardening) 270
Balancing of masses and inertial forces (reciprocating-piston engines) 399
Balancing rate (crankshaft) 400
Ball bearings, see rolling bearings 289
Ball impression hardness 278
Band syncromesh (transmission) 594
Bandless V-belts 307
Bar, unit of pressure (conversion) 16
Barrel, unit of volume (conversion) 20
Barrel-type coil springs 318

PETITIONER'S EXHIBIT 1002
US PATENT NO. 6,557,540

Barrier impact 729
Basic equations (mechanics) 34
Batteries, vibration-proof 869
Battery characteristic data 867
Battery maintenance 871
Battery chargers 873
Battery charging 63, 870
Battery design types 868
Battery faults 871
Battery ignition 490
Battery power 576
Battery systems 576
Battery testers 872
Battery-charging current 873
Battery-charging curves 873
BCD mixing process (semiconductors) 80
BDC, see Bottom Dead Center 385
Bearing-pin sensors 112
Bearings (materials) 284
Bearings, sliding and rolling 282
Beats (definition) 29
Bell-shaped curve (Gaussian/normal distribution) 157
Belt force (belt drives) 306
Belt-drive systems 306
Bending, bending moment, bending stress 42
Benedicks effect (thermal e.m.f.) 75
Bevel gears 297
Bi-Litronic 746
Bimorphous spring element 108
Bingham bodies 230
Binomial distribution 163
Bipolar transistors 79
Bit stuffing (CAN error detection) 886
Black body radiators 57
Black ice (coefficient of friction) 343
Bleeding (grease) 230
Blind rivets 323
Blowby (crankcase ventilation) 521
Bodies, commercial vehicles 732
Bodies, passenger cars 718
Body design (passenger cars) 720
Body roll 353, 613
Body structures (passenger cars) 722
Body templates 718
Boiling curve (gasoline) 240
Boiling range (diesel fuels) 242
Bonding and joining technology 319
Boost air 390
Boost charging (batteries) 873
Boost retarders (braking systems) 685
Booster (car radio) 787
Boron treatment (thermochemical hardening) 272
Bosch Micro-Contact (BMK) 860
Bosch sooting numbers (SZ) 567
Bosch spark plugs 486
Bottom Dead Center (BDC) 385
Box-type body (commercial vehicles) 735
Brake analyzers 702
Brake booster (servo) 656
Brake characteristic 679
Brake control circuit (TCS) 610
Brake cylinders 689, 691
Brake deceleration 648
Brake discs 657
Brake fluids 247
Brake horsepower (passenger-car specifications) 899
Brake line 646
Brake pressure 656, 659
Brake response time 347, 647
Brake test stands 702
Brake testing 702
Brake-circuit configuration 654
Brake-lining wear 656
Brake-lining wear equalization (EBS) 700
Brakes 645
Brakes, engine 683
Brakes, wheel 657
Braking and acceleration diagram 344
Braking distance 344, 347, 648
Braking force 635, 647
Braking operation 344, 646
Braking power 648
Braking progression for GMA 663
Braking resistance 337, 583
Braking system, air-over-hydraulic 676
Braking systems (continuous operation) 595, 644, 649, 682
Braking systems (EU requirements) 650
Braking systems 644, 899
Braking systems for heavy commercial vehicles 674
Braking systems for passenger cars and light commercial vehicles 656
Braking systems, actuation methods 644, 656, 688
Braking systems, continuous 644, 649, 682
Braking systems, design 653
Braking systems, inertia 645
Braking systems, splitting (brake circuits) 654
Braking times 647, 648
Braking torque 647
Braking when cornering 357
Braking work 648,
Braking-energy recovery (electric vehicles) 578

PETITIONER'S EXHIBIT 1002
US PATENT NO. 6,557,540

Braking-force distribution 647, 653, 675
Braking-force metering 689
Braking-force metering device 658
Braking-systems, components 652
Brazing 322
Brazing solder 213,
Breakdown voltage 77
Breakerless transistorized ignition 490
Breaking spark (ignition distributor) 488
Breaking strength 180
Broad-band (oxygen) sensors 524
Broad-band interference source, EMC 891
Browning (corrosion protection) 264
Bucket tappet assemblies (valve timing) 408
Buckling (strength) 43
Bulbs (automotive lighting) 763
Bulk micromechanics (BMM) 90
Bumper protector strips 724
Bus allocation (CAN) 885
Bus bodies 735
Bus configuration (CAN) 884
"Bus-stop" brake 701
Bus systems (microprocessors) 84
Bus/motor coach (definition) 716
Bush-type gear pumps, hydraulic 817
Butane (LPG) 192, 245, 512
Butt-seam welding 320
Bypass oil filters 411

C

C pillar (body structure) 722
Calorific values (fuels) 238
Cam brakes, see Drum brakes 678
Camber angle 621, 602
Cam-follower assemblies (valve timing) 408
Cam-lobe design (valve gears) 409
Camshaft adjustment 501
Camshaft drive assembly (valve gears) 408
CAN, see Controller Area Network 884
Candela (definition) 12
Canister-purge valves 506
Capacitance (capacitor) 17, 61, 66
Capacitive reactance 66
Capacitor-discharge ignition (CDI) system 492
Capacitors 62, 66
Capacity, Ah (starter batteries) 868
Car radios 786
Carbon dioxide (exhaust-gas emissions) 518
Carbon monoxide (exhaust-gas emissions) 245, 518
Carbon-deposit index (diesel fuels) 243
Carbon-graphite bearings 287
Carbonitriding 271
Carburetors 460
Carnot cycle 59, 367, 363
CARTRONIC® 175, 887
Case hardening 271
Case-hardened steel 194
Cast iron (properties) 193
Caster (steering) 620, 639
Castings (sintered metals) 201
Catalytic afterburning: 521
Catalytic converters 448, 505, 509 521, 532
Catalytic converters, three-way 458
Cathodic protection (corrosion) 264
C-brake (engine brake) 683
CD, see Compact Disc 787
Cell rotors (pressure-wave supercharger) 446
Cell voltages 576
Cells, battery 576, 868
Cells, solar 81
Cellular telephone networks 800
Celsius degree, conversion 26
Celsius degree, unit 17
Center electrode (spark plugs) 483
Central air filters 438
Central display and control units (vehicle instrumentation) 781, 802
Central injection unit (Mono-Jetronic) 465
Central locking systems 815
Central Processing Unit (CPU) 84, 886
Centrifugal advance mechanisms (gasoline engine) 489
Centrifugal force 35
Centrifugal force when cornering 352
Ceramic materials 217
Ceramic monoliths (catalytic converters) 449, 451
Ceramic soot filters 451
Ceramics 182
Cetane improvers (diesel fuel) 243
Cetane number (fuels) 241
Changes of condition in cyclic processes 368
Changes of state (gases) 59
Charge cycle 454, 501
Charge stratification in cylinder 383
Charge, electrical 60
Charging and insulation module 865
Charging balance equation (automotive electrical systems) 864
Charging voltage (automotive electrical system) 864
Chart, EC tachograph 794
Chassis cross-member 722

PETITIONER'S EXHIBIT 1002
US PATENT NO. 6,557,540

Chassis dynamometers (brake testing) 526, 702
Chassis frames (commercial vehicles) 734
Chemical elements 176
Chemicals (names of) 250
Child seats (standardized anchorage) 811
Chopper disc (exhaust-gas testing) 532
Chromating (coating) 264
Circuit diagrams (automotive electrics) 839
Circuit families 84
Circuit isolation (compressed-air brakes) 689
Circuit, magnetic 70
Circuit-diagram symbols, American 857
Circuit-diagram symbols, automotive 834
Classification (motor vehicles) 717
Claw-pole alternators 877
Cleaning systems (headlamps) 772
Cleaning, windshield and rear window 770
Clearance (wheel brakes) 681
Clearance lamps 761
Climbing power 341
Climbing resistance 341
Clinching (joining and bonding) 323
Clock pulse generators (microcomputers) 84
Closed center (hydraulic systems) 825
Closed process (combustion) 366
Closing control (power sunroof) 813
Cloud point (lubricants) 230
Clutch disc 590
Clutches 590
C-net communications path 800
CO, see carbon monoxide 518
Coaches, long-distance (definition) 716
Coal hydrogenation 243
Coalescence effect 437
Coatings 265
Coatings, inorganic 264
Coatings, metallic 265
Coatings, non-metallic 264
Coatings, organic 266
Coefficient of cyclic variation (crankshaft) 398
Coefficient of cornering stability 360
Coefficient of friction (tire/road surface) 343
Coefficient of friction, static 39, 343; 635
Coefficient of thermal expansion 181
Coefficient of wear 331
Coefficients of expansion 181, 186, 190
Coefficients of friction 39, 282, 313, 315, 343
Coercive field strength 68, 181
Coil ignition (CI) 477, 487
Coil springs 291
Coking (injectors) 555
Cold-discharge test current (batteries) 868, 872
Cold-flow properties (diesel fuels) 241
Colloid (definition) 180
Color filters 139
Combination brake cylinders 689, 691
Combustion knock 375, 497, 502
Combustion noise (diesel engines) 555
Combustion problems 375, 382
Combustion sequence (IC engines) 374, 381, 518, 560
Combustion stroke 386
Combustion-chamber design (diesel engines) 378, 560
Combustion-chamber design (gasoline engines) 520
Combustion-chamber pressure curve 479
Combustion-chamber pressure sensor 111
Comfort and convenience systems (motor vehicle) 812
Commercial vehicle (definition) 716
Commercial vehicles 595, 716, 732
Commercial-vehicle air filters 439
Commercial-vehicle bodies 732
Commercial-vehicle tires 628
Commercial-vehicle transmissions 595
Common Rail (accumulator) fuel-injection systems (CRS) 535, 551
Communication areas (motor vehicle) 780
Compact alternators 877
Compact Disc (CD) 787
Compact-diode design (claw-pole alternator) 877
Comparative cycle (gas turbines) 428
Comparative data (IC engines) 413
Complete combustion 518
Component codes (circuit diagrams) 854
Components (technical optics) 138
Composite bearings 286
Composite materials 183
Composite positioning (vehicle navigation systems) 796
Composite systems (automotive) 887
Compound electrode (spark plugs) 483
Compound, chemical 180
Compressed-air conditioning (air brakes) 688
Compressibility (brake fluids) 248
Compression (calculation) 417
Compression (engine cylinders) 423
Compression area (diagram) 420
Compression graph (turbochargers) 442

PETITIONER'S EXHIBIT 1002
US PATENT NO. 6,557,540

Compression ratio 520
Compression stroke 386
Compressor efficiency 423
Concentration sensors 117
Conditional safety 726
Conductivity, electrical 76, 215
Conductivity, thermal 181
Conductor color coding (circuit diagrams) 854
Conductor sizes (calculations for automotive electrical system) 858
Conductors in magnetic fields 72
Conductors, metal 76
Confidence interval (statistics) 159
Conformability (bearings) 283
Connecting rod 405
Connections (symbols) 834
Connectors (vehicle electrical systems) 860
Consistency (lubricating grease) 231, 237
Constant throttle (exhaust brake) 683
Constant Volume Sampling (CVS) 526, 561
Constant-displacement pump (automotive hydraulics) 825
Constant-pressure cycle 368, 428
Constant-pressure systems (automotive hydraulics) 825
Constant-pressure turbocharging 443, 444
Constant-pressure valve 537
Constant-velocity joints (final-drive) 602
Constant-volume cycle 368
Constant-volume valves 537
Constriction index (fluid flow) 41
Consumable materials (motor vehicle) 247
Contact breakers (coil ignition) 487
Contact corrosion 256, 261
Contact force (tires) 351
Contact pitting 488
Contact potential 83
Contact potential values 73
Contact pressure (gears) 303
Contact thermometers 119
Content-based addressing (CAN) 884
Continuous braking system 646
Continuous combustion 366
Continuous division, golden section 147
Continuous sound level (noise) 54
Continuously variable transmissions (CVT) 601
Continuous-time control 169
Contrast (definition) 140
Control cycle (antilock braking systems/ABS) 662
Control engineering 167
Control filament (glow plugs) 568
Control methods 169
Control rod (in-line fuel-injection pumps) 538
Control systems (IC engines) 171
Control systems, automotive 171
Control unit, electronic (ESP) 712
Control unit, electronic (ABS/ASR) 608, 695
Control unit, electronic (KE-Jetronic) 470
Control unit, electronic (L-/LH-/L3-Jetronic) 473
Control unit, electronic (Motronic) 498
Control unit, electronic (Park Pilot) 792
Control unit, electronic (seatbelt tensioner and front/side airbag) 808
Control unit, electronic (UIS/UPS) 551
Control valves (steering cylinder) 640
Controlled systems (control engineering) 167
Controlled systems 170
Controlled variables 170
Controlled variables (emission control) 525
Controller Area Network (CAN) 884
Controlling systems, open and closed-loop (control engineering) 167
Control-sleeve in-line fuel-injection pumps 535, 542
Convection (heat transfer) 56
Conventional (3-box) vehicle shape, c_W figure 340
Converter lockup clutches 592
Converters, electrical 124
Convertible (cabriolet), definition 716
Coolant circuit (air-conditioning systems) 778
Coolant circuit 410
Coolant expansion tank 432
Coolant temperature 431
Coolants 249, 430
Cooled exhaust-gas recirculation 435
Cooler-module technology 434
Cooling (engines) 410, 430, 879, 899
Copper conductors (in motor vehicles) 858
Copper losses (alternators) 881
Core hardness (heat treatment) 269
Cornering behavior 352, 359
Cornering force 351, 360
Cornering resistance 339
Corrosion 256
Corrosion inhibitors 243, 249
Corrosion protection 256, 262, 724
Corrosion testing 259
Corrosive atmosphere 364
Coulomb's Law 61

PETITIONER'S EXHIBIT 1002
US PATENT NO. 6,557,540

Coupé (passenger car), definition 716
Coupling of oscillations 30
CPU, see Central Processing Unit 84, 886
Crank sequence (crankshaft configuration) 401
Crankcase ventilation (blowby) 521
Crankcases 407
Crankshaft assemblies 396, 405
Crankshaft bearings 405
Crankshaft vibrations 406
Crankshaft-assembly dynamics 396
Crash-behavior analysis 731
CRC, see Cyclic Redundancy Check 886
Creep (deformation) 47
Creep behavior (strength) 47
Crevice corrosion 259
Critical speeds 353
Crossflow cylinder heads 407
Cross-ply tires 628
Crosswind, response 350
Crosswind, sensitivity 354
CRS, see Common-Rail System 535, 551
Crude oils (characteristics) 244
Cruise Control 714
Cruise-control facility 506, 714
Cryogenic tank (liquid hydrogen) 517
CT (clock/time) code, car radios 788
Cumulative frequency curve (statistics) 156
Curb weight (passenger-car specifications) 899
Curie point 181
Curie temperature tables 208
Current density, permissible 858
Current measurement 62
Current, electric 12, 62, 65, 71
CVS see Exhaust-gas testing 526, 561
Cyclic combustion 366
Cyclic Redundancy Check (CRC) 886
Cycloidal teeth 296
Cyclone prefilters 439
Cylinder deactivation (IC engines) 377
Cylinder heads (IC engines) 407
Cylinder liners (IC engines) 404
Cylinder numbering (IC engines) 395
Cylinder pressure (hydraulic cylinder) 816
Cylinder-charge control (gasoline engines) 452, 500
Cylinders, combination brake 689
Cylinders, hydraulic 816, 822
Cylindrical lenses 138
Cylindrical springs 618

D

DAB, see Digital Auto Broadcasting 789
Damped sprung-mass system 612
Damping characteristics 617
Danger of skidding 705
Dash area (vehicle bodies) 723
Data processing (DP) in motor vehicles 169, 172, 884
Daytime running lamps 763
DC machines 72, 132
DC motors for wiper systems 772
DC relays (materials) 185, 206
DC series-wound motors 578
Deceleration (brakes) 345
Decibel (dB) 52
Decimal system 144
Decoding (traffic bulletins) 798
Decompression exhaust brake 683
Deep-cycle batteries 869
Deep-drawing press 326
Deep-drawing techniques 326
Deflection-force lever arm (automotive suspension) 620
Deformation behavior (vehicle bodies) 728
Degree of reflection (optics) 138
Degrees of protection (electrical machines) 136
Delivery pumps (diesel engines) 536, 543
Delivery rate (hydraulic pumps) 816
Delta connection (3-phase AC) 67
Demagnetization curves 71
Denloc groove (tires) 625
Density (fuels) 238, 242
Density 180
Destination entry, route guidance (navigation systems) 796
Detergent additives (diesel fuels) 243
Device identification codes (circuit diagrams) 849
Devices in the motor vehicle (diagrams/symbols) 836
Devices in the motor vehicle (identification in schematic diagrams) 849
DI diesel engines 535
Diagnosis (integrated), ME-Motronic 506
Diagnosis connector 511
Diagnosis of control units 511, 884
Diamagnetism 68
Diamagnets 184
Diametral pitch (gears) 301
Diaphragm pumps (fuel supply) 460
Diaphragm-type cylinders (commercial-vehicle brakes) 689
Dielectric constant 61
Dielectric displacement 61
Diesel engines 378, 534
Diesel exhaust, composition 560

PETITIONER'S EXHIBIT 1002
US PATENT NO. 6,557,540

Diesel fuel filters 436
Diesel fuel-injection pumps 534
Diesel fuels 241
Differential (drivetrain) 590, 604
Differential, see final drive 602
Diffusion flame 381, 382
Diffusion potential 77
Diffusion process 264
Diffusion rate (charge air) 433
DigiCeiver 787
Digital Auto Broadcasting (DAB) 789
Digital call procedure 801
Digital circuits, integrated 83
Digital instruments 781
Digital networks, cellular phones 800
Digital parametric equalizing (DPE) 787
Digital signal adaptation (DSA) 787
Dilatant flow behavior (viscosity increase) 232
Dilution systems (emissions testing) 527
Dimensional tolerances 279
Dimensions (passenger cars) 719
Dimethylether (DME) 247
Diodes, semiconductor 78
Direct cooling (air cooling) 410
Direct current (DC) 62
Direct injection (DI) 379, 464
Direction of current flow 62
Direction of rotation (IC engines) 395
Directional stability (steering characteristics) 638
Directional-control valves (automotive hydraulics) 820
Dirt sensors 121
Disc brakes 657, 681
Disc radiators 434
Disc wheels 624
Discharge of air (from nozzles) 37
Discharge time (energy-storage device) 334
Discrete-time control 170
Dispersion 138, 180
Displacer, Stirling engine 424
Display (instruments) 784
Display and operator unit, central 781, 802
Display elements, optical 143
Dissociation losses (combustion) 375
Distance calculation (Park Pilot) 793
Distance sensor (ACC) 714
Distributor (ignition) 488
Distributor fuel-injection pumps 535, 543
Distributorless ignition 492
Distributorless voltage distribution (ignition) 482, 495
Disturbance point (control engineering) 168
Disturbances (control engineering) 168
Door latches/locks, car 725
Door locking (busses) 833
Door operation (busses) 832
Doping (semiconductors) 76
Doppler effect 51
Downdraft carburetors 460
Downgrade force 341
DPE, see Digital parametric equalizing 787
Drag coefficient (c_W) 37, 329, 721
Drag coefficient (wind resistance) 340, 721
Draw tempering, steel (hardening) 270
Drawbar power (agricultural tractor) 362
Drawbar pull (agricultural tractor) 362
Drawing methods (sheet-metal processing) 326
Drive batteries 576
Drive belts 307
Drive configurations, hybrid 582
Driver information system (ARI) 786
Driver information systems 780
Driver stages (Motronic) 498
Driver's cab 734
Driver-selected (disengageable) all-wheel drive 605
Drivetrain 588
Drivetrain configurations 589
Drivetrain elements 589
Drive-wheel tires (agricultural tractor) 363
Driving cycles (emissions testing) 526, 562
Driving limits (vehicle dynamics) 706
Drop-center rim (vehicle wheels) 624
Dropping point (lubricants) 232
Drum brakes 657, 678
Drum brakes, servo 680
Drum brakes, Simplex 679
Drum brakes, wedge 679
Dry cells 64
Dry sliding bearings 286
DSA, see Digital signal adaptation 787
Dual system (mathematics) 144
Dual-bed catalytic converters 522
Dual-chamber combustion systems 379
Dual-circuit steering systems 642
Dual-fuel operation (gasoline/LPG) 512
Dual-mass (vehicle) model 612
Dual-mass flywheels (clutch) 590
Dual-spark ignition coils 482, 496
Dual-spring nozzle holders 558
Dummies (crash test) 728
Duo-duplex drum brakes 680
Duo-servo drum brakes 680
Durability, passenger cars 722

PETITIONER'S EXHIBIT 1002
US PATENT NO. 6,557,540

Duroplastics 183, 222
Dust-unloading valves 439
Duty cycle (electrical equipment) 863
Duty types (electric machines) 135
Dwell angle 488, 491, 504
Dwell period 505
Dynamic loadability (rolling bearings) 289
Dynamic route guidance (vehicle navigation systems) 799
Dynamic supercharging 390
Dynamic tire-performance characteristics 636
Dynamic vehicle stability 608, 705
Dynamic viscosity 232
Dynamic-behavior analysis (bodywork) 731
Dynamics of lateral motion (motor vehicles) 350, 705
Dynamics of linear motion (motor vehicles) 338
Dynamised routes 797
Dynatard (engine brake) 683

E

Ease of ignition (diesel fuel) 241
Ease of repair (body structures) 722
EC tachograph 794
Eccentric shaft (rotary engines) 426
Eccentricity (bearings) 282
ECE/EU test cycle (exhaust-gas emissions) 528
Echo depth-sounding method (parking systems) 791
Economic efficiency (gasoline engines) 377
ECOTRONIC carburetor system 462
ECU, see Control Unit, electronic
EDC, see Electronic diesel control 544
Eddy-current sensors 97
Eddy-current speedometers 782
Efficiency (reciprocating-piston engines) 370, 419
Efficiency (alternators) 880
Efficiency (electric drives) 580
Efficiency levels (gas turbines) 428
Efficiency, theoretical cycle (IC engines) 368
Elastokinematics (suspension) 621
Elastomer swelling 248
Elastomers 183, 224
ELB, see Electronically controlled braking system 697
Electric drives (motor vehicles) 575
Electric field strength 61
Electric fuel pumps 455
Electric machines 132
Electric motors 132, 571
Electric power units, vehicles 575
Electric road-going vehicles 575
Electrical conductivity 76
Electrical effects 73
Electrical engineering 60
Electrical loads (automotive electrical system) 863
Electrical power 62, 65
Electrical properties 215
Electricity storage (hybrid power units) 582
Electrochemical corrosion protection 263
Electrochemical equivalent 64
Electrochemical series of metals 257
Electrode gap (spark plugs) 484, 485
Electrode potential (voltaic) series 73
Electrodynamic principle 125
Electrodynamic retarders 685
Electrohydraulic brakes (EHB) 673
Electrohydraulic pumps 819
Electrolysis (electrolyte) 64
Electrolyte density, state of battery charge 867
Electromagnetic compatibility (EMC) 890
Electromagnetic fields 60
Electromagnetism (principle) 126
Electron-beam welding 321
Electron-hole pairs (semiconductors) 76
Electronic accelerators (ETC/drive-by-wire) 452, 501, 606
Electronic carburetor systems 462
Electronic components 78, 836
Electronic control unit, see ECU
Electronic diesel control (EDC) 544
Electronic force limitation (power windows) 812
Electronic heater controls 777
Electronic ignition (EI) 493
Electronic injection-pump control 541, 544
Electronic keys (immobilizers) 769
Electronic knock control (ignition retard) 491
Electronic stability program (ESP) 701, 704, 803
Electronic throttle control (ETC/drive-by-wire) 452, 501, 606, 608
Electronic transmission control 598
Electronically controlled braking system (ELB) 697
Electronic-system testing (gasoline engines) 510
Electrophoretic dip coating 724
Electroplating 265

PETITIONER'S EXHIBIT 1002
US PATENT NO. 6,557,540

Electropneumatic braking systems (EPB) 698
Electropneumatic fanfare horns 766
Electrostatic discharge (EMC) 895
Elongation at fracture (Table) 193
EMC, see Electromagnetic compatibility (EMC) 890
Emissions (exhaust) 518, 560
Emissions limits (pollutants) 533, 563
Emitter, transistor 79
Empirical distribution 157
Emulsion 180, 247
Enameling 265
Energy 15
Energy source (air brakes) 644, 687
Energy storage and supply (air brakes) 689
Energy storage devices, electrical (hybrid drives) 582
Energy storage devices, mechanical (hybrid drives) 581
Energy supply (air brakes) 644, 687
Energy supply (automotive electrical systems) 862
Energy supply (electric drives) 575
Energy transmission (braking systems) 653
Energy units (conversion) 25
Energy-absorbing foam 723
Energy-assisted braking systems 645
Engagement solenoid (starters) 571
Engaging systems (starters) 572
Engine brakes 683
Engine characteristics (calculations) 417
Engine designs 394, 899
Engine diagnosis 510
Engine drag-torque control (MSR) 608, 708
Engine fuel-consumption graph 336
Engine management (diesel engines) 534
Engine management (gasoline engines) 452
Engine oils 234
Engine power control 452, 606
Engine power loss 414
Engine power output (calculation) 418
Engine ring gears (starting systems) 571
Engine speed and vehicle speed 342
Engine swept volume (calculation) 417, 420
Engine temperature sensors 473
Engine testers 510, 553
Engine testing technology 510, 552
Engine torque (calculation) 419
Engine-control circuit (TCS) 610
Engines, internal-combustion (IC) 366
Engines, opposed-cylinder (boxer) 394
Engine-speed reduction (gasoline engines) 377
Enhanced Other Network (EON) 788
Enthalpy (heat content) 56
Enthalpy-entropy diagram 368
Entropy 59
Environmental considerations (automobile recycling) 732
Environmental considerations (electric drives) 575
Environmental considerations (exhaust-emissions control) 519
Environmental considerations (exhaust-gas aftertreatment) 521
Environmental considerations (exhaust-gas recirculation/EGR) 519
Environmental considerations (hybrid drives) 581
Environmental considerations (Lambda closed-loop control) 522
Environmental considerations (soot filters) 451
Environmental considerations (three-way catalytic converter) 522
Environmental stresses on automotive equipment 364
Environmental stresses on the motor vehicle 364
EON, see engine octane number 239
EON, see Enhanced Other Network 788
Epitrochoids (rotary engines) 426
Equalizers (car radio) 788
Equilibrium boiling point (brake fluid) 247
Error detection (CAN) 886
E-series (electrical components) 145
ESP, see Electronic Stability Program 701, 704, 803
Ethanol 190
Ethanol as fuel 516
Ethylene glycol 249, 430
EU requirements (braking systems) 650
Euler's Formula 146
Eureka "147-DAB system" 789
Euro test (exhaust-gas emissions) 528, 562
Evaporation loss, fuel 528
Evaporative emissions control system (fuel) 508
Evaporative-emissions testing 526
Excess air (diesel engines) 382, 560
Excess-air factor (Lambda) 458
Excess-air factor (Lambda) control 522
Excitation (alternators) 875
Excitation (DC machines) 132

PETITIONER'S EXHIBIT 1002
US PATENT NO. 6,557,540

Excitation (EC/electronically commutated motors) 134
Excitation diodes (alternators) 875
Exhaust gas 515, 518, 560
Exhaust pipes 448
Exhaust valves 385, 408
Exhaust-flap brakes 683
Exhaust-gas components 518
Exhaust-gas emission control 519, 560
Exhaust-gas emission limits 533, 563
Exhaust-gas recirculation (EGR) 435, 501, 519
Exhaust-gas system 448
Exhaust-gas testing 526, 561
Exhaust-gas testing equipment 532, 566
Exhaust-gas treatment 509, 521, 561
Exhaust-gas turbocharger (ATL) 392, 442
Exhaust-gas testing cycles 528, 562
Extension spring 292
External combustion 424
External EGR 520
External fuel-mixture control 367
External resistance to vehicle motion 337
External safety (vehicles) 727
External thread (pipes) 318
Eytelwein equation (friction) 306

F

Fabric-base laminates 219
Facet reflectors 743
Fading (brakes) 682
Failure mode and effects analysis (FMEA) 150, 165
Fan drives 827
Fanfare horns 766
Fans (radiator) 432
Farad (unit) 17
Faraday's Laws 64
Fastback (crosswind characteristics) 350
Fatigue limit (steel screws/bolts) 311
Fatigue limit under alternating bending stress 46, 193
Fatigue limit under completely reversed stress 46
Fatigue limit under pulsating stress 46
Fatigue resistance (springs) 291
Fatigue strength of structure 47
Fault memory, 507, 671
Fault-tree analysis (FTA) 166
FE model (self-steering characteristics) 359
Federal Test Procedure (FTP 75) 529
FEM, see Finite Element Method 326
Ferromagnetism 68
Ferromagnets and ferrimagnets 184
FET, see Field-effect transistor 79
Fiber composite materials 183
Fiber-optic sensors 95
FID, see Flame ionization detector 562
Field constant, electrical 61
Field strength, magnetic 68, 73
Field, electrical 61
Field, electromagnetic 60
Field, magnetic 67, 71
Field-dependent resistors 104
Field-effect transistor (FET) 79
Filler metals (high-temperature brazing) 213
Film (substrate) potentiometers 96
Film circuits 87
Filter method (exhaust soot removal) 566
Filterability (diesel fuels) 241
Filters, air 438
Filters, color 139
Filters, diesel fuel 437
Filters, edge, see filters, oil 411
Filters, inline 436
Filters, oil 411
Filters, soot 451
Final compression pressure (FCP) 423
Final controlling elements (control engineering) 168
Final drive ratio (passenger-car specifications) 899
Final-drive units 602
Fine-pitch thread (metric) 317
Finite Element Method (FEM) 326
Finned-tube radiator systems 430
Firing order (IC engines) 395
Fischer-Tropsch synthesis 243
Fittings 318
Fixed-caliper disc brakes 657, 681
Flame hardening 269
Flame Ionization Detector (FID) 562
Flashing frequency 759
Flashing signals 760
Flashpoint (fuels) 230, 242
Flat pintle nozzles 555
Flat-base rims 624
Flatbed body structures (commercial vehicles) 735
Fleet fuel consumption (test cycles) 530
Flexible-disc couplings 602
Float angle (vehicle dynamics) 354, 358, 705
Float angle 355
Float chamber (carburetors) 461
Float glass process 774
Floating car data (traffic telematics) 799
Floating-caliper disc brakes 657, 681

PETITIONER'S EXHIBIT 1002
US PATENT NO. 6,557,540

Floodlamps 763
Flow curves 232
Flow improvers (diesel fuel) 243
Flow meters 115, 474
Flow pressure 230
Flow rates in lines 817
Flow volume (calculation) 41
Flow with change in cross section 41
Flow-control valves (automotive hydraulics) 820
Flow-type pumps 456
Fluid friction 329
Fluid mechanics 41
Fluid-friction clutch, VISCO® 432
Flux (soldering) 321
Flux density, magnetic 67
Flux, magnetic 68
Flyweight (mechanical) governors (diesel engines) 538
Flywheel ring gears 571
Flywheels, dual-mass (clutch) 590
Flywheels, hybrid drive 581
FMEA, see Failure Mode and Effects Analysis 150, 165
Foam, energy-absorbing 723
Focal length (reflector) 739
Fog lamps 755
Fog warning lamps (rear fog lamps) 762
Force 15
Force limitation (power windows) 812
Force of attraction 37
Force sensors 112
Force units, conversion 24
Forced-feed lubrication 410
Forked-pipe radiators 434
Form factor (vibration) 31
Forward-control cab 735
Föttinger converter 592
Four-channel ABS system 660
Four-circuit protection valves 676
Fourier series (definition) 29
Four-layer diodes 81
Four-stroke process (IC engines) 385
Fracture toughness 180
Frame junctions (commercial-vehicle chassis) 734
Frames (passenger cars) 722
Free fall 36
Frequency (definition) 29
Fresh gas, fresh charge 385, 453
Fresnel optics 757
Fretting corrosion 259
Friction 39, 329
Friction between solids 233, 329
Friction clutches 590
Friction force 329
Friction hardening 269
Friction modifier (lubricants) 230
Friction welding 321
Frictional power 329
Front airbag systems 803, 805
Frontal impact 727, 737
FTA, see Fault Tree Analysis 166
FTP 75, see Federal Test Procedure 529
Fuel cells (reaction equations) 586
Fuel cells 584
Fuel consumption 21, 336, 721, 866, 899
Fuel conversion (degree of) 370
Fuel delivery 455, 508
Fuel distributor, K-Jetronic 468
Fuel evaporation 506
Fuel filters 436
Fuel injection 379, 534, 560, 563
Fuel injectors 468, 473, 476, 509
Fuel pumps 455, 460
Fuel pumps, in-tank 457
Fuel regeneration (fuel cell) 585
Fuel vapor 472
Fuel-consumption graph (IC engines) 336
Fuel-delivery control 536
Fuel-delivery measuring methods 553
Fuel-injection pumps, axial-piston distributor-type (VE), mechanically governed 535, 543
Fuel-injection pumps, distributor-type 535, 543
Fuel-injection pumps, in-line 535
Fuels (basic requirements) 335
Fuels (essential data) 239, 246
Fuels (properties) 244
Fuels 238
Fuels for SI engines (gasoline) 238
Fuel-supply pumps (diesel engines) 536, 543
Fuel-supply shutoff 377
Full-depth teeth (gears) 301
Full-flow oil filters 411
Full-throttle fuel enrichment 470
Fully automatic transmissions 597
Fully developed deceleration 648
Fusion welding 321

G

Galvani potential 74
Galvanic cells 64
Galvanic effects 75
Galvanic interference coupling 894
Galvanomagnetic effects 98
Gap reflectors 739
Gas discharge 75, 744

PETITIONER'S EXHIBIT 1002
US PATENT NO. 6,557,540

Gas exchange 366, 384
Gas force (IC engines) 396
Gas forces (reciprocating-piston engines) 396
Gas friction 329
Gas generators (airbag) 809
Gas lasers 328
Gas turbines (IC engines) 366, 428
Gas velocity (calculation) 418
Gaseous-discharge lamps 139, 744
Gasoline (SI) engines 372
Gasoline 238, 244
Gasoline direct injection 373
Gasoline filters 436
Gasoline injection systems 463
Gasoline, see Fuels 238
Gas-shielded metal-arc welding 321
Gassing voltage (lead-acid battery) 873
Gate arrays 87
Gaussian distribution 157
Gear motors and gear pumps (automotive hydraulics) 817
Gear pair with modified center distance 299
Gear pair with reference center distance 299
Gear qualities 299
Gear shifting 594, 899
Gear teeth 296
Gear transmissions 590
Gear types of 297
Gears 296
Gearset (seat adjustment) 814
Gel-type greases 230
General surface corrosion 258
General-purpose batteries 865
Generation of electrical energy (automotive electrical system) 874
Geometric Series 147
Geometrical deviations (tolerances) 280
Geometrical moments of inertia 49
Glare (lighting) 739
Glass ceramics 265
Glasses (materials) 182
Glass-mat-base laminates 219
Glazing 725
Glow plugs 568
Glow sequence 570
Glow-control units 569
Glycol (Glysantin®), see Ethylene glycol 249, 430
Glycol-ether fluids (brakes) 248
Golden section (continuous division) 147
Gough map (tire performance) 634
Governors (diesel engines) 538, 543
Governors, combination (diesel engines) 539
Governors, RQ-, RQV-, RSF-, RSV-< 539
Governors, variable-speed 538
Graded-index optical fiber 141
Gradient sensors 104
Graphical display (instrument cluster) 784
Graphics module (motor vehicles) 781
Graphite (lubricants) 231
Gravitation 37
Gravity braking systems 645
Grooved friction bearing 283
Ground electrode (spark plugs) 483
Grounding points (motor vehicles) 856
Guldin's Rule (Pappus theorem) 148
Gunn oscillators 101

H

H point (hip point) 718
Half-value width (oscillations) 30
Hall effect 74
Hall principle (ignition pulse generator) 490
Hall sensors 103, 107
Hall-effect IC 98
Hall-effect vane switches 103, 107
Halogen lamps 139
Hard metals 195
Hard soldering 321
Hardening 268, 273
Hardness 274
Hardness, Brinell 275
Hardness, Knoop 278
Hardness, Rockwell 274
Hardness, scleroscope 278
Hardness, Shore 278
Hardness, Vickers 276
Hazard-warning flashers 760
HB measurement method (Brinell hardness) 275
HC, see Hydrocarbons 244, 518
Headlamp adjustment 750
Headlamp aiming devices 752
Headlamp cleaning systems 755, 772
Headlamp leveling controls (vertical-aim control) 754
Headlamp systems 740
Headlamps 138, 739
Head-up display (HUD), instruments 785
Heat 56
Heat balance (Stirling engines) 425
Heat exchanger (gas turbine) 428
Heat of evaporation (materials) 181
Heat of fusion, specific 181
Heat range (spark plugs) 484
Heat requirements (dwellings) 57

PETITIONER'S EXHIBIT 1002
US PATENT NO. 6,557,540

Heat transfer 56
Heat treatment (metals) 268
Heatable safety glass 775
Heat-absorption glass 775
Heated lambda sensors 524
Heating (motor vehicles) 776
Heating, catalytic converter 505
Heat-transfer coefficients 57
Heavy metals 195, 198
Heavy-duty (HD) batteries 870
Helical gears 298
Helical springs 292, 618
Helmholtz resonator 451
HF eddy-current sensors 97
High beam (headlamps) 747, 749
High-lubricity oils 236
High-pressure fuel-injection pumps 536
High-pressure lubricants 230, 231
High-pressure metal-diaphragm sensors 112
High-pressure pumps 508, 536, 543, 551
High-voltage distribution 492
High-voltage supply (ignition) 487
Histogram (statistics) 156
Hoist controls (agricultural tractors) 825
Hole (electron gap) 76
Hole-type nozzles 556
Holography 142
Homofocal reflectors 741
Homogenous operation mixture formation 464
Hooke's Law 43
Horns 766
Horsepower (conversion) 25
Hot immersion priming 265
Hot-film air-mass flow meters 116, 475
Hot-wire air-mass flow meters 116, 474
Humidity sensors 118
Hump (wheel rims) 624
Hybrid circuits 87
Hybrid electric bus 583
Hybrid engines 383
Hybrid power units 581
Hydraulic power potential (CRS) 552
Hydraulic accumulators (automotive hydraulics) 827
Hydraulic cylinders (automotive hydraulics) 816, 822
Hydraulic cylinders (suspension systems) 615
Hydraulic diaphragm accumulators 619
Hydraulic level-control systems 613
Hydraulic modulators (ABS) 661, 665, 671, 712
Hydraulic motors 816
Hydraulic pumps 816
Hydraulic systems for tractors 824
Hydraulic valves 820
Hydraulic-fluid control (hydropneumatic suspension) 616
Hydrocarbons (exhaust-gas emissions) 518
Hydrocarbons (properties) 244
Hydrodynamic plain bearings 282, 284
Hydrodynamic retarders 684
Hydrodynamic torque converters 129, 342, 591
Hydrodynamics 233
Hydrogen (properties) 245
Hydrogen accumulators (fuel cells) 585
Hydrogen as fuel (SI engines) 517
Hydrogen storage medium (fuel cell) 585
Hydromechanical efficiency 816
Hydropneumatic springs 613, 619
Hydrostatic drives (automotive hydraulics) 830
Hydrostatic energy converters 129
Hydrostatic press 41
Hydrostatic steering 642
Hysteresis loop 68
Hysteresis loss 68
Hysteresis, braking system 647

I

IC, see Integrated Circuit 82
Ice crystallization point (glycol-water mixtures) 249
Ideal combustion cycle (IC engines) 369
Identification lamps, rotating flashing 763
IDI (indirect injection) diesel engines 535
Idle-speed control 470, 491, 505, 538
Ignition 374, 452, 477
Ignition chambers 374
Ignition coils 481, 487, 492
Ignition distributors 488
Ignition energy, ignition spark 480
Ignition maps 494
Ignition point 389, 478
Ignition spark 477
Ignition spray process (multifuel engines) 384
Ignition systems 479
Ignition systems, overview 520
Ignition systems, electronic 493
Ignition timing and adjustment 478, 489
Ignition voltage 477
Ignition-advance angles 479, 504
Ignition-advance mechanisms 489
Ignition-triggering sensors 104
Illuminance 140

PETITIONER'S EXHIBIT 1002
US PATENT NO. 6,557,540

Image sensors 122
Impact detection (airbag) 805
Impedance, electrical 65
Incandescent lamps 139
Inch (conversion) 19
Incomplete combustion 518
Increment systems (ignition) 494
Independent suspension 623
Inductance (coils) 65, 73
Induction hardening 269
Induction period (lubricants) 231
Induction principle (ignition pulse generator) 490
Induction-type pulse generator (ignition distributor) 490
Inductive sensors 103
Industrial trucks 575
Inert gas welding 321
Inertia of bodies 38
Inertia of plane areas 49
Inertia reel (seat belts) 729
Inertia-drive starters 572
Inertial forces (crankshaft assemblies) 397
Inflation pressures (tires) 631
Infrared method (emissions testing) 532
Infrared system (vehicle immobilizer) 769
Inhibitors (in lubricants) 231
Inhibitors, corrosion 267
Inhibitors, vapor-phase (VCI, VPI) 267
Initial-sample testing 152
Injection pumps (diesel) 534
Injection pumps (diesel), electronic control 541, 544
Injection-pump test benches (diesel) 552
In-line control-sleeve fuel-injection pumps 542
In-line engines (definition) 394
In-line fuel-injection pumps 535
Inorganic materials 182
Inspection planning (quality assurance) 153
Instrument clusters (motor vehicle) 780
Instrument lighting 783
Instrumentation (motor vehicle) 780
Insulating materials, properties of 216
Insulator (spark plugs) 483
Insulators 76
Intake manifolds (carburetors) 460
Intake runners, variable length 391
Intake stroke 374, 386
Intake systems (contamination inhibitors) 241
Intake valves 385, 408
Intake-air cooling 561
Intake-noise damping 439
Integral timing devices (diesel injection) 541
Integrated circuit (IC) 82
Integrated on-board diagnostics (OBD) 506
Integrated sensors 95
Intercrystalline corrosion 259
Interference (vibration and oscillation) 30
Interference coupling (EMC) 894
Interference (automotive electrical system) 890
Interference model (EMC) 894
Interference sources (automotive electrical system) 890
Interference suppression 890
Interior dimensions (passenger cars) 718
Interior noise level (motor vehicles) 53
Interior trim 725
Intermittent duty (electric machines) 135
Internal A/F mixture formation 367 464
Internal combustion (IC) 366
Internal exhaust-gas recirculation (EGR) 520
Internal safety (vehicle body) 727
Internal threads (pipes) 318
Internal-combustion (IC) engines (calculation equations) 417
Internal-combustion (IC) engines 366
Internal-gear pumps 455
Interphase reactions (corrosion) 256
Interval (acoustics) 51
Intrinsic conduction of semiconductors 76
Involute teeth 296
Ionic-current measurement procedure (spark plugs) 484 <
Iron losses, alternator 881
ISO metric screw threads 317
ISO tolerance classes 279
IU characteristic (battery charging) 870, 873

J

Jackknifing 361
Jake brake (engine brake) 683
Japanese test cycle (emissions testing) 531, 563
Joining and bonding techniques 319
Joule cycle (gas turbines) 428
Jump characteristic (Lambda oxygen sensors) 523
Junction field-effect transistors 79

K

Kármán vortex path 115
Kármán vortex volumetric flow meter 475
KE-Jetronic 469

PETITIONER'S EXHIBIT 1002
US PATENT NO. 6,557,540

Kelvin 12, 17 (conversion) 26
Kick-down switch (automatic transmissions) 598
Kilogram (definition) 12, 14
Kinematic viscosity 232
Kinetic energy 35
Kingpin angles 621
Kingpin offset 620, 621, 639
Kirchhoff's first (current) law 62
Kirchhoff's Laws 62
Kirchhoff's Second Law 62
K-Jetronic 467
Knock (diesel engines) 383
Knock control 491, 496, 506
Knock inhibitors (fuels) 239
Knock sensors 108, 497
Knot (unit of speed) 15
"K" shape (vehicle bodies), Drag coefficient (c_W) 340
K-values (screw-thread friction) 314

L

Lambda closed-loop control 469, 473, 505, 522
Lambda oxygen sensors 117, 523
Laminar flow (hydraulics) 817
Laminated composite materials 183
Laminated safety glass (LSG) 774
Laminates (materials) 219
Lanchester balancing system (crankshaft) 401
Laser cutting 328
Laser technology 141, 328
Lateral dynamics (motor vehicles) 350, 705
Lateral force (tires) 634, 659
Lateral runout (wheels) 626
Law of continuity (magnetic flux) 71
Law of induction 72
Layered mixture formation 464
Lead-acid batteries 576, 866
Leaded gasoline 238
Leaf springs 290, 618, 622
Leakage coefficient, magnetic 71
Lean misfire limit (SI engines) 458
Lean-burn (oxygen) sensors 524
Lean-burn catalytic converters 374
Lean-burn control (exhaust-gas emissions) 523
Lean-burn engines 520
Leclanché cells 64
LED, see Light-Emitting Diode 143
Legal units 13
Lens (lighting systems) 748
Level-control systems (air suspension) 613
Lever law 37
License-plate lamps 761
Life factor (gears) 303
Lifting-axle control 614
Light distribution patterns (vehicle headlamps) 744
Light-Emitting Diode (LED) 143
Light metals 199
Light sources 139
Light transmittance (automotive windshield and windows) 775
Light/dark cutoff line (low beam) 741
Light-alloy wheels 625
Lighting source (instrument cluster) 783
Lighting techniques 738
Lights and lamps (motor vehicles) 757
Limit stresses 45
Limit-current principle (Lambda oxygen sensors) 524
Limited-slip differentials 590, 604
Limiting field strength 68
Limp-home mode (engine management) 507
Line filters 436
Linear bus structure (CAN) 884
Linear coefficient of expansion 181
Lines of flux (magnetic field) 72
Liquefied Petroleum Gas (LPG) 245, 251, 512
Liquid Crystal Display (LCD) 143
Lithium-based batteries 576
Litronic 744
L-Jetronic 471
Induction period (lubricants) 231
Intercooling 433, 561
Load control (SI engines) 376
Load dump (voltage peaks) 882
Load index (tires) 631
Load ranges (IC engine) 509
Load sensing, see Directional-control valves 820
Load-bearing capacity (gears) 302
Load-bearing capacity (rolling bearings) 289
Load-bearing components (vehicle bodies) 723
Load-change shock damping 506
Load-levelling systems (air suspension) 613
Loads, permissible 45
Lock nuts 313
Locking devices (threaded fasteners) 310
Logarithmic decrement (definition) 30
Logic circuits 84
Logic devices, programmable (PLD) 87

PETITIONER'S EXHIBIT 1002
US PATENT NO. 6,557,540

Long-distance coaches (bodywork) 736
Longitudinal elements 108
Long-term stability (Lambda closed-loop control) 525
Lorentz force 61, 125
Loudness (acoustics) 54
Loudness level 54
Lower beam (headlamps) 740, 749
Low-temperature sludge (lubricants) 231
LPG, see Liquefied Petroleum Gas 246, 251, 512
Lubricants 230, 333
Lubricating greases 236
Lubricating varnish 230
Lubrication 410
Lubricity 242, 333
Luminance 140
Luminous efficiency 140
Luminous emittance, specific 140
Luminous energy (definition) 140
Luminous flux 140, 740
Luminous intensity (definition) 140

M

M+S tires (winter tires) 628
Mach number (speed of sound) 21
Machine capability (quality assurance) 153
Machines, electrical 132
Magnesium alloys 199
Magnetic flux (magnetic field) 71
Magnetic materials 183
Magnetic quantities 18, 60, 67
Magnetic sheet steel and strip 184, 204
Magnetic-field sensors 103
Magnetization curves 70
Magneto-elastic bearing-pin sensors 112
Magnetoresistive sensors 100
Magnets, ceramic 210
Magnets, metallic 209
Main headlamps 740, 749
Main headlamps, American system 749, 753
Main headlamps, European system 740, 749
Main jet (carburetors) 461
Maintenance-free batteries 868
Major dimensions (passenger cars) 718
Major exhaust-gas components 518
Malleable cast iron 193
Manifold-pressure compensator (LDA) 540
Manipulated variables (control systems) 168
Manually-shifted transmissions 593, 597
Manufacturing accuracy 164
Martensitic iron microstructure 268
Material groups 182
Material parameters 180
Material terminology 180
Material-content curve (tolerances) 281
Materials (permanent magnet) 209
Materials (rolling bearings) 289
Materials, cast iron 193
Materials, ceramic 217
Materials, electrical engineering 215
Materials, gear 305
Materials, laminated 219
Materials, non-ferrous 198
Materials, plastic 220
Materials, sinter metal 200, 207
Materials, soft magnetic 203
Materials, steel and malleable cast iron 193
Mathematics 144
Maximum permeability 181
Maximum speed (passenger-car specifications) 899
Maximum-speed governors (diesel engines) 538
McPherson strut (suspension linkage) 623
ME Motronic 498
Mean pressure (gasoline engines) 376
Mean Time To Failure (MTTF) 166
Measurement (basic terms) 164
Measuring chambers (exhaust-gas emissions) 532
Measuring techniques (EMC) 894
Mechanical (flyweight) governors 538, 543
Mechanical supercharging 391
Mechanics, basic equations 34
Mechatronics 92
MED-Motronic 464, 507
Message format (CAN) 885
Metal adhesives 322
Metal catalytic converters 449
Metal soaps 231
Metal-ceramic bearings 287
Metal-hydride tanks 517
Metallic coatings 229
Metal-oxide semiconductors (MOS) 79
Metals 76, 182
Meter (definition) 12
Metering pumps (steering cylinder) 642
Methanol (fuels) 516
Methanol (properties) 244
Methanol reforming (fuel cells) 585
Microcomputer performance 172
Microcomputers, microprocessors 84, 172, 498
Micromechanical pressure sensors 89
Micromechanics 89
Mineral oils (lubricants) 231

PETITIONER'S EXHIBIT 1002
US PATENT NO. 6,557,540

Mineral-oil fluids (brakes) 249
Miniaturization concepts (sensors) 95
Minibus (definition) 716
Minor components (exhaust gas) 518
Mixed friction 233, 329
Mobile communications (CAN) 884
Mobile radio 800
Modal analysis (vibrational characteristics) 33
Module series (spur and bevel gears) 300
Modulus of elasticity 42
Moldings (vehicle components) 723, 725
Mole (unit), definition 12
Molybdenum disulphide 237
Moments of inertia (crankshaft assemblies) 397
Monitoring system (ESP) 712
Mono-Jetronic 465
Monolex sloping-bead seat wheels 626
Monolith, ceramic 449, 521
Monolithic integration 82
MOS field-effect transistors 79
MOS, see metal-oxide semiconductors 79
MOSFET, see MOS field-effect transistors 79
Motion, rectilinear 34
Motive force 342
Motive power of vehicles 342
Motor octane number (MON) 239
Motor vehicle (definition) 716
Motor vehicles (classification systems) 716
Motor vehicles 334
Motorcycle tires 596
Motorcycles (definition) of 716
Motors, wiper-system 772
Motor-vehicle definitions 716
Motronic 498
Moulding compounds (plastic) 220
Moving-magnet ratiometer 782
MSR, see Engine drag-torque control 608, 708
"M" system (diesel engines) 380
MTTF, see Mean Time To Failure 166
Mufflers 448, 450, 692
Multi-circuit braking systems 645
Multifocal reflectors 741
Multifuel engines 384
Multifunction regulators (automotive electrical system) 882
Multigrade oils 231, 236
Multilayer bearings 283
Multilayer ceramic substrates 87
Multi-leaf springs 290
Multi-line braking systems 646
Multi-master principle (CAN) 884
Multimode (MM) fibers (optical waveguides) 141
Multi-piston power units 394
Multiplate overrunning clutches (starters) 573
Multiple injection (CRS) 552
Multiple-orifice nozzles (combustion process) 379
Multiple-ratio transmissions 592, 593
Multiplex application (CAN) 884
Multipoint fuel-injection systems 463, 467
Multi-purpose passenger cars (definition) 716
Multipurpose trucks (definition) 716
Multistage turbochargers 445
Muscular-energy braking systems 640, 645

N

Narrow V-belts 307
Narrow-band interference (EMC) 891
Natural frequency (definition) 29
Natural frequency of vibration absorbers 32
Natural gas as fuel 512
Natural gas (characteristics) 245
Natural gas, operation on (SI engines) 515
Natural materials 183
Natural-gas engines 515
Navigation systems, vehicle 796
Needle-motion sensors 542
Networked vehicle systems 887
Neutral cornering 355
Newton (unit) 12, 15
Newton's Law 12
Newtonian fluids 232
Nickel-based batteries 576
Nitriding and nitrocarburizing 272
Nitriding of iron 272
Nitrogen oxides (NO_X) in exhaust 518, 560
Nitrogen-oxide emissions 479, 518, 560
NMOG emission limits 533
Noble metals (corrosion) 258
Noble-metal catalytic converters (diesel engine) 561
Noise (alternators) 881
Noise (diesel engines) 383
Noise (passenger-car differential) 603
Noise (stationary vehicle) 52
Noise damping 439
Noise design 55
Noise emissions (motor vehicles) 52
Noise levels 51
Noise levels, perceived 54
Noise limits (motor vehicles) 52
Noise reduction 51
Noise, diesel engine 383

PETITIONER'S EXHIBIT 1002
US PATENT NO. 6,557,540

Nominal capacity (batteries) 868
Nominal/Net/Useful power (definitions) 415
Non-conductors 76
Nonferrous metals 198
Non-laminated toughened safety glass 774
Non-metallic materials 217
Non-methane organic gas (NMOG) 533
Non-volatile memories 84, 173
Normal (Gaussian) distribution 157
Normalizing 273
Notch effect (strength) 44
NO_X, see nitrogen oxides 518, 560
Nozzle shapes 556
Nozzle-opening pressures 558
Nozzles and nozzle holders 554
Nozzles, throttling-pintle 554
NPN transistors 79
Number of teeth spanned (gears) 298
Number systems 144
Numerical aperture (NA) 142

O

OC (open center) directional control valves 820
Occupant safety systems 727, 729, 803
Occupant-classification mat 810
Octane rating (antiknock quality) 238
Octave band spectrum 51
Off-board testers (engine) 511
Off-road tires 628
Ohm's Law 62, 66
Ohmic resistance 62
Oil control rings (piston) 404
Oil coolers 434
Oil filters 411
Oil separation 230
Oil-bath air filters 439
On-board diagnosis (OBD) 511
Opacity measurement (exhaust soot) 566
Open center (hydraulic systems) 820, 824
Open control loops (control engineering) 167
Open process (combustion) 366
Open-circuit potential (corrosion) 257
Opening control (power sunroof) 813
Opening pressure (injectors) 558
Open-loop operation (vehicle handling) 354
Operating temperature, battery systems 576
Operation on alcohol (spark-ignition engines) 516
Operational amplifiers (OP) 93
Opposed-piston engines 394
Optical fibers (optical waveguides) 141
Optical fibers 141
Optical properties (windshield and window glass) 775
Organic materials 183
Orientation (vehicle navigation systems) 796
Oscillation gyrometers 105
Oscillations (types) 612
Outflow volume (calculation) 41
Output power (hydraulic pumps) 816
Outside diameter (spur gears) 298
Overall contact area (spur gears) 298
Overall efficiency (IC engines) 370
Overland bus (definition) 716
Overlap ratio (gears) 298
Overrun fuel cutoff 470, 505
Overrunning clutch, radial-tooth (starters) 573
Overrunning clutch, roller-type (starters) 573
Overrunning-clutch systems (starters) 573
Oversteer 352, 355
Overturning test 728
Overvoltage protection (automotive electrical system) 882
Overvoltage protection, Z-diode (alternators) 883
Oxidants (exhaust-gas pollutants) 518
Oxidation catalytic converters 448, 521
Oxygen concentration sensors 117

P

Painting (body shells) 724
Painting (corrosion protection) 266
Paints (automotive) 228
Panhard rod 622
Paper air filters 38
Paper sizes 20
Paper-base laminates 219
Paraffin precipitation (diesel fuel) 437
Parallel connection 66, 133
Paramagnetism 68
Paramagnets 184
Park Pilot warning coverage 793
Parking lamps 761
Parking systems 791
Parking-brake systems 644, 682
Parking-brake valves 690
Partial throttle efficiency 375
Particle composite materials 183
Particle velocity (definition) 29
Particulates in exhaust gas (measurement) 562
Part-load behavior 414
Passenger car (definition) 716

PETITIONER'S EXHIBIT 1002
US PATENT NO. 6,557,540

Passenger cars 716, 718
Passenger-car air filters 438
Passenger-car bodies 718
Passenger-car dimensions 719
Passenger-car engine-cooling systems 430
Passenger-car tires 628
Passenger-car transmissions 594
Passenger-car types 900
Passenger-compartment surveillance 810
Passing/overtaking 348
Passive safety (vehicles) 727, 737
Peak factor (vibration/oscillation) 31
Peltier effect (thermoelectrics) 74
Pendelum motion 35
Pendelum-motion oscillation amplitudes (motor vehicles) 361
Penetration (lubricants) 231, 234
Perceptibility safety 726
Perforated-pipe silencers 451
Perforating (lasers) 328
Periodic system of elements 179
Peripheral pumps 456
Peripheral testing (engines) 510
Peripherals (microcomputers) 86
Permanent magnets 69, 183
Permanent magnets, rare-earth type 580
Permanent-field starters 571
Permanently-excited synchronous drives 580
Permanent-magnet excitation 132
Permanent-magnet materials 69, 185, 209
Permeability 68, 181
Permissible voltage drop (wiring) 859
Perpendicularity tolerance 279
PES fog lamps 756
PES headlamps 743
Phase displacement angle φ 65
Phon 54
Phonetic alphabets 897
Phosphatizing 264
Photocells, see solar cells 81
Photodiodes 78
Photometers (exhaust-gas emissions) 567
Photometric quantities and units 18, 137, 140
Photovoltaics 81
Physiology of vision 140
PI code, see Program identification number 787
Piezo-ceramic sensors 108
Piezoelectric sensors 105, 108
Pilot injection (diesel engines) 546, 552
Pinion-engaging drive (starters) 571
Pinions (starters) 571
Pipe threads 318
Piston accumulators, hydraulic 619, 826
Piston and crankshaft assembly of the reciprocating-piston engine 394
Piston motors (automotive hydraulics) 818
Piston movement 417
Piston pressure (calculation) 419
Piston pumps (automotive hydraulics) 818
Piston rings 404
Piston velocity 417, 422
Pistons 404
Piston-type fuel-supply pumps 536
Pitch (perceived pitch levels) 54
Pitch (suspension systems) 613
Pitch circle diameter (spur gears) 298
Pitch diameter (conversion) 301
Pitot-tube air-flow sensors 115
Pitting corrosion 258
Plain (sliding) bearings 282
Planetary-gear sets 571, 593
Plasma polymerisation 267
Plastic flow behavior (lubricants) 232
Plastics (trade names) 226
Plastics 183
Plating 265
PLD, see. Programmable Logic Device 87
Plunger-and-barrel assemblies 536
Plunger-type sensors 97
Ply rating, PR number (tires) 630
Pneumatics, automotive 832
PN-junction (semiconductors) 77
Poisson approximation and distribution 163
Polar substances (lubricants) 231
Polarisation, electrical 61
Polarisation, electrolytic 64
Polarisation, magnetic 68, 181
Pollutant emissions, see exhaust gases 513, 518
Poly-Ellipsoid System (PES) 743
Polymer bearings 286, 288
Polytropic exponent 375, 382
Populations (technical statistics) 156
Port-closing sensors 540
Position sensors 96
Positional tolerance 279
Positive belt drives 309
Positive-displacement pumps 455
Positive-displacement superchargers 392, 440
Post-start phase 470, 505
Potential, diffusion 77
Potential, electrical 17, 61
Potentially susceptible devices (EMC) 893
Potentiometers 96
Pourpoint (lubricants) 231

PETITIONER'S EXHIBIT 1002
US PATENT NO. 6,557,540

Powder coating (corrosion-protection) 267
Power (mechanical) 35, 40
Power and torque 15, 40
Power controllers (electric drives) 578
Power curves (electric drives) 579
Power curves (IC engine) 413
Power density (actuators) 130
Power density (motor vehicles) 334
Power factor cos φ 64
Power output (electric drives) 578
Power output (IC engines), definition 414
Power output efficiency (SI engines) 377
Power output per liter, see Power per unit displacement 418, 899
Power output per unit (passenger-car specifications) 899
Power per unit displacement, see Power output per liter 418, 899
Power take-offs (commercial-vehicle transmissions) 595
Power take-up elements 590
Power units, electric vehicle 578
Power units, hybrid 581
Power units, hydrostatic 827
Power-assisted steering 640
Power-brake systems 645, 674
Power-line frequencies (AC) 65
Power-steering systems 640
Power-window drives 812
Power-window motors 812
PR numbers (tire identification) 630
Prechamber systems (IC engines) 381
Precipitation hardening 273
Precrash sensing 811
Pre-engaged-drive starters 572
Preferred numbers 145
Premium-grade gasolines 238
Presentation of measured values (engineering statistics) 156
Pressure build-up time (brakes) 347, 647
Pressure control (brakes) 687
Pressure control valves 509, 696
Pressure in fuel system 455
Pressure plate (clutch) 590
Pressure point (vehicle side-wind characteristics) 350
Pressure regulator (fuel supply) 471
Pressure sensors 89, 109, 509
Pressure units (conversion) 24
Pressure units 16
Pressure vs. volume work diagram 367
Pressure-control valves (automotive hydraulics) 821
Pressure-relief valves (automotive hydraulics) 821
Pressure-wave chargers 446
Pressure-wave supercharging 393
Pressurized (Tox) clinching 323
Primary current limitation (transistor ignition) 491
Primary retarders 684
Printed circuit board (pcb) technology 88
Prisms (technical optics) 138
Probability (statistics) 158
Process capability (quality assurance) 153
Production-planning phase 152
Program identification number (PI code) 787
Program Type (PTY code) 788
Programmable Logic Devices (PLD) 87
Progression system (carburetors) 461
Project specifications manual (quality) 150
Projected vehicle cross-sectional area 721
PROM 84
Propane, LPG 192, 245, 512
Properties of fuels 244
Properties of gases 192
Properties of liquids 190
Properties of metals 193
Properties of solids 186
Proportional valves, electrical 821
PTC, see Thin-film metallic resistors 119
PTY code, see Program Type 788
Pullman saloon (definition) 716
Pulse generators (ignition) 490
Pulse turbocharging 443
Pulsed arc welding 321
Pump shutoff (diesel engines) 541, 544
Pump timing adjustment 542
Pumps, vane-type 543
Push-rod assemblies (valve timing gear) 408
Pyrometric temperature sensing 119
Pyrotechnical seatbelt tensioners 804

Q

Quadratic equation 147
Quality assurance (QA) 150
Quality audits 150
Quantities (nuclear physics) 18
Quantities and units (overview) 14
Quantity of electricity 17
Quench and draw (steel) 271
Quick solders 321

R

Rack-and-pinion steering 639
Rack-travel sensors 540
Radar sensors 107
Radial crushing strength 180

PETITIONER'S EXHIBIT 1002
US PATENT NO. 6,557,540

Radial engines 394
Radial force of crankshaft assembly 396
Radial runout (vehicle wheels) 626
Radial tires 628
Radial-piston distributor-type fuel-injection pumps 535
Radial-piston machines 818
Radial-ply tires 628
Radial-sleeve bearings 282
Radian measure 146
Radiation, electromagnetic 137
Radio Data System (RDS) 787
Radio remote control (alarm systems) 767
Rain sensors 122
RAM, see Random Access Memory 84
Ram-pipe supercharging 390
Random Access Memory (RAM) 84
Random interval (statistics) 158
Random variable (statistics) 157
Ranges (electric vehicles) 576
Ranges (headlamps) 739
Range-selector box (drivetrain) 595
Rare-earth permanent magnets 580
Rating codes (tires) 631
Rating sound level (noise) 53
RDS, see Radio Data System 787
Reactance 66
Reaction time 346, 647
Reaction torque (brake testing equipment) 702
Reactive power, susceptance, reactance 65
Read Only Memory (ROM) 84
Rear hoisting-gear controls (agricultural tractors) 825
Rear mufflers 451
Rear suspension 620
Rear underride guards 737
Rear-end impact 728
Rear-window wiper systems 771
Reciprocating-piston engines (main components) 404
Reciprocating-piston engines with external combustion 424
Reciprocating-piston engines with internal combustion 369, 394
Recirculating-ball hydraulic steering system 643
Recirculating-ball steering 639
Recirculation cooling systems 410
Recrystallization annealing 273
Rectification value (oscillations) 30
Rectifier diodes 78
Recycling (motor vehicle) 732
Reduction gear (starters) 571
Reduction-type catalytic converters 522
Refinery components (fuel) 239
Reflected-light measurement (exhaust soot) 566
Reflection (light) 138
Reflection mufflers 450
Reflector optics 757
Reflectors 138, 741
Refraction of light 138
Regeneration (soot filters) 451
Regenerator (Stirling engines) 424
Regional identification codes (BK), car radio 786
Regular-grade fuels 238
Relaxation 47
Relays (symbols) 835
Release time (braking systems) 648
Reliability 161, 165
Remagnetization losses 70
Remanence 68
Replaceable Bulb Headlamps (RBH) 749
Research Octane Number (RON) 239
Residual arcing 488
Residual gas (proportion) 385, 453
Residual ripple (automotive electrical system) 890
Resistance measurement 63
Resistance to vehicle motion 337, 588
Resistance welding 319
Resistance, climbing 341
Resistance, cornering 339
Resistance, electrical 62, 66, 215
Resistance, rolling 338
Resistance, wind (aerodynamic drag) 37, 339, 721
Resistive (Lambda) oxygen sensors 524
Resonance (definition) 30
Response time, brake 347, 647
Retard mechanism (ignition) 489
Retardation (braking) 337, 344, 648
Retardation control (EBS) 700
Retarders 595, 684
Return pumps (ABS) 671
Return-flow restriction (delivery valves) 537
Returnless fuel systems 472
Reverse state (pn-junction) 77
Reynolds number (drag coefficient) 37
Rheopexy (lubricants) 232
Ride comfort 612
Rigid axles 622
Rigidity (body structures) 722
Rims (vehicle wheels) 624, 630
Riveting 325
Riveting techniques 323
Rivets 325

PETITIONER'S EXHIBIT 1002
US PATENT NO. 6,557,540

Road trains (definition) 716
Road-map memory (vehicle navigation systems) 797
Road-surface adhesion 343, 663
Road-surface state (coefficient of friction) 343
Rocker-arm assemblies (valve timing) 408
Rocker-arm valve gear 408
Roll angle 354, 355
Roll axis 353
Roll bellows (suspension) 618
Roll center 622
Roll steer 356
Rollback limiters 701
Roller friction 329
Roller-cell pumps 455
Rolling bearings 289
Rolling friction 329
Rolling resistance 338
Rollover bars 809
Rollover protection systems 809
Rollover sensing 809
Rollover tests 728
ROM, see Read Only Memory 84
RON, see Research Octane Number 239
Roof frame (body structure) 722
Rotary actuators 127
Rotary engines 426
Rotary oscillations (vehicle dynamics) 361
Rotating distribution (ignition energy) 482
Rotating flow (combustion air) 378
Rotating mass (crankshaft) 397
Rotating voltage distribution 482, 495
Rotating-solenoid actuator 544
Rotational speed, units 15
Rotocap (valve rotation) 409
Roughness average (tolerances) 281
Roughness profile (tolerances) 281
Route computation (vehicle navigation systems) 797
RPM sensors 103
Rubber elements 771
Rubber suspension 619
Rubberizing 267
Rudge hub 625
Rust formation 259

S

SAE viscosity grades 235
Safety circuits (transmissions) 601
Safety glass 774
Safety margins 348
Safety systems, automotive 803
Safety, commercial-vehicle bodies 737
Safety, passenger-car bodies 726
Salient-pole alternators 878
Saloon/sedan (definition) 716
Sample bags (emissions testing) 527
Sampling (statistics) 156
Saturation polarization 68
S-cam (drum brakes) 646
Scavenging efficiency (gas exchange) 385
Scavenging process (two-stroke process) 388
Schematic diagrams (automotive electrical system) 839
Schottky barrier diodes (Schottky diodes) 78
Scooters (definition) 716
Screw threads 317
Sealed-beam headlamps 749
Seam welding 320
Seat adjustment, electrical 814
Seat belts 729
Seat belts, three-point 729, 803
Seat reference point (seat position) 718
Seat-belt buckle tensioner 804
Seat-belt slack 729
Seat-belt tightener systems 729, 803
Seats 725
Second, unit (definition) 12
Secondary braking systems 644
Secondary retarders (permanent brake) 684
Secondary-air injection 521
Section designations (circuit
Section modulus 42, 49
Seebeck effect (thermoelectrics) 74
Seizing (component wear) 331
Selective catalytic converters 522
Select-low control (ABS for commercial vehices) 693
Self-charging (superchargers) 440
Self-discharging (batteries) 870
Self-excited synchronous alternators 875
Self-induction 72
Self-locking screws 313
Self-steering characteristics (motor vehicles) 355, 359
Semiconductor memories 84, 498
Semiconductor pressure sensors 110
Semiconductors 76
Semi-hollow rivets 325
Semi-noble metals (corrosion) 258
Semi-rigid axles 622
Semi-surface electrode gap (spark plugs) 485
Semitrailers, single-axle ABS 692
Semi-trailing arm 623
Sensor integration levels 95

PETITIONER'S EXHIBIT 1002
US PATENT NO. 6,557,540

Sensors (fundamentals) 94
Sensors, acceleration 107, 808
Sensors, combustion-chamber pressure 111
Sensors, differential 97
Sensors, dirt 121
Sensors, distance (ACC) 714
Sensors, fiber-optic 95
Sensors, force 112
Sensors, gradient 104
Sensors, half-differential 97
Sensors, Hall-effect 103, 107
Sensors, ignition-triggering 104
Sensors, image 122
Sensors, inductive 103
Sensors, integrated 95
Sensors, knock 108, 497
Sensors, magnetoresistive 100
Sensors, oxygen concentration (Lambda) 117
Sensors, piezoelectric 105, 111
Sensors, position 96
Sensors, rain 122
Sensors, short-circuiting ring 97
Sensors, speed 103, 670, 695, 712
Sensors, tangential 104
Sensors, temperature 119
Sensors, thermopile 120
Sensors, thick-film pressure 110
Sensors, torque 112
Sensors, vehicle speed 103
Sensors, vibration 107
Sensors, wheel 796
Separately-excited direct-current drive 578
Series connection 63, 66, 132
Series-wound machines (characteristics) 132
Service life (rolling bearings) 289
Service life, MTTF 166
Service-brake system 644, 699
Service-brake valve 689
Servo cylinders (air brakes) 689
Servo unit for central locking 815
Servomotors, ABS/TCS 611
SFTP cycles 530
Shear modulus (modulus of rigidity) 44
Shearing stress 44
SHED tests (evaporative-emissions testing) 528
Sheet steel (vehicle body) 197
Sheet steel for bodywork 197
Sheet-metal processing 326
Sheet-steel panels 193
Shift programs (automotive transmissions) 600
Shift-point controls 600
Shock-absorbing systems 724
Short-circuiting ring sensors 96
Short-stroke linear motors 127
Short-term performance rating (electric drives) 578
Shunt characteristic 133
Shunt-wound machines 132
SI units 12
Side airbags 807
Side force (tires) 634
Side impact 728
Side members (chassis) 722
Side-channel pumps 456
Sidedraft carburetors 460
Side-impact protection systems 807
Side-marker lamps 761
Siemens (unit) 17
Signal conditioning (ECU) 174
Signal processing (ECU) 174
Signaling devices, acoustic 766
Signs and symbols, mathematical 144
Silicone brake fluids 249
Simulation of environmental factors 364
Sine function 146
Single-arm wipers 770
Single-circuit braking systems 645
Single-circuit steering systems 643
Single-component adhesives 322
Single-leaf springs 290
Single-line braking systems 646
Single-mode fibers (optical fibers) 141
Single-piston power units 394
Single-plunger fuel-injection pumps 535
Single-point fuel-injection systems 463, 465
Single-point injection (SPI) 465
Single-pump systems, time-controlled 548
Single-rotor engines 427
Single-spark ignition coils 481, 495
Single-tube shock absorbers 616
Single-winding rotary actuators 127
Sinter (PM) metals for plain bearings 200
Sintered ceramic resistors (NTC) 119
Sintered materials 285
Sintered metals 182
Sintered metals for soft-magnetic components 185, 207
Sintered metals for moulded components and plain bearings 200
Sintered-metal plain bearings 286, 288
Sinusoidal input (steering angle) 357
Skidpad, steady-state (vehicle testing) 355
Skyhook damping 617
SI units, basic (definitions) 12

PETITIONER'S EXHIBIT 1002
US PATENT NO. 6,557,540

Sliding friction 329
Sliding-gear starters 573
Slip 636
Slip angle 351, 355, 360, 634
Small machines (hydraulic) 819
Smart-power ICs 87
SMD, see Surface Mounted Devices 88
Smoke testers 566
Smoke-emission measurement (diesel engines) 566
Smooth running (reciprocating-piston engines) 396, 545
SMT, see Surface Mounted Technology 88
Soft annealing 273
Soft soldering 321
Soft solders 212
Soft-magnetic materials 184, 203
Soil resistance (agriculture) 363
Solar cells 81
Solar modules 82
Solders (soldering) 212, 321
Solenoid fuel injectors 476
Solenoid valves (ABS) 672
Solenoid-controlled axial-piston distributor pumps 546
Solenoid-controlled distributor injection pumps 545
Solenoid-controlled radial-piston distributor pumps 546
Solenoid-plunger sensors 127
Solid angles (light) 140
Solid lubricants 230
Solid-body laser 328
Solids 186
Solids in exhaust gas 518
Solution, chemical 180
Sommerfeld number (bearings) 282
Sone (loudness) 54
Soot (exhaust gas) 518, 566
Soot emissions 382
Soot filters 451
Sound (general definitions) 50
Sound insulation 51
Spark current 481
Spark plugs 482
Sparking rate (four-stroke engine) 487
Spark-plug designation codes 486
Spark-plug electrode gap 484
Spark-plug temperature response 484
SPC, see Statistical Process Control 154, 160
Speakers (passenger car) 788
Specifications (passenger car) 898
Speed droop (diesel fuel injection) 539, 544
Speedometer, see Instrumentation 780
Speeds (conversion) 21
Speeds, critical 353
Spherical triangle 147
SPI, see Single-Point Injection 465
Spiral torsion springs 291
Splash water 364
Splitter box (drivetrain) 605
Splitter groups (transmission) 595
Spot lamps 763
Spot welding, resistance 319
Spray-injection process (diesel engines) 379
Spring dimensioning calculations 290
Spring plate (clutch) 590
Spring steel 196, 294
Springs 290, 618
Spring-type brake actuator 691
Spring-type brake cylinder 691
Spur gears 297
Spur-gear transmissions 590
Squirrel-cage rotor (asynchronous motors) 135
Squish flow (gasoline engines) 375
SRET principle (corrosion testing) 261
Stability in curves 614
Stabilizer fins 352
Stabilizers (automotive suspension) 619
Standard axis separation (gears) 300
Standard bore 279
Standard deviation (statistics) 157
Standard shaft 279
Standard threads, metric 317
Standardization (CAN) 886
Standing waves 30
Star connection (three-phase AC) 67
Star diagram (crankshaft) 400
Start valves (K-/L-Jetronic) 468, 473
Start-assist systems (diesel engines) 568
Starter batteries 865, 866, 899
Starter gearing 300
Starter motors, see Starters 571
Starter pinions 571
Starter protection 574
Starter relays 574
Starters 571
Starting devices (diesel engines) 540
Starting enrichment (KE-Jetronic) 470
Starting systems 571
Starting temperature 862
Start-locking relays 574
Start-repeating relays 574
State of aggregation (materials) 180
Station wagon (definition) 716
Statistical evaluation 162
Statistical Process Control (SPC) 154, 160

PETITIONER'S EXHIBIT 1002
US PATENT NO. 6,557,540

Statistics 156
Stators (electric machines) 132
Steel (vehicle body panels) 197, 723
Steel 193
Steel springs 618
Steel, cast 193
Steering (safety regulations) 729
Steering and steering behavior 638
Steering angle (abrupt change) 357
Steering angle 355, 705
Steering boxes 639
Steering cylinders 641
Steering kinematics 639
Steering operating force 638
Steering-angle curve (with GMA yaw-moment buildup delay) 663
Steering-angle sensors 101
Steering-axis inclination (steering kinematics) 639
Steering-column adjustment 814
Steering-wheel angle 355
Step input (steering angle change) 357
Step-index optical fiber 141
Stepped reflectors (lighting systems) 741
Stick-slip (lubricants) 230
Stirling engines 424
Stop lamps 761
Stopping distance, stopping time 346
Storage of hydrogen in the vehicle 517
Straight-cut teeth 298
Strain 42, 45, 180
Strainers (oil filters) 411
Strain-gauge resistors 110
Streamlined vehicle-body shape (aerodynamic drag) 340
Streamlined vehicle-body shape (crosswind effects) 350
Strength calculations (vehicle bodies) 731
Strength formula 42
Stress concentration factors (notch configurations) 47
Stress corrosion cracking 259
Stress, mechanical 42, 45
Stress-relief annealing 273
Stribeck curve (lubricants) 232
Stub teeth (gears) 301
Stud welding 321
Suction resonators 451
Sulfur in fuels 240, 243
Sunroof drive units, electrical 813
Superchargers 440
Superchargers, centrifugal 440
Superchargers, Roots 441
Superchargers, rotary-piston 442
Superchargers, sliding-vane 441
Superchargers, spiral-type 441
Supercharging process (IC engines) 390
Supertone horns 766
Supplementary functions (ME-Motronic) 500
Suppression level 892
Surface areas of solids 149
Surface characteristics (tolerances) 280
Surface fatigue 331
Surface hardening (laser technology) 328
Surface hardening 269
Surface hardness 269
Surface micromechanics (OMM) 90
Surface roughness 280
Surface-Mounted Devices (SMD) 88
Surface-Mounted Technology (SMT) 88
Surge control 542, 545
Susceptibility, magnetic 184
Suspension 180, 612
Suspension design elements 613
Suspension systems 613
Swelling-mat mounting (catalytic convertors) 449
Swing axle (suspension linkage) 623
Swirl-chamber systems (IC engines) 381
Switches (symbols) 834
Switching diodes 78
Symmetry tolerance 279
Synchronization 594
Synchronous alternators, self-exc ted 875
Synchronous drive units 134, 580
System circuits (assembled-representation diagrams) 856
Systems of units, physical/technical 13

T

Tachograph 794
Tail lamps 761
Tandem wiper systems 770
Tangential force (crankshaft assembly) 396
Tangential sensors 104
Tapered bead seat rim, 5° (vehicle wheels) 624
Tapered bead seat rim, 15° (vehicle wheels) 624, 626
TAS, see Temperature-dependent starting device 540
Taylor gauge test 279
TC, see exhaust-gas turbochargers 392, 442
TCS, see Traction Control System 606, 710
TD system (vehicle wheels) 625
TDC, see Top Dead Center 385
Technical optics 137
Telematic services 798

PETITIONER'S EXHIBIT 1002
US PATENT NO. 6,557,540

Telescopic shock absorbers 616
TEM cell (EMC) 896
Temperature coefficient 181
Temperature measurement, technical 58
Temperature response (spark plugs) 484
Temperature sensors 119
Temperature-dependent starting device (TAS) 540
Tensile strength 45
Tension (mechanical) 42
Terminal designations (circuit diagrams) 852
Terminal diagrams (motor vehicle) 851
Tesla (unit) 18
Test adapters, universal 510
Test benches (injection pumps) 552
Test cycles (emissions testing) 528, 563
Test cycles (fleet fuel consumption) 530
Test equipment (quality assurance) 154
Test procedures, tribological 332
Test program (Emissions testing) 526
Test pulses (EMC) 891
Test sampling (exhaust gas) 526
Test setups, exhaust 527
Test symbols (vehicle lighting equipment) 738
Testing (exhaust emissions) 526
Testing electronic engine systems 510
Testing equipment (diesel exhaust gas) 561
Testing evaporative emissions 526
Testing of initial samples 152
Tex (unit) 23
Theft-deterrent systems (car alarms) 766
Thermal capacity and conductivity 181
Thermal conduction 56
Thermal radiation 56
Thermal radiators 139
Thermal release (diesel engines) 382
Thermal resistance (wall layers) 57
Thermal shields (diesel injectors) 555
Thermal shock (spark plugs) 483
Thermal spraying 265
Thermochemical treatment (metals) 271
Thermocouples 74
Thermodynamic cycle (IC engines) 367
Thermodynamics 59
Thermoelectric effects 74
Thermoelectric series 74
Thermoelectricity 73
Thermoelectromotive force 74
Thermomagnetic effects 75
Thermomanagement 435
Thermometer, see Temperature measurement 58
Thermopile sensors 120
Thermoplastics 183, 220
Thermo-switches 686
Thermo-time switch (cold start) 468, 473
Thick-film circuits 87
Thick-film pressure sensor 110
Thick-film resistors 120
Thief-proofing (central locking) 815
Thin-film circuits 87
Thin-film metallic resistors (PTC) 119
Third-octave band spectrum 51
Thixotropy (lubricants) 232
Thomson effect (thermoelectric power) 75
Thread friction 313
Threaded fasteners 310
Three-finger rule (direction of magnetic field) 72
Three-phase AC 67
Three-phase AC machines 133
Throttle Body Injection (TBI) 465
Throttle valves 454, 460, 500
Throttle-valve potentiometers 462
Throughlighting, instruments 783
Thrown body and falling body (equations) 36
Thrust bearing (clutch) 590
Thrust bearings 282
Thyristor ignition 492
Thyristors 81
Tie rod (vehicle steering) 638
Tightening of threaded fasteners 312
Tightening torques (screws and bolts) 316
Tilting controls (sunroof) 813
Time of day, time zones (conversion) 28
Time units (conversion) 28
Time zones 28
Time, stopping 346
Time-controlled single-cylinder pump systems 548
Timing devices, injection (diesel engines) 541, 544
Timing dynamics (valve gear) 409
Tipping resistance (commercial-vehicle dynamics) 360
Tiptronic® gear-shift strategies 600
Tire categories 628
Tire condition (coefficient of friction) 343
Tire designation symbols 630
Tire designs 628
Tire inflation pressures 636
Tire speed 631
Tire traction 634
Tire treads 633
Tire-pressure monitoring system 111
Tires 628, 899
Tires, CT 629

PETITIONER'S EXHIBIT 1002
US PATENT NO. 6,557,540

Tires, summer tires (standard tires) 628
Titanium alloys 199
TMC, see Traffic Message Channel 788
Toe-in (suspension systems) 620, 639
Tolerance of concentricity 279
Tolerance of form 279
Tolerance of planar regularity 279
Tolerances 279
Tool steel 194
Tooth shape 297
Tooth thickness 298
Toothed drive belts 309
Top coats 264
Top dead center (TDC) 385
Toroid bellows (suspension) 618
Torque 16, 40, 44
Torque calculations 419
Torque control (diesel-engine management) 538
Torque control (MED-Motronic) 507
Torque control (ME-Motronic) 500, 503
Torque converter, hydrodynamic 591
Torque graphs, electric drives 579
Torque graphs, IC engines 413, 452
Torque motors 127
Torque sensors 112, 114
Torr (conversion) 16
Torsion 44
Torsion beam trailing-arm axle 622
Torsion springs 291
Torsion-bar springs 292, 618
Torsion-beam axle 622
Total-loss lubrication 410
Tow-away protection (theft-deterrent systems) 768
Towing vehicle (definition) 716
TR rim (vehicle wheels) 625
Traction batteries (hybrid drives) 583
Traction control system (TCS) 606, 710
Traction, enhanced (TCS) 606
Tractive-force regulation (agricultural tractors) 825
Tractor hydraulics 823
Tractor vehicles (articulated truck) body 733
Tractors (definition) 716
Tractrix principle 361
Tracts, intake and exhaust 407
Traffic Message Channel (TMC) 788
Traffic safety 726
Traffic telematics 798
Trailer vehicles (definitions) 716
Trailer-control valve 691
Trailers (brakes) 649, 674
Trailing arm (suspension) 623
Trailing-arm torsion-beam axle (automotive suspension) 622
Transformers 72
Transient response (motor vehicles) 356
Transistorized ignition (TI) 490
Transistors 78
Translational actuators 127
Transmission (gearbox) 592
Transmission device (air brakes) 645, 689
Transmission lubricants 236
Transmission of force (clutch) 590
Transmission ratio (vehicle specs.) 899
Transmissions, automatic 342, 597
Transmissions, effect on fuel consumption 337
Transmissions, hydraulic automotive 831
Transmissions, semi-automatic 597
Transponder systems (vehicle immobilizer) 769
Transputer 86
Transversal electromagnetic field, see TEM cell (EMC) 896
Transverse contact ratio (gears) 298
Transverse forces 42
Transverse suspension link or wishbone 623
Tread depth and stopping distances 633
Triac 81
Tribochemical reactions 331
Tribological damage 330
Tribological damage analysis 331
Tribology 329
Trigonometric functions 146
Trilex wheel system 626
Trilok torque converter, see Föttinger torque converter 592
Trip recorders and tachographs 794
Trolley bus (definition) 716
Truck assemblies 735
Truck bodies 733
Trucks 716, 733
Trunk radio networks 801
TRX-Denloc system 625, 629
Tubeless tires 629
Tubular heating element (glow plugs) 568
Tuned-intake-tube charging 390
Tungsten inert-gas welding 321
Tuning devices (exhaust systems) 451
Turbines (gas turbines) 366, 442
Turbochargers 442
Turbochargers and superchargers (IC engines) 440
Turbolators (engine cooling) 430
Turn-signal flashing 760
Turn-signal indicators (automotive) 760

PETITIONER'S EXHIBIT 1002
US PATENT NO. 6,557,540

Turn-signal lamps 760
Twin suspension links 623
Twin-flow turbine housings, ATL 443
Twin-tube shock-absorbers 617
Two-bed three-way catalytic converters 449
Two-component adhesives 322
Two-line braking systems 646, 674
Two-stage carburetors 460
Two-stage turbocharger systems 445
Two-step control (exhaust emissions) 525
Two-stroke process 388
Two-way radio networks 801

U

U-engines 394
UIS, see Unit Injector Systems 548
Ultrasonic passenger-compartment protection 768
Ultrasonic remote control 815
Ultrasonic sensors 791
Ultrasonic transit-time processes 101
Ultrasound 50
Underbody preservation 724
Understeer 352, 355
Uniform distribution (A/F mixture) 519
Uninhibited corrosion 256
Unit Injector Systems (UIS) 535, 548
Unit Pump Systems (UPS) 535, 549
Unitized all-steel bodies 722
Units (conversion) 19
Units of angle (conversion) 21
Units of area (conversion) 20
Units of length (conversion) 19
Units of mass (conversion) 22
Units of power (conversion) 25
Units of stress (conversion) 24
Units of temperature (conversion) 26
Units of volume (conversion) 20
Units, statutory 13
Universal (drive) shafts 602
Universal joints 602
Universal test adapters 510
Unleaded gasoline 238
Uplighting (lighting) 783
UPS, see Unit Pump Systems 549
Urban bus (definition) 716
USA test (emissions testing) 529, 562
Useful speed range 414
Useful-signal frequency (EMC) 893
Utrasonic flow measurement 115

V

Vacuum advance mechanisms (ignition timing) 489
Vacuum brake boosters 655
Valence (chemical elements) 176
Valence (electrolytic materials) 64
Valve arrangements, springs 408
Valve deactivation 377
Valve gear 408
Valve guides 409
Valve seats, timing 408
Valve timing 520
Valve timing, variable 387
Valve, delivery 537
Valves, canister-purge 506
Valves, dust-unloading 439
Valves, hydraulic 820
Valves, needle (carburetor) 461
Vane-type supply pumps 543
Vapor Lock Index (VLI) 240
Vapor pressure (fuels) 240
Vapour Phase Inhibitors (VPI) 267
Varactor (variable-capacitance diode) 78
Variable-displacement pumps (automotive hydraulics) 825
Variable-geometry intake manifolds 390, 500
VCI, see Volatile Corrosion Inhibitors 267
Vehicle bodies (delivery trucks and vans) 732
Vehicle bodies 713
Vehicle bulbs 763
Vehicle combinations 716
Vehicle control (ESP) 705
Vehicle dynamics (commercial vehicles) 359
Vehicle dynamics (control in pass. cars), see. ESP 701, 704
Vehicle dynamics 338
Vehicle dynamics control system (ESP) 707
Vehicle dynamics, assessment criteria 35
Vehicle handling (ISO) 354, 361
Vehicle Headlamp Aiming Devices (VHAD 749
Vehicle immobilizers 769
Vehicle information system 802
Vehicle lighting 738
Vehicle safety 726
Vehicle speed and engine speed 342
Vehicle surface area, projected 721
Vehicle testing procedures (EMC) 896
Vehicle wheels 624
Vehicle-body calculations 730
Vehicle-body drag coefficient (c_W) 340
Vehicle-body materials 723
Vehicle-body sheet metal 197, 723
Vehicle-body shell 722
Vehicle-speed limiters 611

PETITIONER'S EXHIBIT 1002
US PATENT NO. 6,557,540

Velocity of sound 50
V-engines 394
Venturi chamber (carburetors) 460
Venturi nozzles (mufflers) 451
Venturi tube (carburetors) 461
Vibration absorbers 617
Vibration absorption 32
Vibration and oscillation 29
Vibration corrosion cracking 259
Vibration damping 29, 31, 616
Vibration isolation 31
Vibration period (definition) 29
Vibration reduction, crankshaft 406
Vibration sensors 107
Vibrational stress 612
Viscosity (diesel fuel) 242
Viscosity grades 233
Viscosity units (conversion) 27
Viscous flow behavior, intrinsic (lubricants) 232
Visibility range when passing/overtaking 349
Vision 720
Visual range (lighting) 739
VLI, see Vapor Lock Index 240
Volatile Corrosion Inhibitors (VCI) 267
Volatility of gasoline 239
Voltage drop, permissible 859
Voltage regulators (alternators) 882
Voltage regulators (automotive electrical systems) 882
Voltage ripple (automotive electrical systems) 890
Voltage, magnetic 71
Volume expansion coefficient 181
Volumes of solids 1 49
Volumetric efficiency (gas exchange) 384
Volumetric efficiency (IC engine cylinder) 414, 453, 503
Volumetric efficiency (automotive hydraulics) 816
VPI, see Vapour Phase Inhibitors 267

W

W charging curves (battery charging) 873
Wafer bonding 91
Wankel engines, see Rotary engines 426
Warm-up 470, 505
Warning elements (Park-Pilot) 792
Warning signals (theft-deterrent systems) 767
Washing systems (car windows) 773
Water cooling 430
Water separation (fuel filters) 437
Water vapor (exhaust) 518
Water vapor 191
Watt (unit) 16
Watt linkage (automotive suspension) 622
Wavelengths 50
Wavelength range 137
Waves, vibration and oscillation (definition) 30
Wear 330
Wear inhibition 332
Wear quantities 331
Weber (unit) 18
Wedge shape (body), drag coefficient (c_W) 340
Weibull distribution 161
Weight 13
Weight-to-power ratio (calculation) 418
Weight-to-power ratio (passenger-car specifications) 899
Welding techniques 319
Welding, flash 320
Welding, gas-shielded 321
Welding, laser 328
Weston normal cells 64
Wet boiling point (brake fluids) 247
Wet road surfaces and aquaplaning 343
Wheatstone bridge 63
Wheel and tow-away protection (car alarm) 768
Wheel covers 625
Wheel imbalance and centering 626
Wheel load from crosswind 351
Wheel loading 627
Wheel lockup control system (ABS) 708
Wheel lockup prevention, see ABS 644, 649, 659, 693, 708, 803
Wheel mounting 624
Wheel position 620
Wheel sensors 796
Wheel slip 606, 635, 659
Wheel-arch filters 438
Wheelbase (passenger cars) 900
Wheels, motor vehicle 624
Wheel-slip angle 351, 355
Wheel-speed sensors 103, 670, 659, 695, 712
Wheel-suspension linkage 620
Whitworth pipe threads 318
Width requirement (commercial vehicles) 360
Wind effect (vehicle dynamics) 350
Windingless-rotor alternators 878
Windshield and rear-window cleaning 770
Windshield antennas 788
Windshields 721, 774

PETITIONER'S EXHIBIT 1002
US PATENT NO. 6,557,540

Windshields and window glass, automotive 774
Windshield-wiper mechanism 770
Winter tires (M+S tires) 628
Wiper blades 771
Wiper motors (DC) 772
Wiper potentiometers 96
Wiper systems and accessories 770
Wire-knit mounting (catalytic convertor) 449
Work (energy), electrical 62
Work, braking 345, 648
Worked penetration 234
Worm gears 297

Y

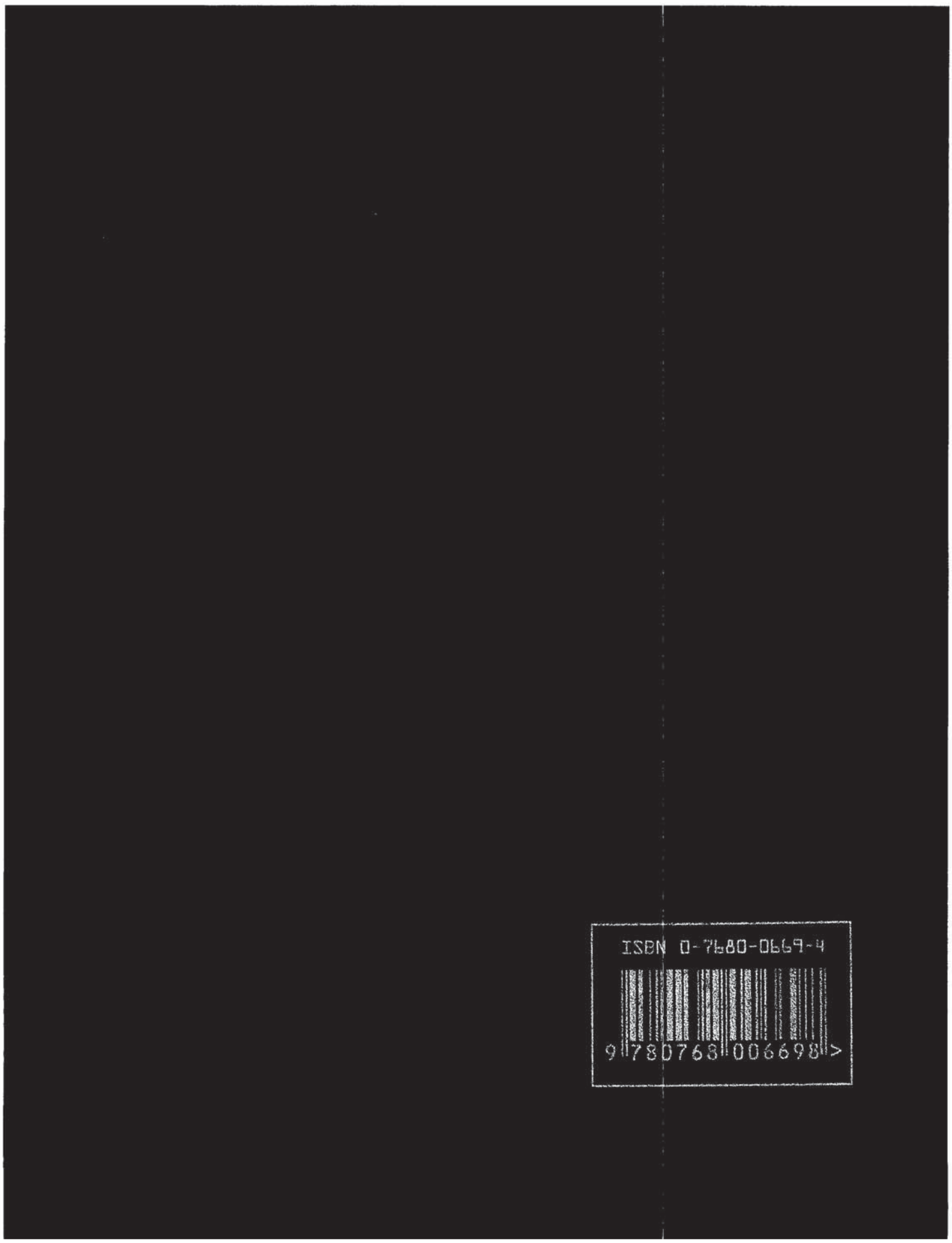
Yard (conversion) 19
Yaw rate 358, 361, 705
Yawing motion 705
Yaw-moment buildup delay (GMA) 662
Yaw-moment coefficients 350
Yaw-rate sensors (gyrometers) 105, 712
Yield point 230
Yield strength (materials) 180

Z

Zener (Z-) diode 78
Zirconium-dioxide oxygen sensor 523

PETITIONER'S EXHIBIT 1002
US PATENT NO. 6,557,540

UNIVERSITY OF CALIFORNIA-LOS ANGELES
L 008 290 180 2



PETITIONER'S EXHIBIT 1002
US PATENT NO. 6,557,540

INFORMATION TO USERS

This manuscript has been reproduced from the microfilm master. UMI films the text directly from the original or copy submitted. Thus, some thesis and dissertation copies are in typewriter face, while others may be from any type of computer printer.

The quality of this reproduction is dependent upon the quality of the copy submitted. Broken or indistinct print, colored or poor quality illustrations and photographs, print bleedthrough, substandard margins, and improper alignment can adversely affect reproduction.

In the unlikely event that the author did not send UMI a complete manuscript and there are missing pages, these will be noted. Also, if unauthorized copyright material had to be removed, a note will indicate the deletion.

Oversize materials (e.g., maps, drawings, charts) are reproduced by sectioning the original, beginning at the upper left-hand corner and continuing from left to right in equal sections with small overlaps. Each original is also photographed in one exposure and is included in reduced form at the back of the book.

Photographs included in the original manuscript have been reproduced xerographically in this copy. Higher quality 6" x 9" black and white photographic prints are available for any photographs or illustrations appearing in this copy for an additional charge. Contact UMI directly to order.

UMI

A Bell & Howell Information Company
300 North Zeeb Road, Ann Arbor MI 48106-1346 USA
313/761-4700 800/521-0600

VW EX1013
U.S. Patent No. 6,557,540

PETITIONER'S EXHIBIT 1002
US PATENT NO. 6,557,540

Modeling and Control of Advanced Technology Engines

by

Anna Stefanopoulou

A dissertation submitted in partial fulfillment
of the requirements for the degree of
Doctor of Philosophy
(Electrical Engineering:Systems)
in The University of Michigan
1996

Doctoral Committee:

Professor Jessy W. Grizzle, Co-Chair
Associate Professor James S. Freudenberg, Co-Chair
Professor Michael G. Parsons
Professor William B. Ribbens
Associate Professor Jeffrey L. Stein
Jeffrey A. Cook Principal Engineering Specialist, Ford Research Laboratory

PETITIONER'S EXHIBIT 1002
US PATENT NO. 6,557,540

UMI Number: 9624736

UMI Microform 9624736
Copyright 1996, by UMI Company. All rights reserved.

This microform edition is protected against unauthorized copying under Title 17, United States Code.

UMI
300 North Zeeb Road
Ann Arbor, MI 48103

© Anna Stefanopoulou 1996
All Rights Reserved

PETITIONER'S EXHIBIT 1002
US PATENT NO. 6,557,540

Dedicated to George, Kaite, and Dolly.

PETITIONER'S EXHIBIT 1002
US PATENT NO. 6,557,540

ACKNOWLEDGEMENTS

My thanks go first to my advisors, Professors Jessy Grizzle and Jim Freudenberg. Their guidance and support made this work possible. I wish to thank Mr. Jeff Cook. I sincerely believe that this work would not exist without his inspiration. His constant encouragement, intuitive wisdom, and resolute leadership were instrumental in completing this work.

I owe special thanks to Professor Ribbens. He served on my dissertation, preliminary, and qualification examination committees, and raised issues for me to consider that ultimately led to a more thorough and complete dissertation. I would like to thank Professor Parsons for giving me the opportunity to come to the University of Michigan. His support during my first year of studies was invaluable. I would also like to thank Professor Stein for serving on my doctoral committee. The insightful comments of Professors Parsons and Stein exemplify the value of cross-disciplinary effort; my thesis would be less without their participation.

I also gratefully acknowledge the financial support of the National Science Foundation (Grant ECS-92-13551) and the Ford Motor Company.

I am indebted to the Ford Motor Company's Control Systems Department. There I was given the opportunity to work and gain immeasurable experience while pursuing my degree. My friends and colleagues Ken, Jing, Paul, Kip, Florian and Bill showed me the art of welding innovative ideas with engineering practice and mathematical reasoning. I would also like to thank Mrdjan, Steve, Ed and Chris for their valuable suggestions and friendly chats during the last months of my studies.

There were many days during the three years of my studies that I found myself working innumerous hours in the 4402 computer laboratory. This laboratory became my home, and my lab-mates Meera, Jon, Raga, Cecilia, Brian, Al, Craig, Erich, Manish, Tyrone, Steve R., Yi-Liang, and Steve H. became my family. I want to thank them for their willingness to help with any problem that arose, and I wish them the best.

There are a number of people without whose friendship my life in Ann Arbor wouldn't have been as meaningful and blissful. Chief among them are Ailan, Tayfun, Ruben, Stephane, and Jong Gwan. I owe a huge debt to all of them.

And, finally, my ultimate thanks go to my wonderful companion Paul, who stood by my side through all these years.

This thesis is dedicated to my father, George, who had decided that I will become an

PETITIONER'S EXHIBIT 1002
US PATENT NO. 6,557,540

engineer even before I was born, to my mother, Kaite, who encouraged all my ambitions, and to my sister, Dolly, who always argued that engineering is a world bleak and monochrome, and filled me with stories of magic, adventure and mystery.

PETITIONER'S EXHIBIT 1002
US PATENT NO. 6,557,540

TABLE OF CONTENTS

DEDICATION ii

ACKNOWLEDGEMENTS iii

LIST OF TABLES vii

LIST OF FIGURES viii

LIST OF APPENDICES x

CHAPTERS

1 Introduction. 1
- 1.1 Background on Advanced Technology Engines. 1
- 1.2 Engine Control. 3
  - 1.2.1 Engine Modeling. 3
  - 1.2.2 Air-Fuel Ratio Control. 4
  - 1.2.3 Exhaust Gas Recirculation. 6
- 1.3 Dynamic Interactions and Performance Tradeoffs. 7
- 1.4 Overview. 8
- 1.5 Contributions of this Dissertation 9

2 Engine with Secondary Throttles. 11
- 2.1 Introduction. 11
- 2.2 Engine Model. 12
- 2.3 Nonlinear Breathing Process. 16
- 2.4 Feedforward Control Design. 18
- 2.5 Demand Map. 20
- 2.6 Feedback Control Design. 21
  - 2.6.1 Feedback Control Design using Secondary Throttles. 23
  - 2.6.2 Fuel Feedback Control Design. 25
  - 2.6.3 Feedback Control Design using Electronic Throttle. 27
- 2.7 Simulation Example. 29
- 2.8 Conclusions. 32

3 Modeling of Variable Cam Timing Engine. 33
- 3.1 Introduction to the VCT Engine Control Problem. 33
- 3.2 Dynamic Engine Model. 35
  - 3.2.1 Breathing Process. 36

PETITIONER'S EXHIBIT 1002
US PATENT NO. 6,557,540

3.2.2 Torque Generation. 38
3.2.3 Feedgas NO_x and HC emissions. 39
3.2.4 Process Delays. 42
3.2.5 Actuators and Sensors. 43
3.3 Region of Validity. 43
3.4 Model Validation. 44

4 Control of Variable Cam Timing Engine. 47
4.1 Feedback Controller Structure. 47
4.2 Performance Tradeoffs. 47
4.2.1 Engine Torque Response versus Feedgas Emissions. 48
4.2.2 Nonlinear Breathing Process and Feedforward Fuel Control 50
4.2.3 Catalytic Converter Efficiency versus Feedgas Emissions. . . 53
4.3 Multivariable Feedback Control Design. 53
4.4 Nonlinear Simulation Example. 58
4.5 PI Feedback Control Design. 58

5 Consequences of Modular Controller Development for the VCT Engine. . . 63
5.1 Decentralized Control of Multivariable Plants. 64
5.2 Multivariable and Decentralized Controller: Design. 64
5.3 Multivariable and Decentralized Controller: Analysis. 69
5.4 Conclusions. 73

6 Conclusions and Directions for Future Work. 74

APPENDICES 77

BIBLIOGRAPHY 126

PETITIONER'S EXHIBIT 1002
US PATENT NO. 6,557,540

LIST OF TABLES

Table

A.1 The 120 steady-state experiments performed at 750 rpm and the associated input variables. 79
A.2 The 150 steady-state experiments performed at 1000 rpm and the associated input variables. 80
A.3 The 150 steady-state experiments performed at 1500 rpm and the associated input variables. 81
A.4 The 180 steady-state experiments performed at 2000 rpm and the associated input variables. 82

PETITIONER'S EXHIBIT 1002
US PATENT NO. 6,557,540

LIST OF FIGURES

Figure

1.1 Typical three-way catalytic converter efficiency curves 5
2.1 Schematic representation of 4-cylinder engine with secondary throttles. 12
2.2 Engine model with secondary throttles. 13
2.3 Trajectories of the air flow into the manifold ($\dot{m}_\theta$ for $\theta = 10$) and the air flow out of the manifold ($\dot{m}_{cyl}$) for several values of secondary throttles (θ_c). 17
2.4 Block diagram of the linearized breathing process. 18
2.5 Static feedforward nonlinear term of the secondary throttles control signal (θ_c) . . 19
2.6 Schematic representation of the three control schemes. 22
2.7 Simulation of the θ_c-scheme and F_c-scheme. 30
2.8 Closed loop response of the θ_c-scheme and DBW-scheme for a square wave in the demanded torque. 31
2.9 Closed loop performance under uncertainty in the fuel puddling dynamics. 31
3.1 Valve lift profiles of a conventional and a variable cam timing engine. By retarding the cam phasing the exhaust valve stays open during the intake event for a longer time period. This causes the induction and reburn of the last part of the exhaust gases which is rich in unburned HC. The resulting diluent, also, lowers the combustion temperature and suppresses feedgas NO_x emissions. The amount of reduction will vary with engine speed and load. 34
3.2 Schematic representation of the unknown input-output relationship of the VCT engine over the region of interest. 35
3.3 Mass air flow rate through the throttle body as a function of manifold pressure for different throttle angles. Note the two distinct operating regimes of sonic and subsonic flow. 37
3.4 Engine pumping mass air flow rate as a function of manifold pressure for five different cam timing values. 38
3.5 Mass air flow rate into ($\dot{m}_\theta$) and out ($\dot{m}_{cyl}$) of the manifold as a function of manifold pressure for two different engine speeds and five cam timing values ($0^o, 10^o, 20^o, 30^o$,and 35^o). 39
3.6 Engine torque as function of A/F for different values of air charge at constant engine speed (1500 RPM). 40
3.7 Feedgas NO_x emission plotted versus A/F for different CAM timing values at constant manifold pressure ($P_m = 0.4$ bar), and engine speed ($N = 2000$ RPM). . . . 41
3.8 Feedgas HC emission versus A/F for different CAM timings at constant manifold pressure ($P_m = 0.4$ bar), and engine speed ($N = 2000$ RPM) 42
3.9 Block diagram of the identified control-oriented VCT engine model. 44

PETITIONER'S EXHIBIT 1002
US PATENT NO. 6,557,540

3.10 Model and engine actual dynamic response to throttle step command. 45
3.11 Model and engine actual dynamic response to cam phasing step command 46
4.1 Diagrammatic representation of the feedback controller structure. 48
4.2 Load response of an engine with variable cam timing mechanism and mechanical throttle for different scheduling schemes of cam phasing: (a) ideal schedule; (b) realizable scheme. 49
4.3 Steady state cam phasing 50
4.4 Torque response (at 750 rpm) using different low-pass filters in the cam phasing dynamics. 51
4.5 Torque response (at 2000 rpm) using different low-pass filters in the cam phasing dynamics. 52
4.6 Bode gain plots of the closed loop transfer functions (frequency in rad/sec). 57
4.7 Simulation response of the conventional and the VCT engine. 59
4.8 Diagrams of the MIMO control scheme, and the "PI-lowpass filter" control scheme. 60
4.9 Bode gain plots of closed loop transfer functions with the MIMO and the "PI-lowpass filter" feedback controllers (frequency in rad/sec). 61
4.10 Simulation response of the multivariable and the PI control scheme. 62
5.1 Bode gain plots of the linearized plant (frequency in rad/sec). 65
5.2 Block diagram of the linearized plant. 66
5.3 Bode gain plots of the MIMO controller and the decentralized controller (frequency in rad/sec). 67
5.4 Simulation using the linearized VCT engine model during cam phasing commands. 68
5.5 Block diagram of the decentralized control scheme. 69
5.6 Block diagram of the fully multivariable scheme. 70
5.7 Block diagram of the simplified multivariable control scheme. 71
5.8 Bode gain plots of the closed loop transfer function (frequency in rad/sec). 72
5.9 Block diagram of the decoupling controller. 72
B.1 Comparison between the identified polynomial $g_2(\theta)$ and the experimental data. . 87
B.2 Comparison between the identified polynomial $\dot{m}_{cyl}$ and the experimental data. . . 92
B.3 Comparison between the identified polynomial T_b and the experimental data. . . . 93
B.4 Comparison between the identified feedgas NO_x and the experimental data. . . . 94
B.5 Comparison between the identified feedgas HC and the experimental data. 95
C.1 The least squares solution w^* to an overdetermined system $Gw = b$. 98
C.2 Simulation model of the mass air flow through the throttle body during sonic flow programmed in the System-Build environment. 105
C.3 Simulation model of the engine pumping mass air flow rate programmed in the System-Build environment. 109
C.4 Simulation model of the brake torque programmed in the System-Build environment. 114
C.5 Simulation model of the feedgas NO_x emissions model programmed in the System-Build environment. 120
C.6 Simulation model of the feedgas HC emissions model programmed in the System-Build environment. 125

PETITIONER'S EXHIBIT 1002
US PATENT NO. 6,557,540

LIST OF APPENDICES

APPENDIX

A Engine Mapping 78

B Nonlinear Static Maps for the VCT Engine 86

C Regression Analysis and Simulation Modeling 96

PETITIONER'S EXHIBIT 1002
US PATENT NO. 6,557,540

CHAPTER 1

Introduction.

1.1 Background on Advanced Technology Engines.

Over the last two decades there has been a dramatic evolution in powertrain control systems, largely driven by government regulations : (i) stringent Federal and California emissions standards, (ii) increased fuel economy to comply with mandated Corporate Average Fuel Economy (CAFE), and (iii) minimum safety and reliability standards that are independent of age, environment, and varying fuel properties. These requirements create challenging control problems for two reasons:

- It is increasingly important to achieve control over transient behavior and meet performance objectives over the life of the vehicle. This requires the development of high performance and robust powertrain controllers.
- The performance objectives are often conflicting, or at best interrelated. One way to potentially meet these requirements is to introduce additional design parameters via innovative mechanical configurations (new actuators). The design parameters, control variables in system terminology, provide additional degrees of freedom to optimize the performance of the engine over its wide range of operation. The continuously variable transmission is an example of a recently implemented actuator that affects overall powertrain performance. Other actuators currently under consideration are electronic throttle, variable cam timing, camless valves, and direct injectors.

Historically, new actuators (exhaust gas recirculation valve, air bypass valve, fuel injectors) and sensors (exhaust gas oxygen sensor, mass air flow meter) have been introduced each time designers needed to meet additional engine performance requirements [15]. Performance standards and convenience pressed for the development of spark timing control. This additional control was used to advance or retard spark timing resulting in improved fuel economy and power. During the Eisenhower administration, federal emission legislation required emission control. This was accomplished by positive crankcase ventilation systems (PCV) used to minimize emissions from the crankcase, and secondary air systems used to oxidize hydrocarbons (HC) in feedgas emissions. Stricter emissions standards were met by

PETITIONER'S EXHIBIT 1002
US PATENT NO. 6,557,540

introducing external exhaust gas recirculation (EGR) to reduce oxides of nitrogen (NO_x) formation in feedgas emissions. Mandates in fuel economy led to the development of the idle speed regulation by the introduction of the air bypass valve. Development of the catalytic converter allowed further emission reduction, but required precise air-fuel ratio control, which was accomplished with the introduction of the exhaust gas oxygen sensor, and fuel injectors. The development and implementation of the corresponding control strategies were based on the relative independence of the different subsystems at low frequencies. Individual feedback loops were wrapped around sensors and actuators available for each subsystem (multiple single-input single output, SISO approach). In advanced technology automotive engines, the coupling between subsystems is strong, and imposes performance tradeoffs. Without knowledge of this interaction the powertrain control problem involves an extensive scheduling effort to define the new optimum operating points, and requires a laborious tuning process to calibrate the subsystem controllers to avoid unintentional excitations. Good control design in advanced technology automotive engines requires informed decisions of the performance tradeoffs early in the design process, and it is one of the subjects addressed by this dissertation.

In this dissertation we show that control design in advanced technology automotive engines necessitates a systematic modern control theoretical approach. In advanced technology automotive engines, the multiple SISO approach (decentralized controller architecture) reaches its limitations. In the following chapters we present a feasibility analysis of the engine control system for two innovative mechanical configurations of the spark ignition (SI) engine : (i) an SI engine equipped with secondary throttles placed in the intake ports of the cylinders, and (ii) an SI engine equipped with a variable cam timing (VCT) mechanism. Both mechanical designs affect the breathing process of the engine and are introduced to reduce emissions, increase fuel economy, and maintain drivability during rapid changes in the throttle position imposed by the driver (acceleration/ deceleration). Both actuators can be viewed as special cases of camless engine; the functionality of the secondary throttles is similar to the variable intake valve timing and lift, and the variable cam timing engine addresses the case of a variable intake and exhaust valve timing with fixed valve overlap. This study is an assessment of the achieved performance when compared to conventional engines, and an investigation of the effects of the new technology on the implementation of the complete powertrain control strategy. This work is based on the systematic approach of (i) deriving or identifying the dynamic model for the advanced technology engine design, (ii) validating the model using engine-dynamometer experimental data, (iii) studying the subsystem interconnections and making decisions on the performance tradeoffs in transient and steady-state engine operation, (iv) designing a controller that achieves a reasonable tradeoff in the performance requirements, and (v) investigating the controller complexity and the associated engine performance.

PETITIONER'S EXHIBIT 1002
US PATENT NO. 6,557,540

1.2 Engine Control.

Engine performance is primarily characterized by emission production, fuel efficiency and drivability. These in turn are affected by four fundamental engine variables: air charge, air-fuel ratio (A/F), exhaust gas recirculation (EGR) and spark timing. Automatic control of these variables has improved engine performance allowing optimum operation independent of aging, history, or environment [66], and has increased the convenience and safety level of the modern automobile [15]. A key contributor to the accomplishments in the area of engine control has been the availability of accurate and simple (control oriented) engine models. In the early 70's, control applications in the automotive industry paralleled achievements in engine and powertrain modeling. In this dissertation we model two innovative mechanical configurations of the SI engine, and use them for the analysis and synthesis of A/F and EGR controllers to achieve engine performance requirements. To serve as an introduction to this work, we review the most significant engine modeling efforts, and provide a brief description of the A/F and EGR control tasks and existing control designs.

1.2.1 Engine Modeling.

In this section we discuss the accomplishments in the area of engine modeling and its contributions to the analysis and development of engine control. The evolution of the engine models has three significant phases: (i) thermodynamic models, (ii) input-output models, specific to each application or engine configuration, and (iii) nonlinear models, physically based (generalized) for wide range of operation.

In the first of these phases, detailed thermodynamic methods were employed to understand the exact phenomena, to identify the variables that govern them, and ultimately to represent them with compact mathematical equations [3]. Numerical simulations allowed the designers to gain understanding of the engine behavior by performing numerical experiments, and testing the engine performance. The first non-thermodynamic models can be found in [32, 33, 34], where the authors developed crankangle event based models for compression ignition engine to perform stability analysis studies. Nonlinear dynamical models for SI engines have been developed in [65, 66], where spark, A/F, and EGR were optimized to minimize emissions while maintaining fuel economy. In these articles, the authors used control theoretical techniques to achieve performance improvements. Modern control methods were applied to linear engine models in [7] demonstrating the capabilities of control theoretical approaches in automotive applications. The need for precise transient A/F control emerged from the increasingly demanding emission requirements. Unknown fuel dynamics often misled control engineers to over-compensate for lean or rich A/F responses, so identification of fuel puddling and wall-wetting became a pressing problem. The first efforts led to the derivation of an input-output model of the fuel dynamics [75], and later to a more detailed characterization of transient A/F response [85, 1].

In the early 80's nonlinear dynamic models with wide range of operation (covering most

PETITIONER'S EXHIBIT 1002
US PATENT NO. 6,557,540

urban driving cycles) were developed [18, 17, 86, 58]. The work in [17] provides the most comprehensive model including actuator and sensors, and [86] incorporates exhaust emission and rotational dynamics. The effort in engine modeling has been expanded to include transmission and driveline characterization [60, 11]. In [13] the authors derive linearized models and study an important issue of engine control, namely, how multi-rate sampling affects engine control design. By the end of the 80's control engineers had developed a significant number of engine models, and a comprehensive list of them and discussion of their development can be found in [60] and in [62].

Currently, stringent requirements on emission, fuel economy, and safety require high performance and robust controllers. Complete, but generic, powertrain models are developed in [11, 23, 16, 35, 52], and are combined with modern control techniques in [10, 12, 76] to satisfy these requirements. Meeting the new performance requirements often requires accurate information and characterization of complicated phenomena [48], which is facilitated by the increased computational power in on-board control systems. In [61] the author addresses the challenging problem of reducing the development time needed to obtain accurate models, and provides a systematic approach to powertrain modeling and control effort.

1.2.2 Air-Fuel Ratio Control.

Vehicle feedgas emissions consist of carbon monoxides (CO), hydrocarbons (HC), and oxides of nitrogen (NO_x). In the early 1970s, three-way catalytic (TWC) converters were introduced to oxidize (HC and CO) and reduce (NO_x) pollutant species in the exhaust gases. The efficiency with which the undesirable exhaust gases are reduced to acceptable levels, or are converted to desirable gases, is a function of A/F. The sensitivity of the catalytic converter efficiency to A/F is shown in Figure 1.1. In this figure it can be seen that there is a very narrow range of A/F where high conversion efficiency for the primary three pollutants is attained. The A/F value were the highest efficiency is attained is the stoichiometric value (for standard fuels, $A/F = 14.64$). Due to this sensitivity, A/F control is an important task in controlling vehicle tailpipe emissions. In the 70's, A/F was based on regulation of fuel flow into the cylinders via carburaters [73], and later, with fuel injectors [69, 88]. After the development of the exhaust gas oxygen (EGO) sensor, electronic feedback fuel control was possible. Electronic feedback fuel control has since been used to keep A/F close to the stoichiometric value based on the A/F signal at the EGO sensor. Achieving precise A/F in both steady-state and transient engine operations is a challenging problem due to unpredictable inputs of the driver, the switching type EGO sensor, transport delays that limit accurate response during transients and the combined dynamics of the hot-wire anemometer used for the mass air flow sensing, the throttle body, the intake manifold, and fuel puddling dynamics.

For this reason, many studies have been conducted on A/F feedback control. These studies may be divided into two categories, the first of which addresses the scarcity and

PETITIONER'S EXHIBIT 1002
US PATENT NO. 6,557,540

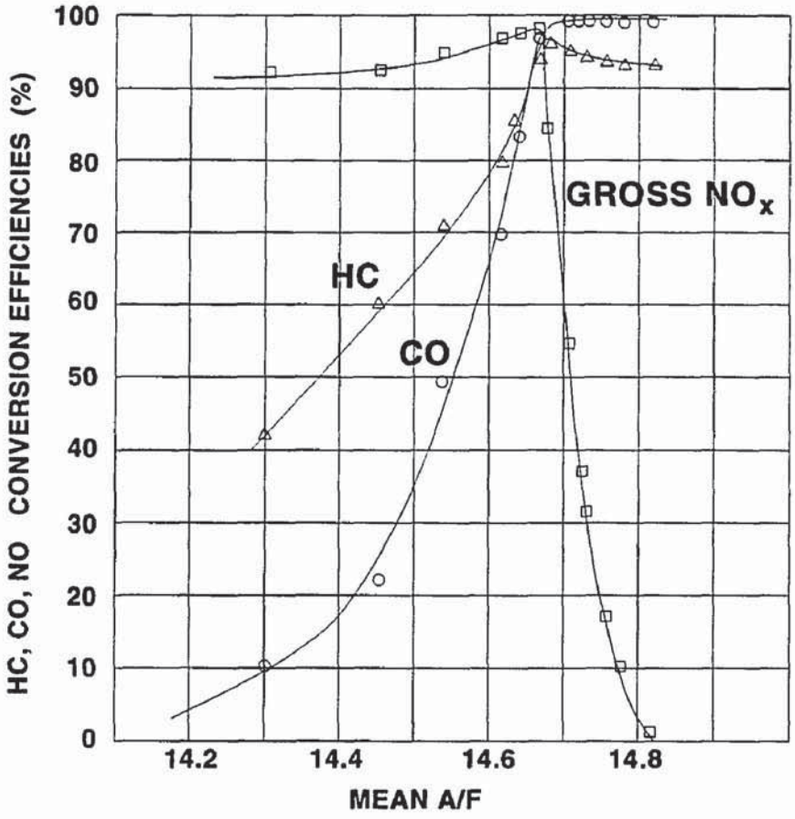


Figure 1.1: Typical three-way catalytic converter efficiency curves

nonlinearity of the conventional sensors. The emphasis in these studies is on the reconstruction of signals available for feedback, and the accurate and robust knowledge of the system states. The second category of studies addresses new engine configurations, i.e., modification of combustion parameters [3], and introduction of new actuators [8, 5] and sensors [64]. The new parameters in these engine configurations can improve A/F, but they often affect other engine variables. In this category of A/F control problems, the control designer has to identify and account for these interactions in order to meet the overall engine performance requirements. The work in this dissertation lies in the second category of A/F control studies. We control A/F for two different engine configurations after the introduction of new actuators. In the first problem, A/F excursions are minimized by the implementation of secondary throttles used to control air flow into the cylinders. The presence of the secondary throttles however can adversely affect drivability by making the engine seem sluggish. In the second problem, VCT is used to reduce feedgas emissions. This new control variable may cause disturbances in the A/F response of the engine. Both of these actuator configurations impose challenging multivariable problems that must be addressed by the control designer.

PETITIONER'S EXHIBIT 1002
US PATENT NO. 6,557,540

Previous work on the first category of A/F control studies consists of proportional-integral control and classical pole placement techniques, both in the discrete and continuous time domains [59, 46]. Furthermore, nonlinear analysis using describing functions has been used to study limit cycle behavior of the A/F response due to the switching type EGO sensor [63]. Multi-variable control with observers [57, 36] has been suggested as solutions to the problem of high performance and robust A/F control. Nonlinear sliding mode fuel injection controllers have been developed and tested in [10, 12, 54] providing an elegant alternative to the traditional gain scheduling of linear controllers, and show promising results even when using a switching EGO sensor. Individual A/F cylinder control using a single EGO sensor based on multi-rate sampling and periodic control techniques have given an answer to the alleviation of air charge maldistribution problems [28]. In related work, estimation of the air charge maldistribution in the cylinders is used in [47] along with a novel nonlinear observer technique. Use of nonlinear estimation also occurs in [36], were an extended Kalman filter is used for compensating the dynamics of fuel puddling. Adaptive compensation for the fuel dynamics has been successfully employed in [49] and [82]. In both studies the objective is the reconstruction of the A/F signal using a switching EGO sensor based on a fuzzy logic algorithm in [49], and a model-based approach in [82]. On-line identification techniques of the model used in [81, 39, 71] give promising results. In [71] the authors use a neural network that deals effectively with the long delay in the A/F process. On-line identification, observer design, and robust nonlinear control design techniques are areas of great importance to transient A/F control.

The second category of A/F control studies includes primarily engine control based on in-cylinder pressure measurements [64], and an electronically throttled engine [8, 39, 5]. The development of the electronic throttle control (ETC) or drive-by-wire (DBW) throttle system is an important research tool that provides a way of regulating the changes in air flow into the manifold caused by the primary throttle movement. These schemes show very good results in regulating A/F, and reducing emissions. In Chapter 2 we use this idea, and introduce secondary throttles in the inlet runners to allow coordination of air flow and fuel flow to achieve good A/F response during transients. The A/F performance improvement is shown to be achieved without slowing the engine torque response, and thus no tradeoff is made with drivability.

1.2.3 Exhaust Gas Recirculation.

Exhaust gas recirculation (EGR) was introduced in the early 1970s to suppress the formation of oxides of nitrogen (NO_x). The inert exhaust gases dilute the inducted air-fuel charge and lower the combustion temperature which reduces NO_x feedgas emissions.

Conventionally, exhaust gas recirculation is accomplished by controlling the exhaust gas that is supplied from the exhaust manifold to the intake manifold through a vacuum actuated valve. The EGR control algorithm is a simple PI or PID loop that adjusts the

PETITIONER'S EXHIBIT 1002
US PATENT NO. 6,557,540

amount of exhaust gas to the scheduled steady-state point which is a function of engine speed, coolant temperature and engine load (or another load related variable). EGR alters the breathing process dynamics and consequently the torque response. Careful steady-state and transient control design is necessary to maintain good engine torque response, and for this reason, EGR is typically turned off in transient engine operations, engine warm-up, and idling.

An innovative mechanical design approach to controlling EGR is the development of the variable cam timing (VCT) mechanism. By retarding the cam timing, combustion products which would otherwise be expelled during the exhaust stroke are retained in the cylinder during the subsequent intake stroke. This is a method of phasing the camshaft to control residual dilution and achieve the same results with the conventional external EGR system, thus providing an innovative solution to an old problem. The development of the VCT engine model and controller is addressed in Chapter 3 (engine model), Chapter 4 (control design), and Chapter 5 (implementation issues). With this work we show that dynamic VCT control is feasible.

1.3 Dynamic Interactions and Performance Tradeoffs.

To meet their stringent performance requirements, automotive engines have to be operated efficiently during both steady-state and transient operations. Past and current practice has been to optimize the additional design parameters that new actuators introduce only in steady-state using static engine mapping. The optimum operating points are defined by overlaying static maps of components that have to cooperate. Performance compromises in steady-state are alleviated with the introduction of feedforward terms that allow more freedom in achieving the design goals. However, the new Federal Test Procedure (FTP) for driving cycles consists of transient and high speed maneuvers, where the dynamic engine response is as important as the static engine behavior. These performance requirements press automotive engine designers to consider interactions between different processes at higher frequencies. Furthermore, the new actuators in the advanced technology automotive engines affect several subsystems, and cause severe performance tradeoffs. In this dissertation we show that the interaction between subsystems is a decisive factor in the control design of these highly multivariable engines. In the following chapters we identify the interactions that the secondary throttles and variable cam timing actuators introduce to the engine. These interactions are manifested through performance tradeoffs that the control engineer has to account for early in the design process. Briefly stated, *the secondary throttles and variable cam timing alter the engine breathing process which in turn affects fuel economy, emissions, and engine torque response over a wide range of operating conditions.* In designing controllers, we shall encounter three fundamental performance tradeoffs which are inherent to the advanced technology automotive engines.

PETITIONER'S EXHIBIT 1002
US PATENT NO. 6,557,540

(i) Fuel economy and emissions.

An approach for increasing fuel economy is to reduce energy losses. Engine operation (maintaining the same load) in high manifold pressure reduces the intake stroke pumping work required from the cylinders. High manifold pressure is associated with faster manifold filling dynamics, and therefore, changes in the throttle position are followed by rapid changes in the air charge. These changes introduce high bandwidth disturbances to the A/F response. Unless A/F control can successfully reject these disturbances, fuel economy (the initial design goal) will be followed by emission degradation.

(ii)NO_x feedgas emissions and catalytic converter efficiency.

Exhaust gas recirculation, used to suppress NO_x formation, alters the engine volumetric efficiency, and changes the breathing process dynamics. Exhaust gas recirculation and mass air flow into the cylinders are interconnected over a wide range of frequencies. High bandwidth control of feedgas NO_x rapidly alters the air charge and causes A/F excursions. In these cases, reduction in feedgas emissions is associated with reduction of the catalytic converter efficiency and may cause an increase in tail pipe emissions.

(iii) NO_x feedgas emissions and engine torque response.

NO_x feedgas reduction using exhaust gas recirculation affects the engine breathing process. Exhaust-gas recirculation affects adversely the air charge and the mixture formation which is crucial to good engine torque response. The EGR control design must address the affects of the mixture dilution to the engine torque response both in steady-state and transient operations. Moreover, an open loop design is necessary since the conventional automobile is not equipped with an on-line torque sensor.

1.4 Overview.

Chapter 2 addresses the problem of controlling an engine equipped with secondary throttles. The new control variables affect the nonlinear breathing process and are introduced to allow joint management of air and fuel flow into the cylinders. A nonlinear feedforward map is developed as a solution to a control authority problem inherent to the two distinct operating regimes of the breathing process. A linear multivariable feedback is designed to limit air fuel excursions and track a torque command during transient operations. This novel approach provides an alternative to current drive-by-wire schemes and possesses major advantages for enhancing the safety level of the modern automobile.

Another innovative engine design is the variable cam timing engine. The effects of cam timing and secondary throttles in the breathing process are similar. The understanding gained from the control problem in Chapter 2 is applied to the modeling of the VCT engine. A mathematical representation for the variable cam timing engine is identified in Chapter 3. The variable cam timing engine allows the joint management of fuel flow and internal exhaust gas recirculation to minimize exhaust emissions, increase fuel economy and satisfy drivers' performance requirements over a wide range of operating conditions. The

PETITIONER'S EXHIBIT 1002
US PATENT NO. 6,557,540

mathematical representation is formulated by physically based differential equations; all parameters and key nonlinearities used are determined from regressed engine data. The models are experimentally validated by engine dynamometer testing.

In Chapter 4, a control scheme is developed to minimize feedgas NO_x and HC emissions and to maintain air fuel ratio at stoichiometry, while providing satisfactory torque response during rapid changes in throttle position. Control of the VCT engine is a challenging problem due to the strong interconnections between the cam phasing and A/F loop, and sensor limitations. Consequently we design a multivariable and a decentralized controller, and analyze how the multivariable controller achieves better performance than the decentralized controller. The impact of the control architecture (multivariable vs. decentralized) upon the dynamic response of the VCT engine is analyzed in Chapter 5. Finally, in Chapter 6 we summarize the results of this dissertation and discuss directions for future research.

1.5 Contributions of this Dissertation

The contributions of this dissertation are :

- An existing nonlinear dynamical engine model by Crossley and Cook [16] was modified to include the effects of secondary throttles placed before the intake ports of the cylinders on the performance of the SI engine. The model, based on physical engine characteristics, is a powerful tool in studying the effects of innovative actuation that can affect the breathing process of the SI engine.

- Identification of different control authority regions for regulating the steady-state air flow into the cylinders. This result, although well known in the thermodynamic community [37], has not been acknowledged by control engineers. Our ability to affect (or not affect) the air flow into the cylinders is an important consideration in engine control, because the air flow into the cylinders is a variable that affects the overall engine performance in the following manner: (i) drivability, by altering the air charge, (ii) fuel economy, by changing the pumping losses during the intake event, and (iii) emissions, by causing A/F excursions.

- Derivation of a new control-oriented engine model that represents an SI engine equipped with a variable cam timing mechanism over a wide range of operating conditions. The model includes the breathing process, torque and emission generation, and sensor/actuator dynamics. Based upon extensive laboratory measurements, a phenomenological engine model structure was elucidated. With respect to the basic model of [16], the VCT mechanism alters the mass air flow into the cylinders, the self-EGR, the torque response, and the emissions of the engine. The developed model reflects all these innovations. It has been validated with engine-dynamometer experimental data and used in the design and development of the VCT engine controller.

PETITIONER'S EXHIBIT 1002
US PATENT NO. 6,557,540

- A rigorous analysis of the consequences of the multivariable versus decentralized controller architecture on the dynamic response of the VCT engine. A multivariable and a decentralized controller were designed, and it was demonstrated that the multivariable controller can manage the performance tradeoffs better than the decentralized controller. Moreover, the multivariable controller structure was simplified, without detrimental consequences in the system dynamic response, providing a paradigm of how a control designer may carry out her/his task in light of the requirement for a modular controller architecture implementation.

PETITIONER'S EXHIBIT 1002
US PATENT NO. 6,557,540

CHAPTER 2

Engine with Secondary Throttles.

2.1 Introduction.

A challenging control problem is to keep the A/F close to stoichiometry during rapid changes in the throttle position. Rapid changes in the throttle position strongly influence the cylinder air charging process, mixture formation and transient performance of the engine. These rapid throttle movements reflect the driver's demand for changes in torque and vehicle acceleration.

A controller is developed in this chapter to keep the A/F close to stoichiometry so that the Three Way Catalyst (TWC) operates with high efficiency, and to track the driver's torque demand during rapid changes in throttle position. The torque set point to be achieved is a function of throttle position and engine speed. This function, when evaluated for all possible throttle positions and engine speeds, forms a nonlinear map; we will call this the "demand map".

The control of the A/F around stoichiometry is usually based on regulating the fuel flow to follow the air flow changes imposed by the driver. The associated feedback control systems do not have enough bandwidth to accommodate fast transients caused by the throttle movement due to the long delay in the induction-compression-combustion-exhaust cycle. The addition of a feedforward term for the fuel set-point does not completely alleviate this problem. Developments in the area of drive-by-wire (DBW) throttle systems [22, 8, 39, 5] indicate the need of an air control scheme in addition to the fuel control. This need motivates the following work that moves a step beyond the DBW scheme by developing a joint air-fuel management system which allows full control authority of the primary throttle position to the driver.

The control scheme presented here is based on the introduction of secondary throttles before the intake ports of the cylinders (Fig. 2.1). The new control variables (θ_c) regulate the air flow into the cylinders. These control variables in combination with the fuel injectors (F_c) achieve low A/F excursions and good tracking of torque demand by adjusting the air flow and the fuel flow into the cylinders. The control variables θ_c smooth out rapid changes of the charging process during throttle movements so that the fuel control path is able to

PETITIONER'S EXHIBIT 1002
US PATENT NO. 6,557,540

maintain stoichiometry.

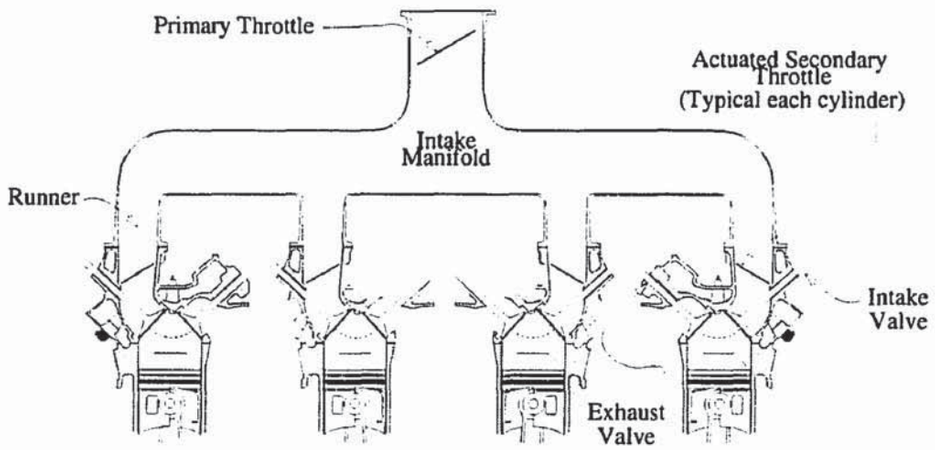


Figure 2.1: Schematic representation of 4-cylinder engine with secondary throttles.

The torque and A/F errors used by the controller are calculated by measuring the difference between actual and desired values. We assume direct measurement of the achieved torque[1]; we also use a linear EGO sensor for A/F measurement.

2.2 Engine Model.

This section gives an overview of the modifications of the nonlinear mathematical representation of the engine model developed in [16] and [23]. This model is a continuous-time nonlinear, low-frequency[2] phenomenological model with uniform pulse homogeneous charge, and lumped parameter approximation of breathing and rotational dynamics. The nonlinear mathematical representation of the engine model with secondary throttles is derived, based on physical engine characteristics, by modulating the mass air flow into the cylinders by a simple multiplication with a signal (θ_c). The signal (θ_c) takes values from 0 (closed) to 1 (wide open) and represents the effective area in the inlet runners. In this model all nonlinearities are regressed over engine-dynamometer data. The choice of parameters against which to regress the data is based upon physical principles explained in [37] for SI engines. Figure 2.2 shows the engine model with secondary throttles.

Breathing process dynamics

The manifold was analyzed as a single control volume with the throttle plate controlling

[1]We are assuming here that a reliable and accurate torque measurement is available, such as could be obtained from in-cylinder pressure sensor.

[2]In this model mass flow rate, manifold pressure, and torque are represented by their average values over an engine event.

PETITIONER'S EXHIBIT 1002
US PATENT NO. 6,557,540

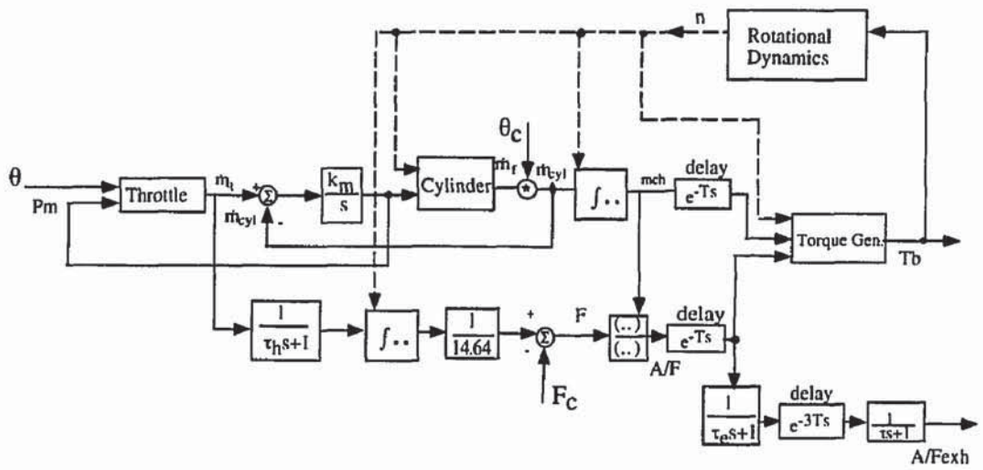


Figure 2.2: Engine model with secondary throttles.

mass air flow into the manifold, and the engine cylinders in combination with the secondary throttles controlling mass air flow out of the manifold. Based on the "Filling and Emptying Models" described in [37], manifold acts as a plenum, where the rate of change of the manifold pressure (P_m) is proportional to the mass air flow rate into the manifold ($\dot{m}_\theta$) minus the pumping mass air flow rate ($\dot{m}_{cyl}$) into the cylinders. The manifold dynamics are described by the following first order differential equation (see [60]) that relates the rate of change of the manifold pressure (P_m) to the flow rates into and out of the manifold ($\dot{m}_\theta$ and $\dot{m}_{cyl}$, respectively)

$$\frac{d}{dt}P_m = K_m(\dot{m}_\theta - \dot{m}_{cyl}), \text{ where } K_m = \frac{R \cdot T}{V_m} . \tag{2.1}$$

Based on the nominal manifold temperature (T), the manifold volume (V_m), and the specific gas constant $R = 287\ \frac{J}{Kg \cdot K}$, the constant K_m was calculated to be equal to $0.413\ \frac{bar}{g}$. This model is an engine event averaged representation of the intake manifold filling dynamics. The dynamic manifold pressure obtained by this model is not the instantaneous manifold pressure.

The mass air flow rate into the manifold ($\dot{m}_\theta$) through the primary throttle body is a function of throttle angle (θ), the upstream pressure (P_o), which we assume to be the atmospheric, i.e., $P_o = 1$ bar, and the downstream pressure, which is the manifold pressure (P_m). When the manifold pressure is less than half of atmospheric pressure, i.e., $P_m/P_o < 0.5$, the flow $\dot{m}_\theta$ through the throttle body is described as sonic flow and depends only on the primary throttle position. The function describing $\dot{m}_\theta$ in the two flow regimes is given

PETITIONER'S EXHIBIT 1002
US PATENT NO. 6,557,540

in [56] and [65] by :

$$\begin{aligned} \dot{m}_\theta &= f(\theta)g(P_m) \\ f(\theta) &= 2.821 - 0.05231\theta + 0.10299\theta^2 - 0.00063\theta^3 \\ g(P_m) &= \begin{cases} 1 & \text{if } P_m \le P_o/2 \\ \frac{2}{P_O}\sqrt{P_m P_o - P_m^2} & \text{if } P_m > P_o/2 \end{cases} . \end{aligned} \tag{2.2}$$

The conventional engine pumping mass air flow rate ($\dot{m}_f$) is a function of manifold pressure (P_m) and engine speed (N) and is given in [16] by :

$$\dot{m}_f = -0.366 + 0.008979NP_m - 0.0337NP_m^2 + 0.0001N^2P_m \quad . \tag{2.3}$$

The secondary throttles are restricting the air flow rate out of the manifold and into the cylinders, so the mass air flow rate into the cylinders ($\dot{m}_{cyl}$) is modeled by :

$$\dot{m}_{cyl} = \theta_c \cdot \dot{m}_f \quad . \tag{2.4}$$

Process delays

The discrete nature of the combustion process causes delays in the signal paths: between the mass charge formation and the torque generation there exists a delay equal to the compression stroke duration, and between the exhaust manifold and the exhaust gas oxygen (EGO) sensor there exists a delay which equals 3 times the intake event duration.

Exhaust process dynamics

The dynamics of the exhaust manifold and the linear EGO sensor are modeled by a first order differential equation with time constant equal to 0.15 sec and 0.20 sec, respectively.

Fuel path dynamics

The fuel puddling dynamics are important in accurate transient A/F control [8], [36], and [55]). In general, it is difficult to accurately model the fuel puddling dynamics [49] because the parameters of the model depend strongly on the fuel characteristics and the temperature of the engine during operation [82]. The model for the fuel puddling dynamics is given in [1] by

$$\begin{aligned} \dot{M}_{fp}(t) &= -\tfrac{1}{\tau_f}M_{fp}(t) + X\dot{M}_{fi}(t) \\ \dot{M}_f(t) &= (1-X)\dot{M}_{fi}(t) + \tfrac{1}{\tau_f}M_{fp}(t) \\ \text{where,}\quad \dot{M}_{fi} &: \text{injected fuel flow (Kg/sec)} , \\ \dot{M}_{fp} &: \text{fuel film mass flow (Kg/sec)} , \\ \dot{M}_f &: \text{cylinder port fuel mass flow (Kg/sec)} , \\ \text{and}\quad X &: \text{fraction of the injected fuel which is deposited on the manifold as fuel film.} \end{aligned} \tag{2.5}$$

The exact model of the fuel dynamics used for the engine with the secondary throttles was

PETITIONER'S EXHIBIT 1002
US PATENT NO. 6,557,540

developed in [1] :

$$
\begin{aligned}
&M_f = \tfrac{(1-X)\tau_f s+1}{\tau_f s+1} M_{fi}, where \\
&X = 0.3 + \tfrac{0.7}{90}\theta = 0.3 + \tfrac{0.7}{90}10 = 0.38, \\
&\theta = 10 : \text{angle in degrees of the primary throttle,} \\
&\text{and } \tau_f = 0.1 \text{ sec, resulting} \\
&M_f = \tfrac{0.62 \cdot s+1}{0.1 \cdot s+1} M_{fi}.
\end{aligned}
\tag{2.6}
$$

Precise transient A/F control during rapid changes in the throttle position by the driver requires feedforward compensation of the fuel command since the inherent delay in the A/F feedback loop prohibits rapid corrections through the feedback fuel command. The feedforward fuel command is regulated on the basis of the estimated cylinder air charge. The estimated cylinder air charge is calculated based on the mass air flow measurement at the mass air flow sensor (hot wire anemometer positioned upstream the throttle body), and integrated during the intake event. The estimated cylinder air charge is divided by 14.64 (nominal A/F) to provide the feedforward fuel flow command used in the A/F loop. The dynamics of the air flow meter are included in the model by a first order lag with a time constant equal to 0.13 sec.

Torque generation

The torque generated by an engine depends on the ignition of the cylinder charge, the mixture formation, and engine specific physical parameters. Analytical curve fitting techniques to dynamometer-engine experimental data are applied in [16] to estimate the steady-state brake torque generation given by:

$$
\begin{aligned}
T_b = \quad & -181.3 + 379.36 m_a + 21.91 A/F - 0.85 A/F^2 + 0.26\sigma - 0.0028\sigma^2 \\
& 0.027N - 0.000107N^2 + 0.00048N\sigma + 2.55\sigma m_a - 0.05\sigma^2 m_a + 2.36\sigma m_e
\end{aligned}
$$

where,

m_a : mass air charge (g/intake event) ,
A/F : air-to-fuel ratio ,
σ : degrees of spark advance before top dead center ,
N : engine speed (rad/sec) , and
m_e : exhaust gas recirculation (g/intake event).

(2.7)

For simplicity in this study, we used the above equation with spark advance equal to 30 degrees ($\sigma = 30$), and exhaust gas recirculation equal to zero ($m_e = 0$).

Rotational dynamics

A very simplified model of the rotational dynamics is used for the engine with secondary throttles model. The rotational motion of the engine crankshaft is given in terms of the engine and the vehicle moment of inertia (J), angular acceleration ($\dot{\omega}$ in $\frac{rad}{sec^2}$), and the difference between the net torque generated by the engine (T_b in Nm) and the load torque

PETITIONER'S EXHIBIT 1002
US PATENT NO. 6,557,540

on the shaft (T_l in Nm).

$$\Sigma T = T_b - T_l = J\dot{\omega}. \tag{2.8}$$

The load torque in the shaft is calculated in [23] using experimental data. It can be represented as a function of the drag due to the engine friction (c_{de}), the aerodynamic drag (c_{dv}), and the selected gear ratio (gr) :

$$\begin{aligned} T_l &= (c_{de} + c_{dv} gr)\omega^2 \ , \\ c_{df} &= 0.00015, \ \text{drag due to the engine friction} \ (\tfrac{Nm \cdot sec^2}{rad^2}), \\ c_{dv} &= 0.001, \ \text{aerodynamic drag} \ (\tfrac{Nm \cdot sec^2}{rad^2}), \ \text{and} \\ gr &= 0.197 \ (\text{3rd gear}). \end{aligned} \tag{2.9}$$

The total inertia is a combination of the engine inertia (J_e), and the vehicle inertia reflected through the drivetrain, and is given by:

$$\begin{aligned} J &= J_e + m_v (r_w gr)^2 \ \tfrac{Nm \cdot sec^2}{rad} \ \text{where,} \\ J_e &: \text{engine inertia,} \\ m_v &: \text{vehicle mass} \\ r_w &: \text{wheel radius} \\ gr &: \text{gear ratio} \end{aligned} \tag{2.10}$$

From vehicle data we selected $J_e = 0.14 \ \frac{Nm\,sec^2}{rad}$, $m_v = 920 \ kg$, and $r_w = 0.28 \ m$.

2.3 Nonlinear Breathing Process.

This section concentrates on the nonlinear dynamics of the engine breathing process. The study of the breathing process behavior is used to investigate and determine the operating regions where the secondary throttles (θ_c) have control authority in regulating the air charge into the cylinders. The air charge for every intake event is a function of the mass air flow rate into the cylinders and the engine speed, and it is directly related to the torque produced throughout the power stroke. Control over the transient and the steady state value of the mass air flow is necessary to meet the objectives of good torque tracking and maintaining the A/F at stoichiometry. The signal θ_c must influence the static and dynamic behavior of the manifold pressure, the air flow into the manifold through the primary throttle position, and the air flow into the cylinders through the secondary throttles.

For the basic model (without the secondary throttles) the steady state operating point occurs at the intersection of the two trajectories of the mass air flow rates. This point is the nominal point shown in Fig. 2.3. With the introduction of the secondary throttles it is possible to scale the engine pumping rate ($\dot{m}_f$) by different values depending upon the effective area of the passage that is regulated by opening and closing these new valves

$$\dot{m}_{cyl} = \theta_c \cdot \dot{m}_f \quad . \tag{2.11}$$

PETITIONER'S EXHIBIT 1002
US PATENT NO. 6,557,540

Figure 2.3 shows the new trajectories of the air flow rate into the cylinders and the resulting new equilibria (set points in Fig. reffig:intersections) for the breathing process. For sufficiently large $\theta_c < 1$, the steady state value of the mass air flow into the cylinder $\dot{m}_{cyl}$ is adjusted by causing the new equilibrium to shift from the sonic flow regime to the subsonic region. A closer investigation of the two regimes illustrates their significance in the new control scheme.

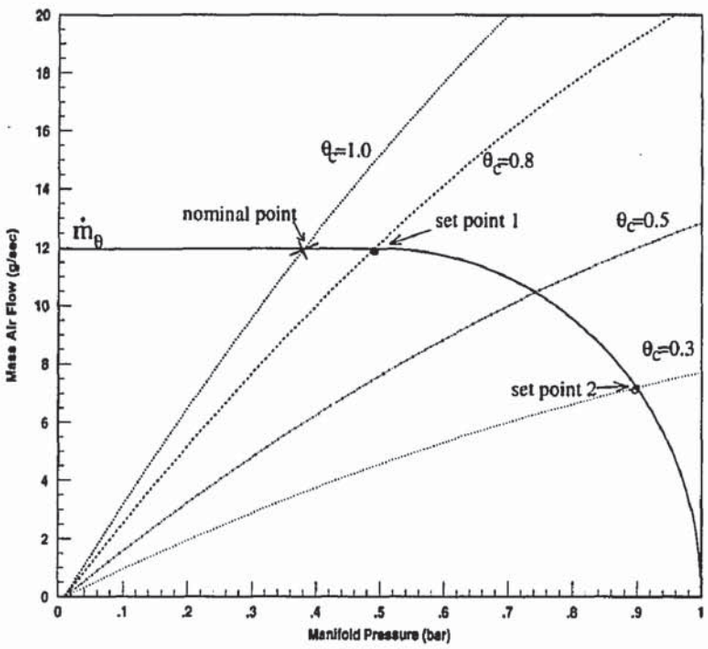


Figure 2.3: Trajectories of the air flow into the manifold ($\dot{m}_\theta$ for $\theta = 10$) and the air flow out of the manifold ($\dot{m}_{cyl}$) for several values of secondary throttles (θ_c).

When the flow through the primary throttle body is sonic and therefore does not depend on the manifold pressure, we operate in the flat region of $\dot{m}_\theta$ in Fig. 2.3. Small changes in θ_c cause no change in the steady state value of the mass air flow in and out of the manifold. For this reason, when the model of the breathing process is linearized, the secondary throttles have zero control authority on regulating the steady state mass air flow into the cylinders. This can be shown by the following transfer function between the control signal $\Delta\theta_c$ and the mass air flow into the cylinder $\Delta\dot{m}_{cyl}$ (see Fig. 2.4) :

$$\frac{\Delta\dot{m}_{cyl}}{\Delta\theta_c} = \frac{1}{1+\frac{k_m k_1}{s}} = \frac{s}{s+k_m k_1} \quad . \tag{2.12}$$

The DC gain of the above transfer function is clearly zero. The usual technique of incorporating an integrator to regulate the steady state mass air flow into the cylinders cannot be used here, since the transfer function has a zero at the origin that cancels the integrator pole. It is also instructive to see this on a block diagram level. Figure 2.4 shows the linear

PETITIONER'S EXHIBIT 1002
US PATENT NO. 6,557,540

dynamics of the breathing process for sonic flow after the introduction of the secondary throttle. Note that the integrator loop, which is an intrinsic part of the manifold dynamics in sonic flow, rejects the signal θ_c in steady state. Thus, the control signal $\Delta\theta_c$ cannot adjust the air charge into the cylinder by "smoothing" the effect of rapid throttle changes. Consequently, the control command $\Delta\theta_c$ has zero control authority on the A/F and the steady state value of the engine torque.

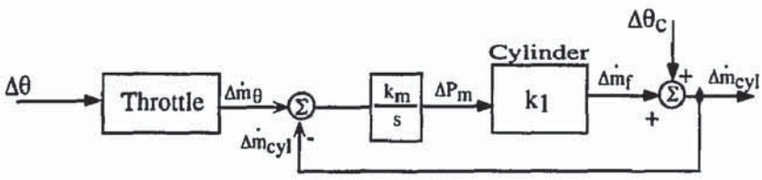


Figure 2.4: Block diagram of the linearized breathing process.

In the case where the flow is subsonic, i.e., $P_m/P_o > 0.5$, the air flow into the manifold depends on the primary throttle position and on the manifold pressure; thus, the linear model of the engine breathing process is different from the above, and the application of linear techniques such as LQG/LTR is possible. The slope of the function that describes $\dot{m}_\theta$ (see Fig. 2.3) indicates the control authority of its operating point. It is clear now that the control authority of the secondary throttles around the set-point 2 in Fig. 2.3 is preferable to that around the set-point 1. Around set-point 2, the secondary throttles can be used to "smooth" the abrupt changes of air flow by regulating the air flow rate into the cylinders at a slower rate.

In conclusion, a nonlinear feedforward design of the θ_c set-points that allows operation in the subsonic flow regime, where the secondary throttles have maximal control authority, is necessary. This map will provide the steady state position of the new control variables.

2.4 Feedforward Control Design.

The natural nominal position of the secondary throttles is wide open, i.e., $\theta_c = 1$. However, recall from Section 2.3 that under these conditions the secondary throttles often have zero control authority in adjusting the steady state value of the mass air flow into the cylinders. A solution that uses a control signal (θ_c), which consists of a nonlinear feedforward term ($\theta_{c_{fw}}$) plus a feedback term ($\theta_{c_{fb}}$) is proposed. The feedforward design ensures maximal control authority and smooth engine operation.

The nonlinear feedforward term ($\theta_{c_{fw}}$) is designed to satisfy the following three conditions: (i) it is a smooth and non-decreasing function of the primary throttle position (θ) and the engine speed (N), i.e., $\theta_{c_{fw}} = \theta_{c_{fw}}(\theta, N)$; (ii) the engine should deliver its maximum power output when operated at or close to wide open throttle (WOT), and (iii) maximal control authority should be available without sacrificing combustion stability and

PETITIONER'S EXHIBIT 1002
US PATENT NO. 6,557,540

performance. To achieve these objectives over a wide range of engine operating conditions we should consider the effects of combustion stability, thermodynamic performance indices and idle operating conditions. For example, it is unclear if the higher manifold pressure associated with the secondary throttles results in higher volumetric efficiency. Presently such an extended analysis has not been completed. Based only on a control authority analysis, the following map has been developed (see Fig. 2.5):

$$\theta_{c_{fw}} = \begin{cases} 0.55 & \text{if } 0^o < \theta < 12^o \\ 0.6445 - 0.0126 \cdot \theta + 1.3125 \cdot 10^{-4} \cdot \theta^2 + 2.1875 \cdot 10^{-5} \cdot \theta^3 & \text{if } 12^o \leq \theta < 20^o \\ 1 - (\frac{\theta - 60}{65})^2 & \text{if } 20^o \leq \theta < 60^o \\ 1 & \text{if } 60^o \leq \theta < 90^o \end{cases}$$

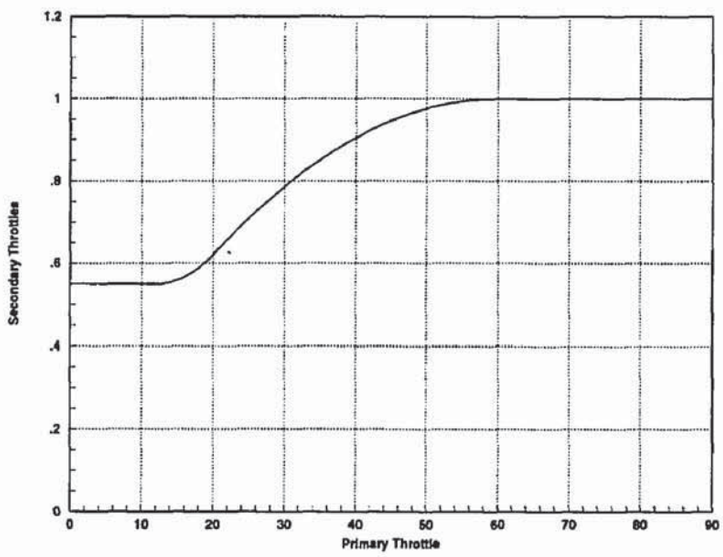


Figure 2.5: Static feedforward nonlinear term of the secondary throttles control signal (θ_c)

The reasoning behind this map is briefly explained. First, usual driving conditions in urban areas correspond to partly open primary throttle (θ) interrupted by rapid requests for acceleration and deceleration (which are the main causes of A/F excursion). At partly open throttle, the maximum power of the engine is not required and hence $\theta_{c_{fw}} < 1$ is acceptable. In addition, $\theta_{c_{fw}}$ has been adjusted to ensure that the breathing process is operating near set-point 2 in Fig. 2.3. When the primary throttle is at or near WOT, the secondary throttles must smoothly operate close to the wide open position to ensure that maximum engine output can be achieved. Under WOT conditions, $P_m/P_o \approx 1$. Therefore, the secondary throttles are operating in the maximal control authority region, however, they have freedom of movement only towards one direction. The secondary throttles can reduce the passage of the inlet runners and regulate the transient air flow rate into the cylinders during acceleration to cause lower A/F excursions. On the other hand, not much

PETITIONER'S EXHIBIT 1002
US PATENT NO. 6,557,540

can be done when the driver closes the primary throttle: the secondary throttles cannot open further ($0 < \theta_c \leq 1$) to "smooth" the abrupt decrease of the air flow into the manifold by providing additional air. Finally, when the primary throttle is nearly closed, there is a minimum position for the secondary throttles below which idle stability issues have to be addressed.

The above map has been used to investigate the contribution of the new control actuator to driveability improvement and emission reduction. Thermodynamic evaluation is needed to determine the interaction of the new control variables with the various engine performance indices. An initial assessment of the influence of the suggested feedforward scheme shows that the feedforward term is beneficial to the manifold dynamics. The engine operates at $P_m/P_o \approx 0.9$, i.e., manifold almost fully charged, which causes considerably faster manifold filling dynamics during part throttle driving. This can be seen by evaluating the time constant of the breathing dynamics at several operating points (see Fig. 2.3). Achieving fast quasi-steady conditions close to atmospheric pressure in the intake manifold can eliminate wide variation in the time constant of the fuel puddling dynamics. This might reduce the uncertainty inherent in the fuel flow transient behavior. A reduction of the pumping losses is also expected due to the low manifold vacuum, however the additional complication in the intake system of the engine might decrease the volumetric efficiency. Further investigation of all the above issues will determine the effect of the new control scheme on fuel economy. For control purposes, usage of the feedforward term shown in Fig. 2.5 makes linearization fruitful and allows linear feedback design.

2.5 Demand Map.

In the engine with the secondary throttles the input is the primary throttle position (driver's command). It is measured but not controlled. The torque set-point (T_{des}) is calculated from the primary throttle position (θ) and the engine speed (N) measurements. This requires a demand map, similar to the one used in DBW schemes [22], to determine the torque set-point for any throttle position and engine speed. This map is a nonlinear and well-defined map, i.e., torque has a unique value for specific throttle position and engine speed. To generate this map we run the simulation model of the engine with the secondary throttles for different throttle positions and gear ratios, and record the corresponding steady-state torque and engine speed response. The torque from the demand map will be used as the desired torque when the torque error is calculated to adjust the control signals.

PETITIONER'S EXHIBIT 1002
US PATENT NO. 6,557,540

2.6 Feedback Control Design.

In the following Sections we compare the A/F closed loop response of the engine with the secondary throttles (θ_c-scheme) with the conventional[3] A/F closed loop response (F_c-scheme), and with the A/F closed loop response of an engine equipped with electronic throttle (DBW-scheme). The comparison is based on simulation results using the nonlinear dynamic model described in Section 2.2. In this section we design three linear multivariable controllers for the three different schemes.

The main objective of the three control designs is to minimize the A/F excursion during rapid changes in pedal position. This is achieved with integral control, by augmenting the states of the system with the integrated state of A/F error. A secondary objective for the closed loop performance of the engine with the secondary throttles, and the engine with the electronic throttle is to maintain good torque response, during these transients. Good torque response amounts to (i) maintaining similarity of the rate of torque change in the first phase of the acceleration-deceleration with the conventional engine torque response, (ii) avoiding torque hesitation during the acceleration phase, and (iii) achieving in steady-state the desired torque response. This objective is accomplished with the introduction of the integrated state of torque error in the control design of the engine with the secondary throttles (θ_c-scheme), and the control design of the engine with the electronic throttle (DBW-scheme). With this objective we ensure that the θ_c and the DBW schemes have torque response similar to the conventional engine. This is an important objective and cannot be ignored, since the two schemes can "decouple" the driver from the engine (particularly the cylinders). The controller will try to filter the rapid changes in air charge (lowpass the disturbance) to minimize A/F excursions causing very slow engine torque response. Thus, designing the two schemes based on A/F regulation only, will cause unacceptable drivability. The three schemes can be summarized as :

F_c-scheme : During acceleration/deceleration, the driver changes the primary throttle position (θ), and fuel command is used to minimize A/F excursions caused by the rapid changes in the throttle position. The fuel regulation is based on A/F, torque, and throttle position measurements. The A/F is measured using a linear EGO sensor. These measurements improve the conventional fuel regulation, which is a PI feedback controller based on the A/F measurement, and a feedforward compensator based on the mass air flow (MAF) or manifold pressure (MAP) measurement.

θ_c-scheme : As above, the driver controls the primary throttle position (θ), and the controller regulates secondary throttle position (θ_c) and fuel command (F_c) to mini-

[3]This scheme is called conventional because we use only the fuel command to control A/F at stoichiometry during rapid changes in throttle position. In the other two schemes ("non-conventional") we coordinate fuel and air flow into the cylinders to maintain stoichiometry. Although we call the F_c-scheme as conventional A/F control, neither the control strategy nor the measurements used are conventional.

PETITIONER'S EXHIBIT 1002
US PATENT NO. 6,557,540

mize A/F excursions and maintain good torque response. In this scheme we use the same measurements as above, i.e., A/F, torque, and throttle position measurements.

DBW-scheme : In this scheme, the driver controls the pedal position, and the controller regulates the throttle position (θ_e), and the fuel command (F_c) to precisely control A/F and track the torque demand (T_{des}). The measurements used in this scheme are identical to the ones used in the previous schemes.

The control structure of the three different schemes is schematicaly shown in Fig. 2.6.

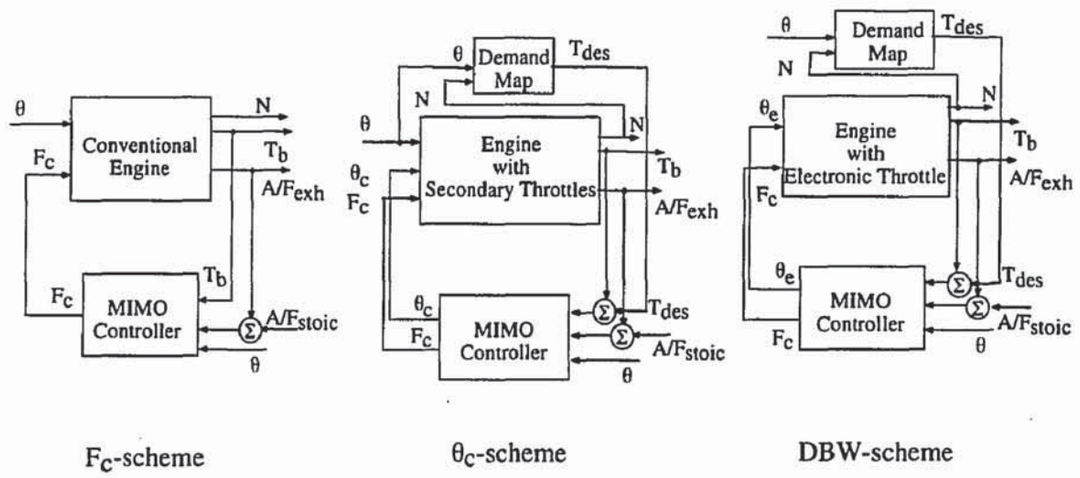


Figure 2.6: Schematic representation of the three control schemes.

The multivariable control law used for all the three designs is based in LQG design methodology. Robustness of the three control designs to actuator uncertainty is an important issue of the feasibility of the different control configurations. The engine model used in the design of the multivariable controller does not include neither θ_c actuator dynamics nor electronic throttle actuator dynamics. Furthermore, there is a great level of uncertainty in the fuel puddling dynamics. For this reason, we adjust the observer gain in all three designs so that the LQG controller can asymptotically approach the robustness properties of the LQR design.

The operating point about which we choose to linearize the engine model lies in the acceleration curve of the engine and third gear was used in the powertrain rotational dynamics. The nominal primary throttle position used was $\theta = 20°$, and the nominal set-point for the secondary throttles was 61% open, resulting in manifold pressure $P_m = 0.96$ bar. The air flow into the cylinders was 15.4 g/sec at 3000 RPM producing 31.5 Nm of torque. The same amount of torque is produced by the conventional engine at a primary throttle position of $\theta = 11.8°$, with a manifold pressure of 0.51 bar. Note that this operating point falls into the low control authority region explained in Section 2.3.

PETITIONER'S EXHIBIT 1002
US PATENT NO. 6,557,540

2.6.1 Feedback Control Design using Secondary Throttles.

The engine model with the secondary throttles is linearized at throttle position equal to 20 degrees, secondary throttles equal to 61% open, engine speed equal at 3000 rpm. The state variables of the linearized model are manifold pressure, A/F at the EGO sensor, mass air flow, angular velocity, fuel puddle, and states associated with second order Padé approximation of the delays in the processes and signals. The state space representation of the linearized model of the engine with the secondary throttles is given by :

$$\dot{x}(t) = Ax(t) + Bu(t) + B_r r(t)$$
$$y(t) = Cx(t)$$

$$\text{where } u = \begin{bmatrix} \theta_c \text{ (sec. throttles)} \\ F_c \text{ (fuel command)} \end{bmatrix}, \quad r = \theta \text{ (primary throttle)},$$

$$\text{and } y = \begin{bmatrix} T_b & \text{(torque meas.)} \\ A/F_{exh} & \text{(meas. at the EGO sensor)} \end{bmatrix},$$

and

$$A = \begin{bmatrix} -0.079 & 139.786 & 0 & 0 & 0 & -1.013 & 0 & 0 & 0 & 0 & 0 \\ 0.019 & -100 & 10.7952 & 0 & 0 & 0 & 0 & 0 & 0 & 0 & 0 \\ -0.0289 & 0 & -74.61 & 0 & 0 & 0 & 0 & 0 & 0 & 0 & 0 \\ 0 & 0 & 0 & -6.667 & 0 & 2 & 0 & 0 & 0 & 0 & 0 \\ -0.0001 & 0 & -0.485 & 0 & -7.692 & 0 & 0 & 0 & 0 & 0 & 0 \\ 0 & 0 & 0.01 & 0 & -1.587 & -0.001 & 0 & 0 & 0 & 0 & -2.529 \\ 0 & 0 & 0 & 0 & 0 & 0 & 61.40 & 288.55 & 0 & 0 & 0 \\ 0 & 0 & 0 & 0 & 0 & 0 & -0.0333 & 0.20 & 5.067 & 0 & 0 \\ 0 & 0 & 0 & 333.33 & 0 & 0 & 0 & -33.33 & -566.667 & 0 & 0 \\ 0. & 0. & 0. & 0. & 0. & 0. & 0. & 0. & 2. & -5. & 0. \\ 0 & 0 & 0 & 0 & 3.846 & 0 & 0 & 0 & 0 & 0 & -10. \end{bmatrix},$$

$$B = \begin{bmatrix} 0 & 0 \\ 25.9675 & 0 \\ -10.2811 & 0 \\ 0 & 0 \\ 0 & 0 \\ 2.361e+03 & -8.254e+04 \\ 0. & 0. \\ 0. & 0. \\ 0. & 0. \\ 0. & 0. \\ 0. & 2. \end{bmatrix}, \quad B_r = \begin{bmatrix} 0 \\ 0.4908 \\ 0.3622 \\ 0 \\ 0.0038 \\ 44.6284 \\ 0 \\ 0 \\ 0 \\ 0 \end{bmatrix},$$

$$C = \begin{bmatrix} -0.0231 & 410.86 & 0 & 0 & 0 & -2.978 & 0 & 0 & 0 & 0 & 0 \\ 0 & 0 & 0 & 0 & 0 & 0 & 0 & 0 & 0 & 2.5 & 0 \end{bmatrix}.$$

During changes in throttle position, it is important to maintain A/F at stoichiometry and maintain zero tracking error in the torque response. This is accomplished by augmenting

PETITIONER'S EXHIBIT 1002
US PATENT NO. 6,557,540

the state vector with the integral of the error in the A/F response ($\dot{q}_2 = A/F_{stoic} - A/F_{exh}$), and the integral of the error in the torque response ($\dot{q}_1 = T_{b_{des}} - T_{b_m}$):

$$\dot{q} = y - \begin{bmatrix} T_{b_{des}} \\ A/F_{stoic} \end{bmatrix} . \tag{2.13}$$

We augment the input and state vector as follows :

$$\hat{r} = \begin{bmatrix} \theta \\ T_{b_{des}} \\ A/F_{stoic} \end{bmatrix} , \text{ and } \hat{x} = \begin{bmatrix} x \\ q \end{bmatrix}. \tag{2.14}$$

The resulting augmented system is :

$$\underbrace{\begin{bmatrix} \dot{x} \\ \dot{q} \end{bmatrix}}_{\dot{\hat{x}}} = \underbrace{\begin{bmatrix} A & 0 \\ C & 0 \end{bmatrix}}_{\hat{A}} \underbrace{\begin{bmatrix} x \\ q \end{bmatrix}}_{\hat{x}} + \underbrace{\begin{bmatrix} B \\ 0 \end{bmatrix}}_{\hat{B}} u + \underbrace{\begin{bmatrix} B_r & 0 \\ 0 & -I \end{bmatrix}}_{\hat{B}_r} \hat{r}, . \tag{2.15}$$

The controller feedback gain

$$u = -K\hat{x} = \begin{bmatrix} -K_1 & -K_2 \end{bmatrix} \begin{bmatrix} x \\ q \end{bmatrix}$$

is found by solving the LQR problem. The weighting matrices R_{xx} and R_{uu} in the minimization of the cost function

$$J = \int_0^\infty (x' R_{xx} x + u' R_{uu} u)\, dt$$

were tuned so that the closed loop objectives (defined in Section 2.6) are satisfied. The resulting K_1 and K_2 feedback gains are :

$$K_1 = \begin{bmatrix} 0.0004 & 0.0411 & 0.0060 & 0.0156 & -0.0173 & 0.0000 & 0.0000 & 0.0000 & 0.0004 & 0.0190 & -0.0352 \\ 0.0000 & 0.0023 & -0.0122 & -0.0247 & 1.8198 & -0.0004 & -0.0001 & -0.0001 & -0.0014 & -0.0810 & 2.5977 \end{bmatrix}$$

$$K_2 = \begin{bmatrix} 0.0099 & 0.0450 \\ 0.0014 & -0.3130 \end{bmatrix} . \tag{2.16}$$

For the complete LQG/LTR controller design we need to estimate the states (x) using an Kalman filter. The real symmetric positive semi-definite matrix representing the intensities of the state noises Q_{xx}, and the real symmetric positive definite matrix representing the intensities of the measurement noises Q_{yy} were assumed diagonal. Loop transfer recovery

PETITIONER'S EXHIBIT 1002
US PATENT NO. 6,557,540

in the input was employed and the resulting observer gain is given by :

$$L = \begin{bmatrix} 0.2582 & -0.6951 \\ 0.0001 & -0.0001 \\ -0.0001 & 0.0003 \\ -0.4108 & 0.3324 \\ 0.0016 & 0.0000 \\ -6.3386 & 0.2615 \\ -56.4934 & 79.6739 \\ 6.4796 & -18.2527 \\ -0.5916 & 1.2789 \\ -0.0322 & 0.4568 \\ 0.0018 & -0.0001 \end{bmatrix}. \tag{2.17}$$

The combined observer and controller state-space representation is described by the following equations:

$$\begin{aligned} \dot{x}_e &= Ax_e + Bu + B_r r_1 + L(y - y_e) \\ y_e &= Cx_e \\ u &= -K_1 x_e - K_2 q \\ \dot{q} &= y - \begin{bmatrix} r_2 \\ r_3 \end{bmatrix} \quad , \text{ where } x_e \text{ is the estimated state,} \end{aligned} \tag{2.18}$$

and finally,

$$\begin{aligned} \frac{d}{dt}\begin{bmatrix} x_e \\ q \end{bmatrix} &= \begin{bmatrix} A - LC - BK_1 & -BK_2 \\ 0 & 0 \end{bmatrix}\begin{bmatrix} x_e \\ q \end{bmatrix} + \begin{bmatrix} L \\ I \end{bmatrix} y + \begin{bmatrix} B_r & 0 \\ 0 & -I \end{bmatrix} \hat{r} \\ u &= \begin{bmatrix} -K_1 & -K_2 \end{bmatrix}\begin{bmatrix} x_e \\ q \end{bmatrix} . \end{aligned} \tag{2.19}$$

2.6.2 Fuel Feedback Control Design.

The control structure of the conventional fuel control configuration is shown in Section 2.6. We used the engine model described in Section 2.2 without the secondary throttles. The model is linearized at throttle position equal to 11.8 degrees, and engine speed equal at 3000 rpm. The state space representation of the linearized model is given by:

$$\begin{aligned} \dot{x}(t) &= Ax(t) + Bu(t) + B_r r(t) \\ y(t) &= cx(t) \end{aligned}$$

where $u = F_c$ (fuel command), $r = \theta$ (primary throttle) , and
$y = A/F_{exh}$ (meas. at the EGO sensor),

PETITIONER'S EXHIBIT 1002
US PATENT NO. 6,557,540

$$A = \begin{bmatrix} -0.079 & 139.785 & 0 & 0 & 0 & -1.013 & 0 & 0 & 0 & 0 \\ 0.0173 & -100 & 26.852 & 0 & 0 & 0 & 0 & 0 & 0 & 0 \\ -0.0280 & 0 & -10.908 & 0 & 0 & 0 & 0 & 0 & 0 & 0 \\ 0 & 0 & 0 & -6.67 & 0 & 2 & 0 & 0 & 0 & 0 \\ -0.0001 & 0 & -0.0019 & 0 & -7.692 & 0 & 0 & 0 & 0 & 0 \\ 0 & 0 & 0.024 & 0 & -1.5874 & -0.001 & 0 & 0 & -2.53 & 0 \\ 0. & 0. & 0. & 0. & 0. & 0. & 100. & 900. & 0. & 0. \\ 0 & 0 & 0 & -222.2 & 0 & 0 & -33.3 & -233.3 & 0 & 0 \\ 0. & 0. & 0. & 0. & 0. & 0. & 0. & 2. & -5. & 0. \\ 0 & 0 & 0 & 0 & 3.84 & 0 & 0 & 0 & 0 & -10 \end{bmatrix},$$

$$B = \begin{bmatrix} 0 \\ 0 \\ 0 \\ 0 \\ 0 \\ -8254.3 \\ 0 \\ 0 \\ 0 \\ 2 \end{bmatrix}, \quad B_r = \begin{bmatrix} 0.0000 \\ 0.0000 \\ 0.8710 \\ 0.0000 \\ 0.0060 \\ 0.0000 \\ 0.0000 \\ 0.0000 \\ 0.0000 \\ 0.0000 \end{bmatrix},$$

$$c = \begin{bmatrix} 0 & 0 & 0 & 0 & 0 & 0 & 0 & 0 & 2.5000 & 0 \end{bmatrix}.$$

The control objective in the conventional engine (A/F control is based on regulating the fuel flow) is to maintain A/F at stoichiometry during changes in pedal position. For this reason, we used integral control, and the augmented the input and state vector are given by :

$$\hat{r} = \begin{bmatrix} \theta \\ A/F_{stoic} \end{bmatrix}, \text{ and } \hat{x} = \begin{bmatrix} x \\ q \end{bmatrix}. \tag{2.20}$$

The resulting augmented system is :

$$\underbrace{\begin{bmatrix} \dot{x} \\ \dot{q} \end{bmatrix}}_{\dot{\hat{x}}} = \underbrace{\begin{bmatrix} A & 0 \\ c & 0 \end{bmatrix}}_{\hat{A}} \underbrace{\begin{bmatrix} x \\ q \end{bmatrix}}_{\hat{x}} + \underbrace{\begin{bmatrix} B \\ 0 \end{bmatrix}}_{\hat{B}} u + \underbrace{\begin{bmatrix} B_r & 0 \\ 0 & -1 \end{bmatrix}}_{\hat{B}_r} \hat{r}, \tag{2.21}$$

We set the LQR problem and adjusted the R_{xx} and R_{uu} of the cost function to minimize the A/F excursions. The resulting controller feedback gains are given by :

$$\begin{aligned} K_1 &= \begin{bmatrix} 0 & 0 & -0.027 & -0.035 & 1.877 & -0.0006 & 0.0016 & 0.0045 & -0.195 & 2.801 \end{bmatrix} \\ k_2 &= -0.9487\,. \end{aligned} \tag{2.22}$$

We assumed that torque measurements are available to better estimate the states. In the observer design we accounted for the fuel puddling dynamics by adjusting the Kalman filter

PETITIONER'S EXHIBIT 1002
US PATENT NO. 6,557,540

gain using loop transfer recovery in the input. The resulting observer gain is :

$$L = \begin{bmatrix} 0.3080 & -0.8831 \\ 0.0001 & 0.0004 \\ -0.0001 & 0.0022 \\ -0.5737 & 0.3602 \\ 0.0059 & 0.0000 \\ -20.1610 & 0.0494 \\ 4.7225 & -12.2339 \\ -0.0597 & 1.4371 \\ 0.0019 & 0.5101 \\ 0.0066 & 0.0000 \end{bmatrix}. \tag{2.23}$$

The combined observer and controller state-space representation is described by the following equations:

$$\begin{aligned} \dot{x}_e &= Ax_e + Bu + B_r r_1 + L(y - y_e) \\ y &= \begin{bmatrix} T_b \\ A/F_{exh} \end{bmatrix} = Cx_e \\ u &= -K_1 x_e - k_2 q \\ \dot{q} &= A/F_{exh} - r_2 = [0,1] \cdot y - r_2 \quad \text{where } x_e \text{ is the estimated state,} \end{aligned} \tag{2.24}$$

and finally,

$$\begin{aligned} \frac{d}{dt}\begin{bmatrix} x_e \\ q \end{bmatrix} &= \begin{bmatrix} A - LC - BK_1 & -Bk_2 \\ 0 & 0 \end{bmatrix}\begin{bmatrix} x_e \\ q \end{bmatrix} + \begin{bmatrix} L \\ 0 \quad 1 \end{bmatrix} y + \begin{bmatrix} B_r & 0 \\ 0 & -1 \end{bmatrix} \hat{r} \\ u &= \begin{bmatrix} -K_1 & -k_2 \end{bmatrix}\begin{bmatrix} x_e \\ q \end{bmatrix}. \end{aligned} \tag{2.25}$$

2.6.3 Feedback Control Design using Electronic Throttle.

In an engine equiped with a electronic throttle, the driver controls the accelerator pedal position, but the actual throttle position that regulates the air flow into the manifold is electronically controlled. The engine model described in Section 2.2 is modified to include the new control command, and linearized at throttle position equal to 11.8 degrees, engine speed equal at 3000 rpm. The state space representation of the linearized model is given by :

$$\begin{aligned} \dot{x}(t) &= Ax(t) + Bu(t) \\ y(t) &= Cx(t) \end{aligned} \tag{2.26}$$

where $u = \begin{bmatrix} \theta_e \text{ (electr. thr. command)} \\ F_c \text{ (fuel command)} \end{bmatrix}, y = \begin{bmatrix} T_b & \text{(torque measurement)} \\ A/F_{exh} & \text{(meas. at the EGO sensor)} \end{bmatrix},$

PETITIONER'S EXHIBIT 1002
US PATENT NO. 6,557,540

and

$$A = \begin{bmatrix} -100 & 26.852 & 0 & 0 & 0 & 0 & 0 & 0 & 0.017 & 0 \\ 0 & -10.908 & 0 & 0 & 0 & 0 & 0 & 0 & -0.028 & 0 \\ 0 & 0 & -6.667 & 0 & 2 & 0 & 0 & 0 & 0 & 0 \\ 0 & -0.002 & 0 & -7.692 & 0 & 0 & 0 & 0 & -0.0001 & 0 \\ 0 & 244.19 & 0 & -1.587e+05 & 0 & 0 & 0 & 1.575 & 0 & 0 \\ 0 & 0 & 0 & 0 & 0 & 100 & 900 & 0 & 0 & 0 \\ 0 & 0 & -222.22 & 0 & 0 & -33.33 & -233.33 & 0 & 0 & 0 \\ 0. & 0. & 0. & 0. & 0. & 0. & 2. & -5. & 0. & 0. \\ 139.786 & 0 & 0 & 0 & -1.013 & 0 & 0 & 0 & -0.076 & 0 \\ 0 & 0 & 0 & 3.846 & 0 & 0 & 0 & 0 & 0 & -10 \end{bmatrix},$$

$$B = \begin{bmatrix} 0.0000 & 0.0000 \\ 0.8710 & 0.0000 \\ 0.0000 & 0.0000 \\ 0.0060 & 0.0000 \\ 0.0000 & -82543 \\ 0. & 0 \\ 0. & 0. \\ 0. & 0. \\ 0. & 0. \\ 0. & 2. \end{bmatrix}, C = \begin{bmatrix} 410.86 & 0 & 0 & 0 & -2.978 & 0 & 0 & 0 & 0.023 & 0 \\ 0 & 0 & 0 & 0 & 0 & 0 & 0 & 2.5 & 0 & 0 \end{bmatrix}.$$

Changes in the accelerator pedal position imposed by the driver represent changes in the demanded torque. In the case of electronically throttled engine, the driver is disconnected from the engine, and does not cause "disturbances" in the A/F loop. However, we have to maintain good engine torque response to satisfy drivability requirements. This is accomplished by augmenting the states with the integral of the error in the torque response. In this control scheme, A/F control is limited only by sensor/actuator limitations and uncertainties in the modeling. The integrated states, the input vector, and the augmented state vector are given by:

$$\dot{q} = y - \begin{bmatrix} T_{b_{des}} \\ A/F_{stoic} \end{bmatrix}, \quad r = \begin{bmatrix} T_{b_{des}} \\ A/F_{stoic} \end{bmatrix}, \quad \text{and } \hat{x} = \begin{bmatrix} x \\ q \end{bmatrix}. \tag{2.27}$$

The resulting augmented system is :

$$\underbrace{\begin{bmatrix} \dot{x} \\ \dot{q} \end{bmatrix}}_{\dot{\hat{x}}} = \underbrace{\begin{bmatrix} A & 0 \\ C & 0 \end{bmatrix}}_{\hat{A}} \underbrace{\begin{bmatrix} x \\ q \end{bmatrix}}_{\hat{x}} + \underbrace{\begin{bmatrix} B \\ 0 \end{bmatrix}}_{\hat{B}} u + \underbrace{\begin{bmatrix} 0 \\ -I \end{bmatrix}}_{\hat{B}_r} r, \tag{2.28}$$

The control design followed is similar to the earlier design in Section 2.6.1. The controller feedback gains are given by :

$$K_1 = \begin{bmatrix} 0.4046 & 0.9368 & 0.1478 & -0.0005 & 0.00 & -0.0016 & -0.0047 & 0.1574 & -0.0233 & -0.0009 \\ 2.7691 & -0.8089 & -0.5292 & 1.9192 & -0.0290 & 0.0199 & 0.0551 & -2.277 & -0.0005 & 3.0441 \end{bmatrix}$$

$$K_2 = \begin{bmatrix} 0.1000 & 0.3135 \\ 0.0031 & -9.9951 \end{bmatrix}, \tag{2.29}$$

PETITIONER'S EXHIBIT 1002
US PATENT NO. 6,557,540

and the observer gain L is given by :

$$L = \begin{bmatrix} 0.0000 & 0.0004 \\ -0.0001 & 0.0020 \\ -0.4094 & 0.3463 \\ 0.0016 & 0.0000 \\ -6.3390 & 0.3095 \\ 7.3912 & -11.4118 \\ -0.5880 & 1.3235 \\ -0.0300 & 0.4716 \\ 0.2397 & -0.8408 \\ 0.0018 & -0.0001 \end{bmatrix}. \tag{2.30}$$

The combined observer and controller state-space representation is given by :

$$\begin{aligned} \dot{x}_e &= Ax_e + Bu + L(y - y_e) \\ y_e &= Cx_e \\ u &= -K_1 x_e - K_2 q \\ \dot{q} &= y - \begin{bmatrix} r_1 \\ r_2 \end{bmatrix} \quad \text{where } x_e \text{ is the estimated state,} \end{aligned} \tag{2.31}$$

and finally,

$$\begin{aligned} \frac{d}{dt}\begin{bmatrix} x_e \\ q \end{bmatrix} &= \begin{bmatrix} A - LC - BK_1 & -BK_2 \\ 0 & 0 \end{bmatrix}\begin{bmatrix} x_e \\ q \end{bmatrix} + \begin{bmatrix} L \\ I \end{bmatrix} y + \begin{bmatrix} 0 \\ -I \end{bmatrix} r \\ u &= \begin{bmatrix} -K_1 & -K_2 \end{bmatrix}\begin{bmatrix} x_e \\ q \end{bmatrix}. \end{aligned} \tag{2.32}$$

2.7 Simulation Example.

The purpose of this example is to illustrate some of the properties of the closed loop system using the secondary throttles, and compare them with the conventional fuel control scheme, and the electronic throttle control scheme. Figure 2.7 is a simulation of the nominal response of the θ_c-scheme and the F_c-scheme for a 10% step change in primary throttle position, which corresponds to 16% step change in torque demand. The θ_c-scheme has $\pm 0.14\%$ A/F excursion and essentially zero A/F and torque error after 50 intake events. A dynamic model of the catalytic converter is needed to evaluate the effects of these A/F excursions to tailpipe emissions. The dynamic catalytic converter response depends on the amplitude and the frequency of the A/F excursions, and a control oriented model of this behavior is not available. The integrated error of A/F during a rapid throttle movement can be used, however, as a measurement of engine emissions during that period. The integrated error of A/F for the F_c-scheme is 0.0402 and for the θ_c-scheme is 0.0051, which indicates a possible reduction of engine emissions. Also, the engine reaches the specified torque faster than in the F_c-scheme, improving drivability significantly. Note that the conventional fuel pulsewidth duration control does not affect the torque performance of the engine.

PETITIONER'S EXHIBIT 1002
US PATENT NO. 6,557,540

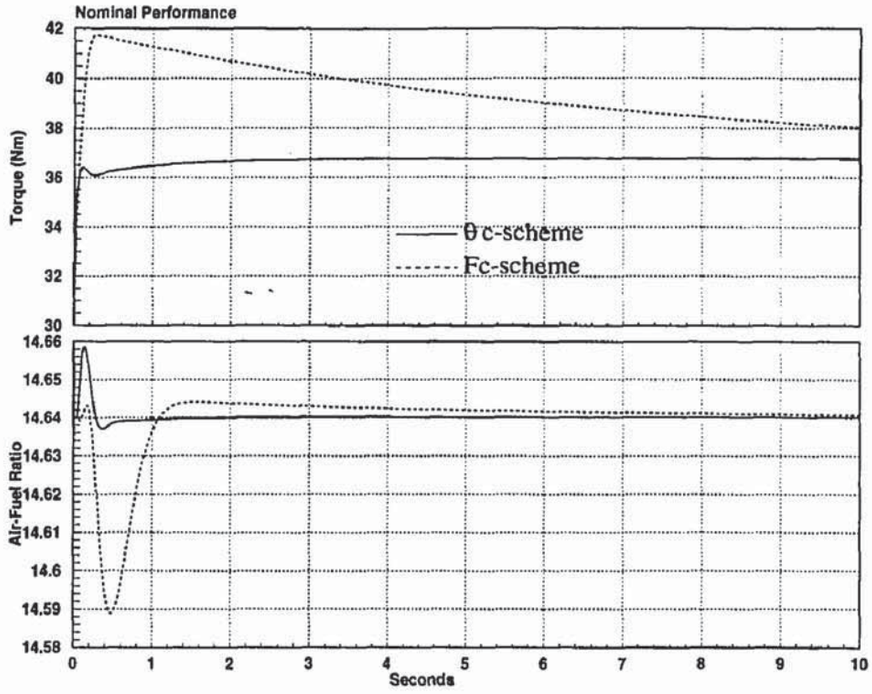


Figure 2.7: Simulation of the θ_c-scheme and F_c-scheme.

The simulation in Fig. 2.8 demonstrates the torque tracking performance of the proposed scheme in comparison with the DBW-scheme. The emissions performance is equivalent in the two systems. Both responses are well within the high-efficiency window of the catalyst, though the absence of the lean spike in the A/F in tip-in conditions in the DBW-scheme is immediately noticeable. In DBW throttle systems the engine is decoupled from the disturbances caused by the rapid throttle movements which are imposed by the driver. The closed loop system has the feature of isolating the high bandwidth torque demands by breaking the linkage between the driver and the primary throttles, facilitating smooth A/F control during transient engine operation. To achieve the same good A/F results we will need to form a smoother torque response in the engine.

The performance of the θ_c-scheme was also tested under uncertainty in the fuel puddling dynamics due to its importance in accurate transient A/F control. Figure 2.9 shows the torque and A/F response of the above control schemes using a time constant of 0.2 sec in the puddling dynamics (see Section 2.2). The simulation results show a limited performance degradation of the closed loops, however the θ_c-scheme maintains the improvement of the torque response better than the other two methods. We have the same comparative results between the F_c-scheme and the θ_c-scheme: integrated A/F error in F_c-scheme is 0.0547, and in θ_c-scheme is 0.0084. The A/F response of the DBW-scheme slightly degrades and the A/F integrated error is 0.0085. Therefore, the θ_c-scheme maintains emissions results

PETITIONER'S EXHIBIT 1002
US PATENT NO. 6,557,540

comparable to the DBW-scheme.

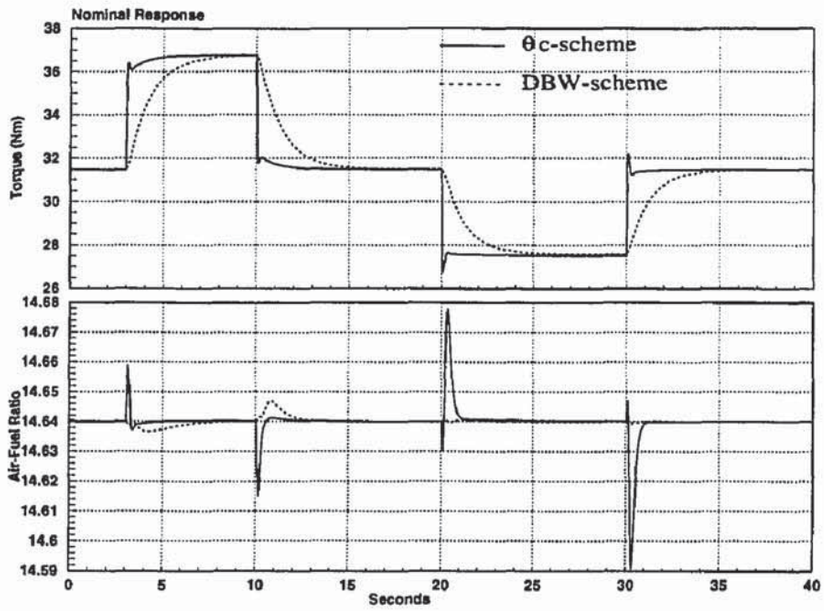


Figure 2.8: Closed loop response of the θ_c-scheme and DBW-scheme for a square wave in the demanded torque.

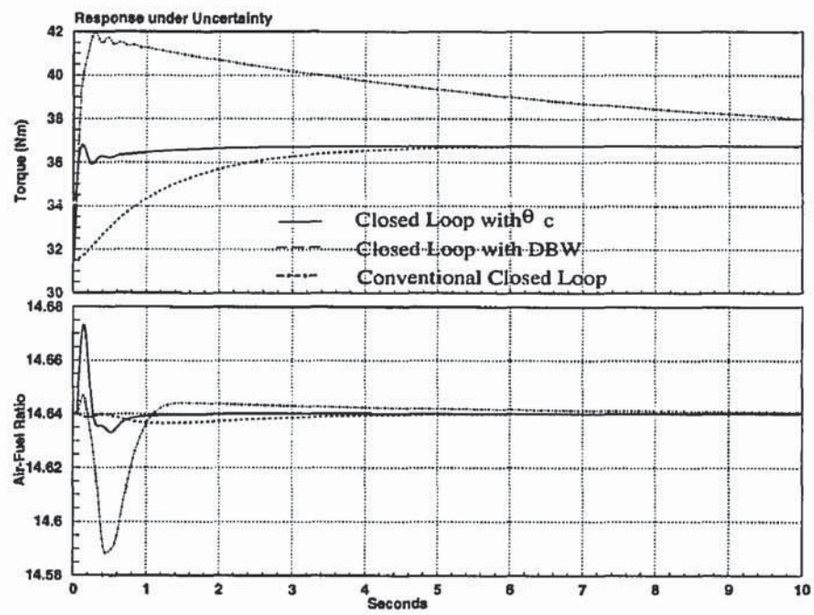


Figure 2.9: Closed loop performance under uncertainty in the fuel puddling dynamics.

PETITIONER'S EXHIBIT 1002
US PATENT NO. 6,557,540

2.8 Conclusions.

In this chapter, we investigated a control scheme for transient A/F and torque control during rapid changes in the throttle position. The air and fuel management scheme based on the secondary throttles seems promising in enhancing the engine performance. This work is very important in understanding the breathing process dynamics and its nonlinear behavior. The developed control scheme addresses the principles of controlling the breathing process which is a fundamental process to emissions, fuel economy, and torque response. The secondary throttles can be replaced by electronically controlled intake valves. Variable intake valve timing and lift is a special case of a camless engine, and the modeling and control design of the engine with the secondary throttles contributes to the development of dynamically controlled camless engines. Another special case of the camless engine is an engine with variable camshaft timing that allows control of the intake and exhaust valve timing with fixed overlap. This topic will be pursued in the following chapters.

PETITIONER'S EXHIBIT 1002
US PATENT NO. 6,557,540

CHAPTER 3

Modeling of Variable Cam Timing Engine.

3.1 Introduction to the VCT Engine Control Problem.

Variable cam timing schemes have been studied extensively and have been found to reduce emissions [45, 79] increase fuel economy [21, 41, 26] and improve full load performance [40]. The primary emphasis of this work is on reducing emissions while satisfying drivability requirements at part load and medium engine speed. Variable cam timing can inhibit the production of oxides of nitrogen (NO_x) and reduce the amount of unburned hydrocarbons (HC) emitted to the exhaust system [45]. By retarding the cam timing, combustion products which would otherwise be expelled during the exhaust stroke are retained in the cylinder during the subsequent intake stroke. The contribution of this diluent to the mixture in the cylinder reduces the combustion temperature and suppresses NO_x formation. In addition, this process often reduces HC emissions since the internally recirculated exhaust gas subjected to the additional combustion cycle is generally from the crevice volumes at the piston/cylinder wall interface and is rich in unburned HC. The effect is to reduce the base HC and NO_x emission levels of the engine with respect to a conventional powerplant, resulting in lower tailpipe emissions at equivalent catalytic converter efficiencies. Of course, VCT obviates the requirement for external exhaust gas recirculation (EGR) systems commonly used for NO_x reduction. Furthermore, by retarding the cam phasing, the amount of fresh air into the cylinder is reduced. This results in the need for a higher manifold pressure in order to maintain the same load. Operation in high manifold pressure is advantageous since it is associated with reduced intake stroke pumping work [31, 83], and therefore, increased fuel economy. One type of VCT engine utilizes a hydraulically actuated mechanism to rotate the camshaft relative to the crankshaft and advance the valve timing with respect to the engine induction and exhaust strokes. This is illustrated in the valve lift profiles shown in Fig. 3.1.

The goal in the following chapters is twofold: (i) reduce feedgas NO_x and HC emissions, and (ii) provide satisfactory torque response to meet vehicle and customer performance requirements during changes in throttle position. Rapid throttle movements reflect the driver's demand for changes in torque and vehicle acceleration, and strongly influence the

PETITIONER'S EXHIBIT 1002
US PATENT NO. 6,557,540

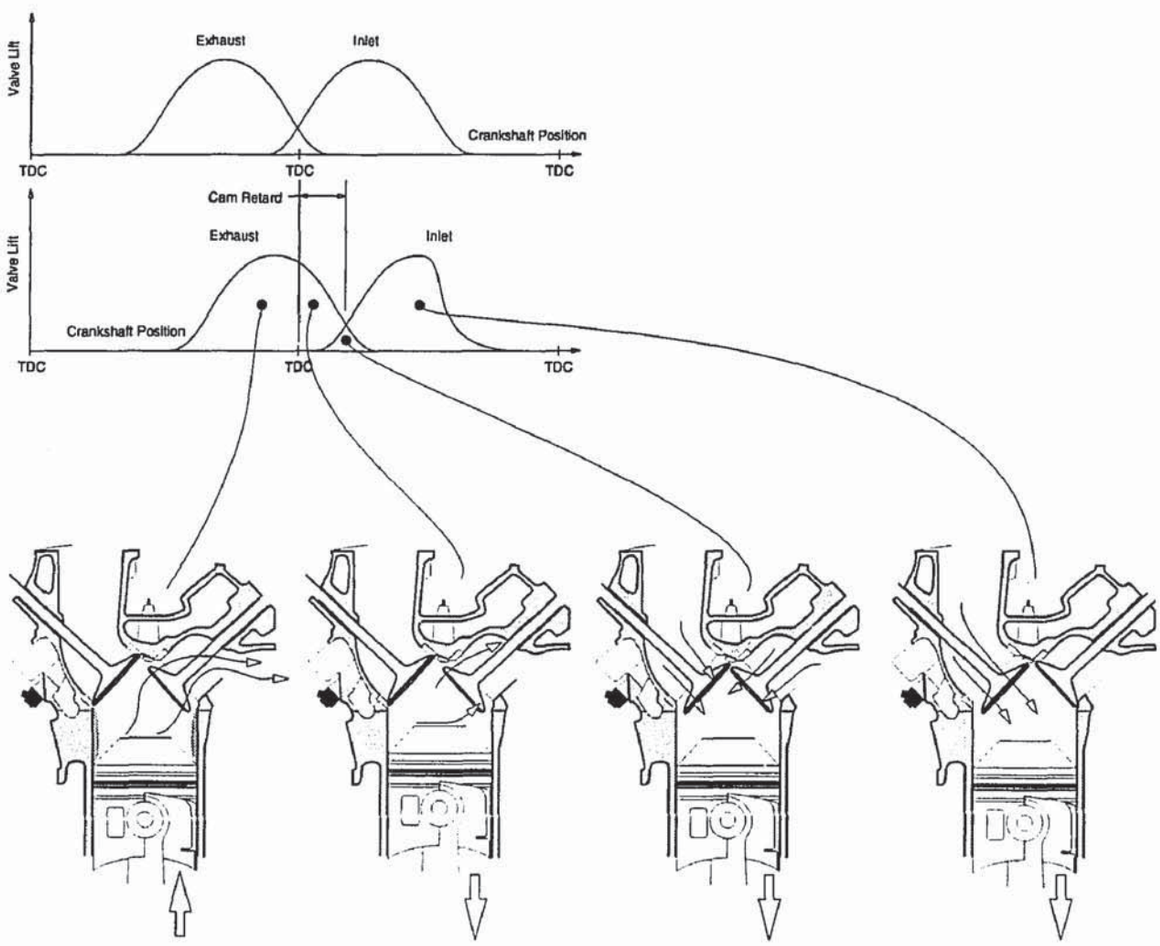


Figure 3.1: Valve lift profiles of a conventional and a variable cam timing engine. By retarding the cam phasing the exhaust valve stays open during the intake event for a longer time period. This causes the induction and reburn of the last part of the exhaust gases which is rich in unburned HC. The resulting diluent, also, lowers the combustion temperature and suppresses feedgas NO_x emissions. The amount of reduction will vary with engine speed and load.

PETITIONER'S EXHIBIT 1002
US PATENT NO. 6,557,540

cylinder air charging process, mixture formation and transient performance of the engine. For both tailpipe HC and NO_x emissions, the primary control objectives are to (i) reduce the NO_x and HC feedgas by changing the cam timing of the engine, and (ii) maintain the A/F at stoichiometry at all times since this corresponds to the point of maximum efficiency of the catalytic converter. The additional complexity is that rapid throttle movements imposed by the driver are now accompanied by changes in cam phasing in order to minimize the amount of NO_x and HC in the feedgas. These changes affect the cylinder air charge, and can cause large A/F excursions which makes the task of A/F control even more challenging.

3.2 Dynamic Engine Model.

The development of a control-oriented model involves the understanding of the region of interest and the input-output relationship that need to be identified (see Fig. 3.2). Details about the region of interest can be found in Appendix A.

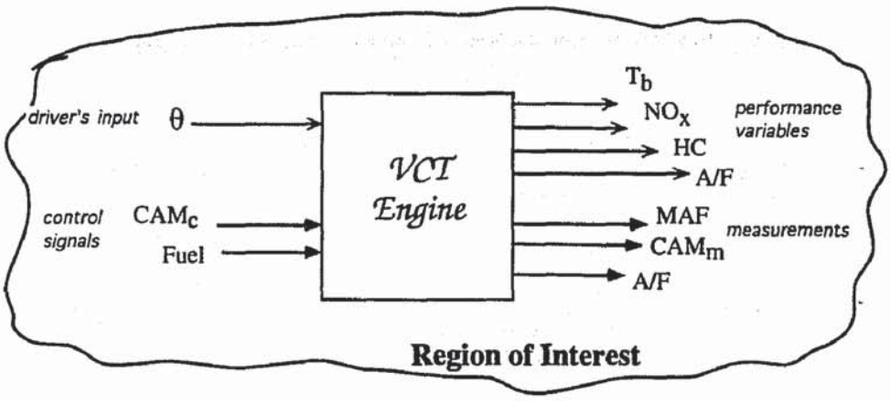


Figure 3.2: Schematic representation of the unknown input-output relationship of the VCT engine over the region of interest.

The VCT engine model is derived based on physical principles and described by measurable parameters. It is a continuous, nonlinear, low-frequency[1], phenomenological representation of an eight cylinder experimental VCT engine, based on [16], with appropriate modifications for variable cam timing.

The dynamic elements of the engine model are described by physically based equations, whereas the pseudo-static elements are described by empirically based expressions as in [16]. The structure of the VCT engine model was identified by engine-dynamometer experiments; the VCT mechanism was found to alter the mass air flow into the cylinders, the self EGR, the engine torque response, and exhaust emissions. The mass air flow through the throttle body, engine pumping rate, brake torque generation and feedgas NO_x and HC emissions

[1]This model represents dynamics averaged over an engine event.

PETITIONER'S EXHIBIT 1002
US PATENT NO. 6,557,540

generation are complex functions, depend on many engine parameters, and are difficult to model analytically, so they are included as nonlinear static empirical relations. Their parameters are determined from regressed dynamometer-engine steady-state data using the least squares approach. Physically based differential and difference equations are used to describe the dynamic elements of the engine, such as inlet manifold dynamics and the delayed processes in the signal paths. The identification of these parameters is based on the dynamic response of the experimental engine mounted in thedynamometer to small step inputs. Furthermore, the model includes actuator and sensor dynamics, and some important computational delays. The following subsections describe each of the engine components, and, at the end of this chapter, the identified model is validated against actual engine-dynamometer data.

3.2.1 Breathing Process.

The model of the breathing process is a very important part of the engine modeling task because it affects most engine performance indices: fuel economy, emissions, drivability. The dynamic equation for the manifold is based on the principles of conservation of mass, thermodynamic energy and momentum which are satisfied by assuming uniform pressure and temperature in the plenum between the throttle body and the intake valves. To use the state equation, the air into the intake manifold is assumed to be homogeneous. The model of the breathing process is based on an averaged representation over an engine event and does not allow the study of high frequency phenomena as acoustic and inertia effects that occur during the intake stroke [48].

Based on the previous assumptions the manifold acts as a plenum, and its dynamics can be described by the following first order differential equation (as in [16]) that relates the rate of change of the manifold pressure (P_m) to the mass air flow rates into and out of the manifold ($\dot{m}_\theta$ and $\dot{m}_{cyl}$, respectively)

$$\frac{d}{dt}P_m = K_m(\dot{m}_\theta - \dot{m}_{cyl}), \text{ where } K_m = \frac{R \cdot T}{V_m} \quad . \tag{3.1}$$

The constant $K_m = 0.12\frac{bar}{g}$ has been identified from dynamic experimental data. Its physically based value can be derived from $K_m = \frac{R \cdot T}{V_m}$, where $R = 287\ \frac{J}{Kg \cdot K}$ the specific gas constant, $T = 288\ K$ the nominal temperature, and $V = 7\ lt = 0.007\ m^3$ the manifold volume, resulting in $K_m = 11808 \cdot 10^5\ \frac{J}{Kg \cdot m^3} = 0.118\frac{bar}{g}$.

For the derivation of the mass air flow through the throttle body, we assumed one-dimensional, steady, compressible flow of an ideal gas as developed in [56]. The mass air flow rate into the manifold ($\dot{m}_\theta$) through the primary throttle body is a function of throttle angle (θ), the upstream pressure (P_o), which we assume to be atmospheric, i.e., $P_o = 1$ bar, and the downstream pressure, which is the manifold pressure (P_m). The function describing

PETITIONER'S EXHIBIT 1002
US PATENT NO. 6,557,540

$\dot{m}_\theta$ (shown in Fig. 3.3 for different values of θ) is described by

$$\dot{m}_\theta = g_1(P_m) \cdot g_2(\theta)$$
$$g_1(P_m) = \begin{cases} 1 & \text{if } P_m \leq P_O/2 \\ \frac{2}{P_O}\sqrt{P_m P_O - P_m^2} & \text{if } P_m > P_O/2 \end{cases} \tag{3.2}$$
$$g_2(\theta) = F(1, \theta, \theta^2, \theta^3)$$

where $g_2(\theta)$ is a third order polynomial of throttle angle. The exact equation $g_2(\theta)$ can be found in Appendix B.1.

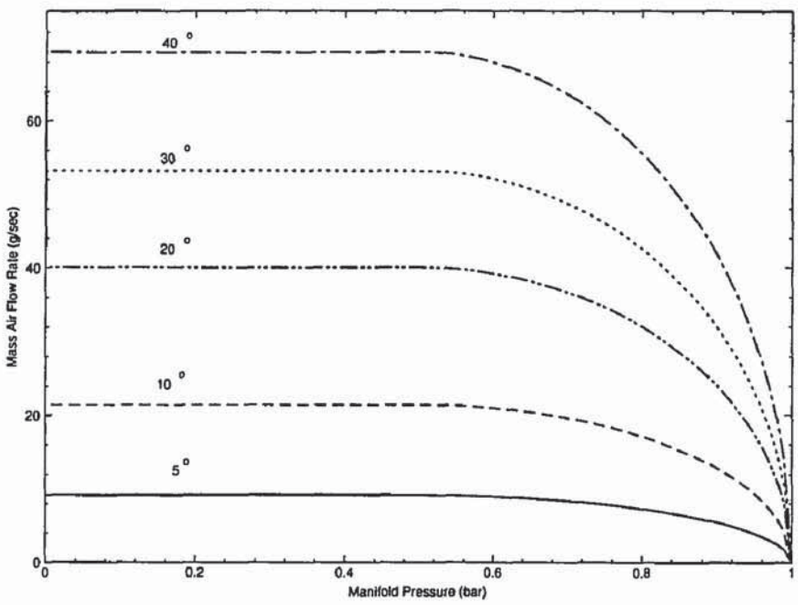


Figure 3.3: Mass air flow rate through the throttle body as a function of manifold pressure for different throttle angles. Note the two distinct operating regimes of sonic and subsonic flow.

The pulsating mass air flow out of the manifold and into the cylinders (during the intake event) is a complicated function of engine characteristics including pressure losses in the intake valve, as well as losses from the wall friction, and inertia [60]. It can be represented, however, by an empirical relationship assuming quasi-steady operating conditions, and averaging the mass air flow into the cylinders over an engine event (180 degrees of crankshaft revolution). The empirical relationship can be developed by treating the engine as a pump and assuming constant intake temperature and exhaust gas pressure. The engine pumping mass air flow rate ($\dot{m}_{cyl}$) is a function of the cam phasing (CAM), the manifold pressure (P_m), and the engine speed (N). The resulting polynomial is of degree three, and a third order polynomial in each individual variable:

$$\dot{m}_{cyl} = F(1, CAM, CAM^2, CAM^3, P_m, P_m^2, P_m^3, N, N^2, N^3) \ . \tag{3.3}$$

The exact identified polynomial can be found in Appendix B.2. Figure 3.4 shows the

PETITIONER'S EXHIBIT 1002
US PATENT NO. 6,557,540

variation of mass air flow rate with manifold pressure (P_m) for different values of cam phasing (CAM) at constant engine speed (1000 RPM).

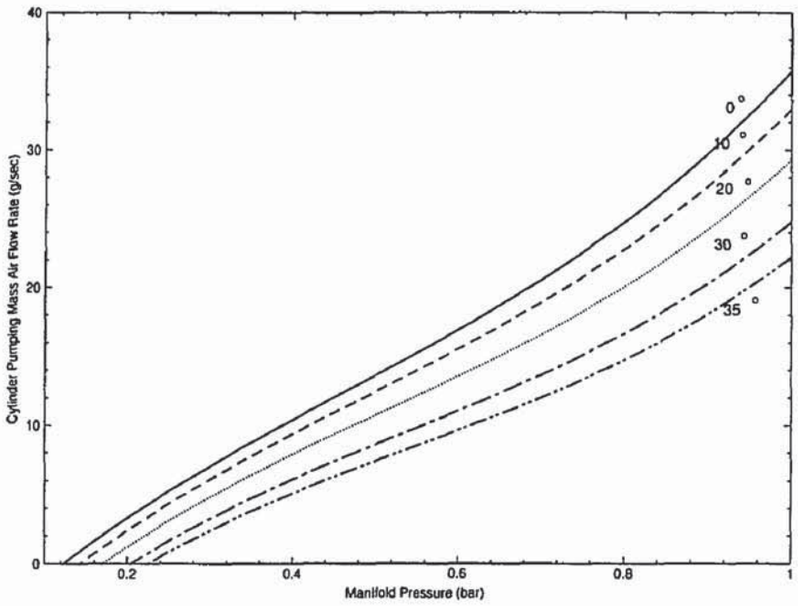


Figure 3.4: Engine pumping mass air flow rate as a function of manifold pressure for five different cam timing values.

The equilibrium of the breathing process occurs when $\dot{m}_\theta = \dot{m}_{cyl}$, and the steady-state manifold pressure and mass air flow into the cylinders is obtained at the intersection of $\dot{m}_\theta$ with $\dot{m}_{cyl}$. Figure 3.5 shows different operating conditions and the corresponding equilibrium points for several throttle positions, engine speeds and cam timings. Note that cam timing affects the steady state mass air flow the same way as the secondary throttles (see Fig. 2.3).

3.2.2 Torque Generation.

The generation of engine torque is a complex process that depends on geometric cylinder and valve features, thermodynamic properties of the unburned and burned gases, the mass and energy equation and the combustion process. The brake torque model derived in this dissertation is an empirical relationship of independent and measurable parameters by assuming fuel, air, and the residual gas uniformly mixed, and quasi-steady operation averaging the individual cylinder torque generation over one engine event. Therefore, engine torque (T_b) can be mapped as a function of the air charge (m_a), the air fuel ratio (A/F), and the engine speed (N). Spark timing is scheduled at minimum spark advance to achieve best torque (MBT). The modeled torque equation is a polynomial of degree three, and a

PETITIONER'S EXHIBIT 1002
US PATENT NO. 6,557,540

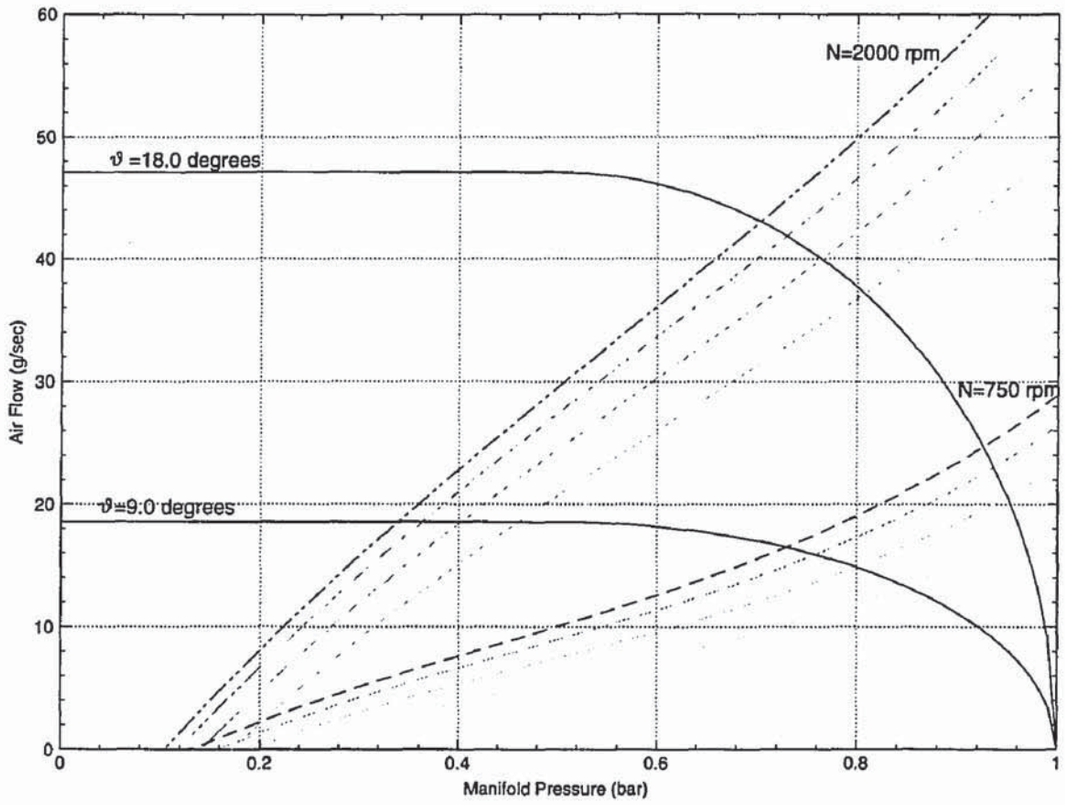


Figure 3.5: Mass air flow rate into ($\dot{m}_\theta$) and out ($\dot{m}_{cyl}$) of the manifold as a function of manifold pressure for two different engine speeds and five cam timing values ($0^o, 10^o, 20^o, 30^o$,and 35^o).

third order polynomial in each individual variable :

$$T_b = F(1, m_a, {m_a}^2, {m_a}^3, A/F, A/F^2, A/F^3, N, N^2, N^3) \quad . \tag{3.4}$$

The exact equation of brake torque is contained in Appendix B.3. The variation of torque with A/F for different values of cylinder air charge (grams per intake event) at constant engine speed (1500 RPM) is shown in Fig. 3.6.

3.2.3 Feedgas NO_x and HC emissions.

We call NO_x emissions the group of nitric oxides NO and nitric dioxides NO_2 produced inside the engine cylinder. In SI engines, experiments and chemical equilibrium considerations indicate that at typical flame temperatures NO_2/NO ratios are negligible small. The principle source of NO is the oxidation of atmospheric (molecular) nitrogen since gasoline contains negligible amounts of nitrogen. Nitric oxide forms in high-temperature burned gases. The higher the burned gas temperature the higher the rate of NO formation. Residual gas plus recycled exhaust reduce the combustion temperature, and consequently reduce the NO formation. The most important engine variables affecting NO_x are the burned gas

PETITIONER'S EXHIBIT 1002
US PATENT NO. 6,557,540

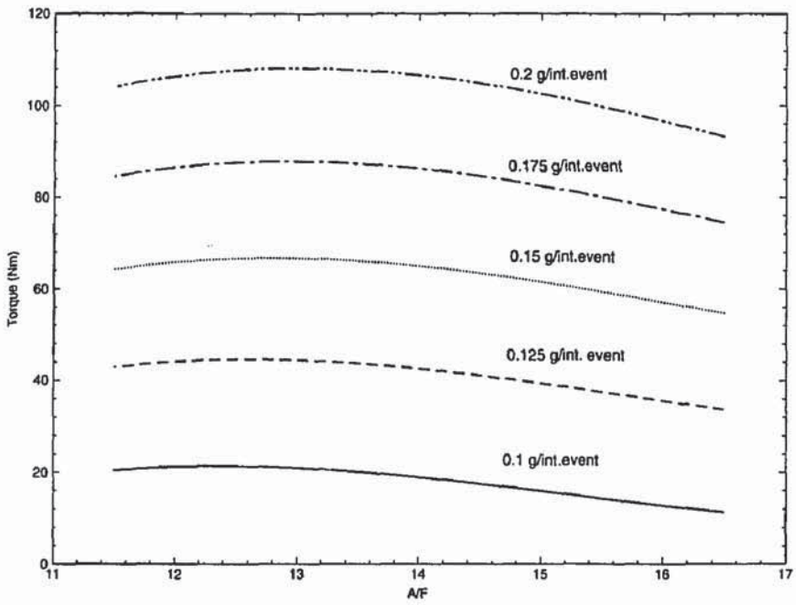


Figure 3.6: Engine torque as function of A/F for different values of air charge at constant engine speed (1500 RPM).

fraction of the unburned mixture, the A/F and the spark timing. For simplicity, the spark timing is scheduled at MBT. Regression of data from the dynamometer and the emission analyzer result in an empirical relationship for the feedgas NO_x emissions. The quasi-static NO_x can be described by a polynomial of engine speed (N), cam phasing (CAM), air fuel ratio (A/F), and manifold pressure (P_m). The four variable regression applied in the NO_x emission data results in an eighth degree polynomial. The modeled NO_x equation is a second, first, third and second order polynomial of engine speed (N), cam phasing (CAM), air fuel ratio (A/F), and manifold pressure (P_m), respectively :

$$NO_x = F_1(1, N, N^2) \cdot F_2(1, CAM) \cdot F_3(1, A/F, A/F^2, A/F^3) \cdot F_4(1, P_m, P_m^2) \quad . \tag{3.5}$$

The exact coefficients from the regression analysis can be found in Appendix B.4. Figure 3.7 shows the NO_x dependency on A/F and CAM phasing. Studies about the prediction of dynamic NO_x emissions based on the static engine mapping [80] show that the dynamic NO_x is also a function of the dynamic cylinder wall temperature. This dependency is not included in this study and might result in higher predicted NO_x emissions than the actual during an acceleration-deceleration maneuver.

Feedgas HC emissions are the result of incomplete combustion of the hydrocarbons in the fuel. HC formation is based on four complex mechanisms even under the assumption of fuel, air, and residual gas uniform mixture. The mechanism of flame quenching at the combustion chamber walls results in a layer of unburned HC attaching to the cylinder wall that is consequently scraped off by the piston off the cylinder walls [37], and exits the

PETITIONER'S EXHIBIT 1002
US PATENT NO. 6,557,540

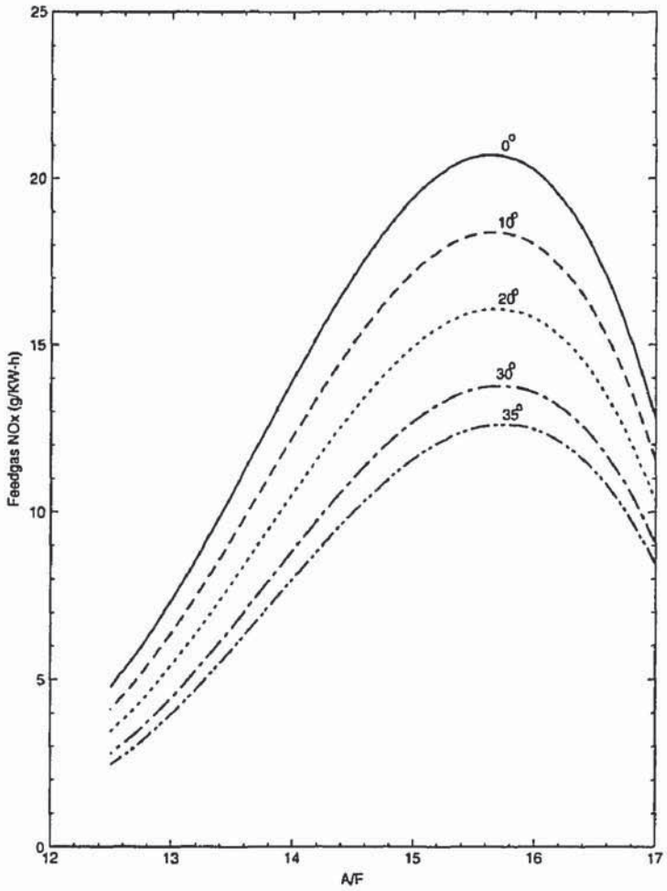


Figure 3.7: Feedgas NO_x emission plotted versus A/F for different CAM timing values at constant manifold pressure ($P_m = 0.4$ bar), and engine speed ($N = 2000$ RPM).

cylinder during the last phase of the exhaust stroke. By retarding the cam phasing we keep this last part of the exhaust gases in the cylinder and reburn it.

The feedgas HC emissions can be modeled by an empirical function of independent engine variables. The emitted amount of HC increases sharply as manifold pressure P_m decreases. For this reason the modeled HC emission equation is a polynomial of the engine speed (N), cam phasing (CAM), air fuel ratio (A/F), and inverse manifold pressure ($\frac{1}{P_m}$). Observing the data trend led us to include a term of modulated cam phasing ($\frac{CAM}{P_m \frac{1}{16}}$), which significantly improves the statistical measures of the regression analysis. The derived equation describing HC emissions is given by :

$$HC = F_1(1, N, N^2) \cdot F_2(1, A/F, A/F^2) \cdot F_3(1, \frac{1}{P_m}) + F_4(1, CAM, \frac{CAM}{P_m \frac{1}{16}}) \quad . \tag{3.6}$$

Figure 3.8 shows the variation of HC emissions with A/F and cam phasing at constant manifold pressure ($P_m = 0.4$ bar), and engine speed ($N = 2000$ RPM).

PETITIONER'S EXHIBIT 1002
US PATENT NO. 6,557,540

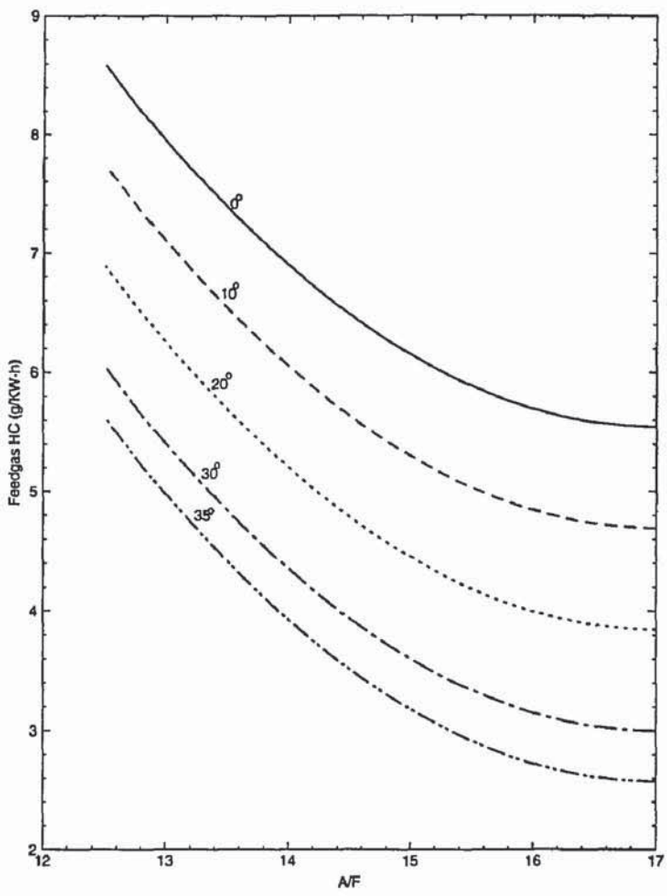


Figure 3.8: Feedgas HC emission versus A/F for different CAM timings at constant manifold pressure ($P_m = 0.4$ bar), and engine speed ($N = 2000$ RPM) .

The exact function that represents the HC emissions can be found in Appendix B.5. In [30] it is shown that dynamic feedgas HC emissions can be accurately predicted by the regression anlysis of the static measurements.

3.2.4 Process Delays.

The fundamental sampling rate for an n cylinder engine at engine speed N (revolutions per minute) is $\frac{1}{\Delta T} = \frac{N \cdot n}{120}$, where ΔT (seconds) is the fundamental sampling time interval. The discrete nature of the engine causes delays in the signal paths. For the engine studied, a delay of $4\Delta T$ seconds is assumed between the induction of the air and fuel mixture into the cylinders, and the corresponding torque response. The delay of $4\Delta T$ seconds corresponds to the induction-to-power stroke physical delay. We should note here that even though we cannot measure torque, its modeled value is used as a performance variable together with NO_x and HC emissions in the control design. The NO_x and HC emissions are steady

PETITIONER'S EXHIBIT 1002
US PATENT NO. 6,557,540

state measurements (average values) and cannot be measured in a dynamic manner. Their identified static nonlinear maps, however, will be included in the VCT model in the same dynamic manner as the torque generation function.

A delay of $9\Delta T$ seconds is also identified between the mass charge formation and the time when its corresponding exhaust gas reaches the EGO sensor. This delay corresponds to a $4\Delta T$ seconds delay of the induction-to-power stroke process, a $4\Delta T$ seconds delay of the power-to-exhaust stroke process, and a ΔT seconds delay of the transport process in the exhaust manifold. To achieve good combustion properties, the fuel is injected on closed intake valves, i.e., during the exhaust stroke prior to the intake event. Including the computational delay involved in the fuel pulse width calculation, a total delay of $2\Delta T$ seconds is estimated between the commanded fuel pulse width and the formation of its corresponding charge.

3.2.5 Actuators and Sensors.

The dynamics of the VCT actuator have been identified using parametric identification methods from the Matlab system identification toolbox and are described by the following transfer function :

$$\frac{CAM_{actual}}{CAM_{commanded}} = \frac{-0.706s + 705.8}{s^2 + 16.13s + 705.8} \quad . \tag{3.7}$$

Also, a reduced order model has been developed for the same actuator for control purposes, and is given by

$$\frac{CAM_{actual}}{CAM_{commanded}} = \frac{-0.013s + 26.959}{s + 26.959} \quad . \tag{3.8}$$

The dynamics of the EGO sensor are modeled as a first order lag followed by a preload (relay or switching-type) nonlinearity. The preload nonlinearity in the EGO sensor is viewed as a coarse form of quantization which can be adjusted in a later design phase. The time constant of the EGO sensor is typically 70 msec.

A hot wire anemometer is used to measure the mass air flow rate through the throttle body. A first order lag with time constant equal to 27 msec is used to describe the air meter dynamics. Finally, cam phasing measurements are received with a delay of ΔT seconds.

3.3 Region of Validity.

The block diagram of the identified control-oriented VCT engine simulation model is shown in Fig. 3.9. The data collected for the identification of the VCT engine model lie between 750 rpm and 2000 rpm, which covers most of the operating region in the current FTP cycle for this engine. The data collected represent engine operation for throttle positions less than 25 degrees; operation beyond this region requires extrapolation and should be used cautiously.

PETITIONER'S EXHIBIT 1002
US PATENT NO. 6,557,540

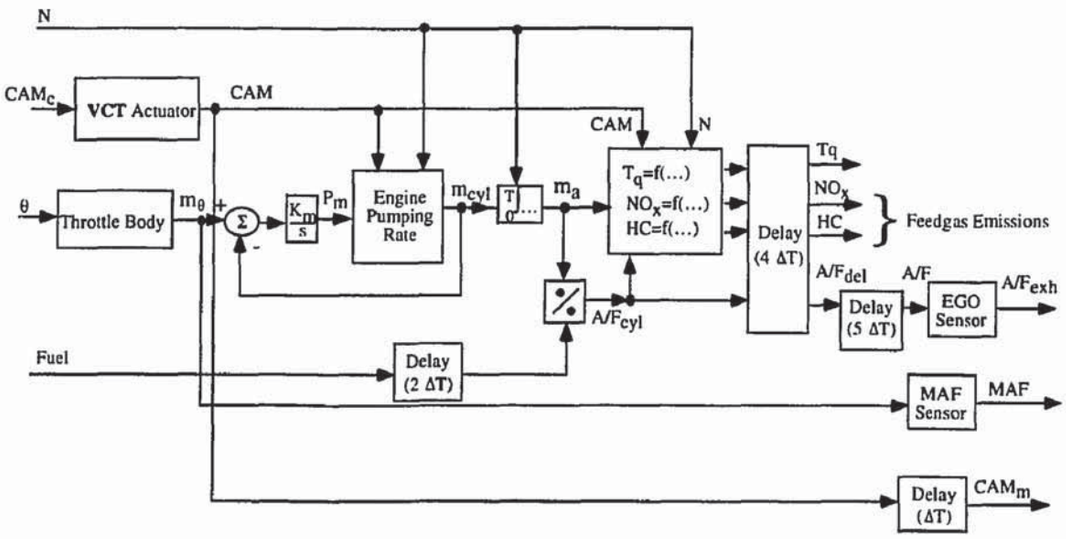


Figure 3.9: Block diagram of the identified control-oriented VCT engine model.

The derived model does not include fuel puddling dynamics, which is one of the important causes of A/F excursions during transient operation. This issue can be addressed by evaluating the sensitivity of the designed control scheme to the uncertain dynamics.

The VCT engine model also does not include the rotational dynamics of the dynamometer. Engine speed is a slowly varying state with respect to breathing and A/F dynamics, and therefore constant engine speed is assumed for the control design phase. The implemented controller, however, must be scheduled with respect to engine speed.

3.4 Model Validation.

The test work here involves the comparison of the identified model response with actual engine data to small step inputs. The set of data used for the validation is different from the set of data used for the model development. Figure 3.10 shows the response of manifold pressure (P_m), measured mass air flow (MAF), and the generated torque (T_b) to a step change in throttle position. Figure 3.11 shows the response of the actual cam position (CAM), manifold pressure (P_m) and generated torque (T_b) to a step change in cam position. Note that since this dynamic experiment lies in the sonic regime, the steady-state torque response is independent of the cam phasing. However the large torque drop during the cam phasing transition might be crucial to drivability requirements. It is important to note here that the large torque drop predicted by the model captured accurately the actual engine response to a misfire that occurred during the rapid change in the cam phasing. The test-cell technician who helped with the experiments felt that the identified model outperformed the measurements in predicting the torque response during rapid changes in cam timing.

PETITIONER'S EXHIBIT 1002
US PATENT NO. 6,557,540

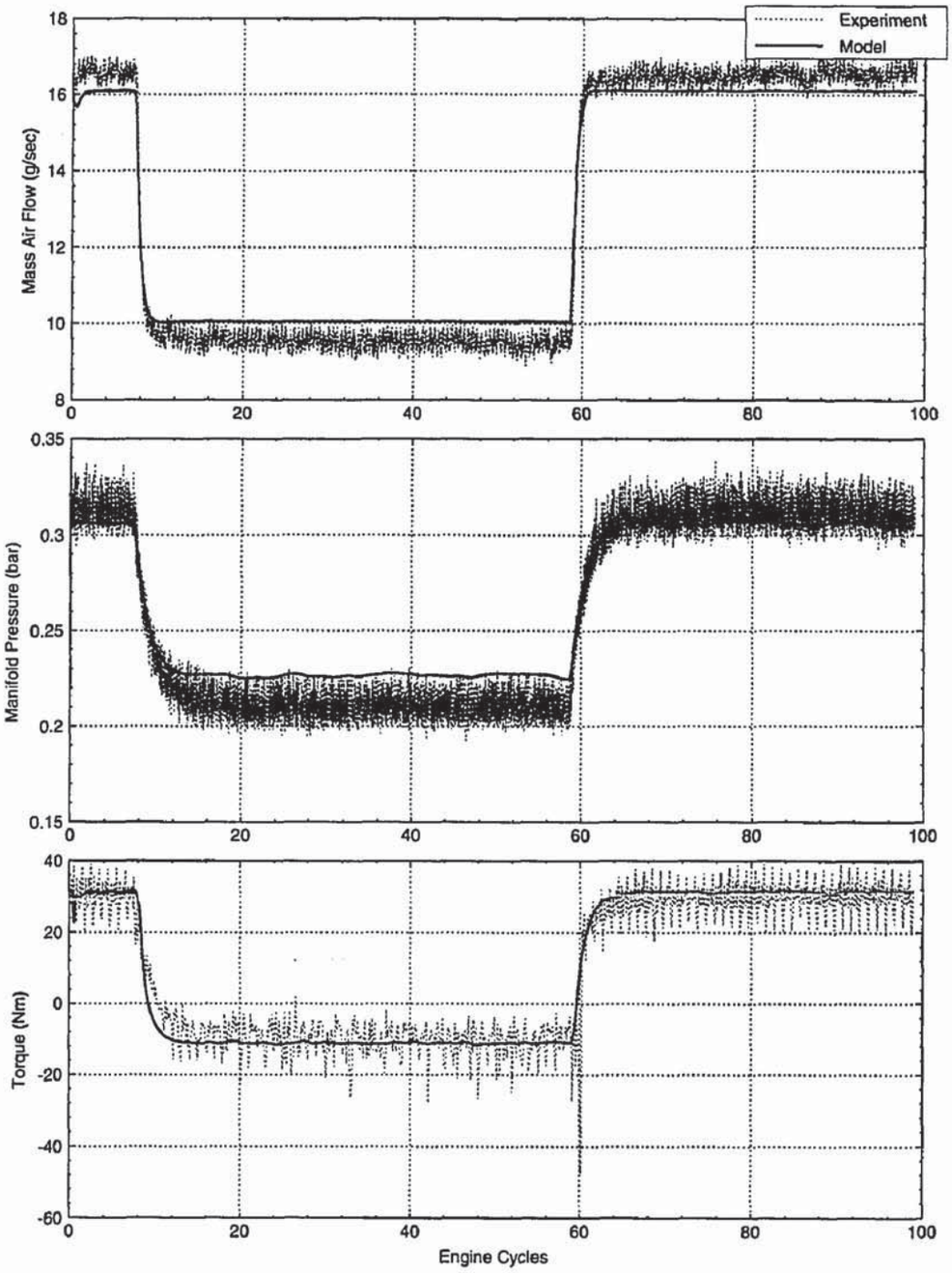


Figure 3.10: Model and engine actual dynamic response to throttle step command.

PETITIONER'S EXHIBIT 1002
US PATENT NO. 6,557,540

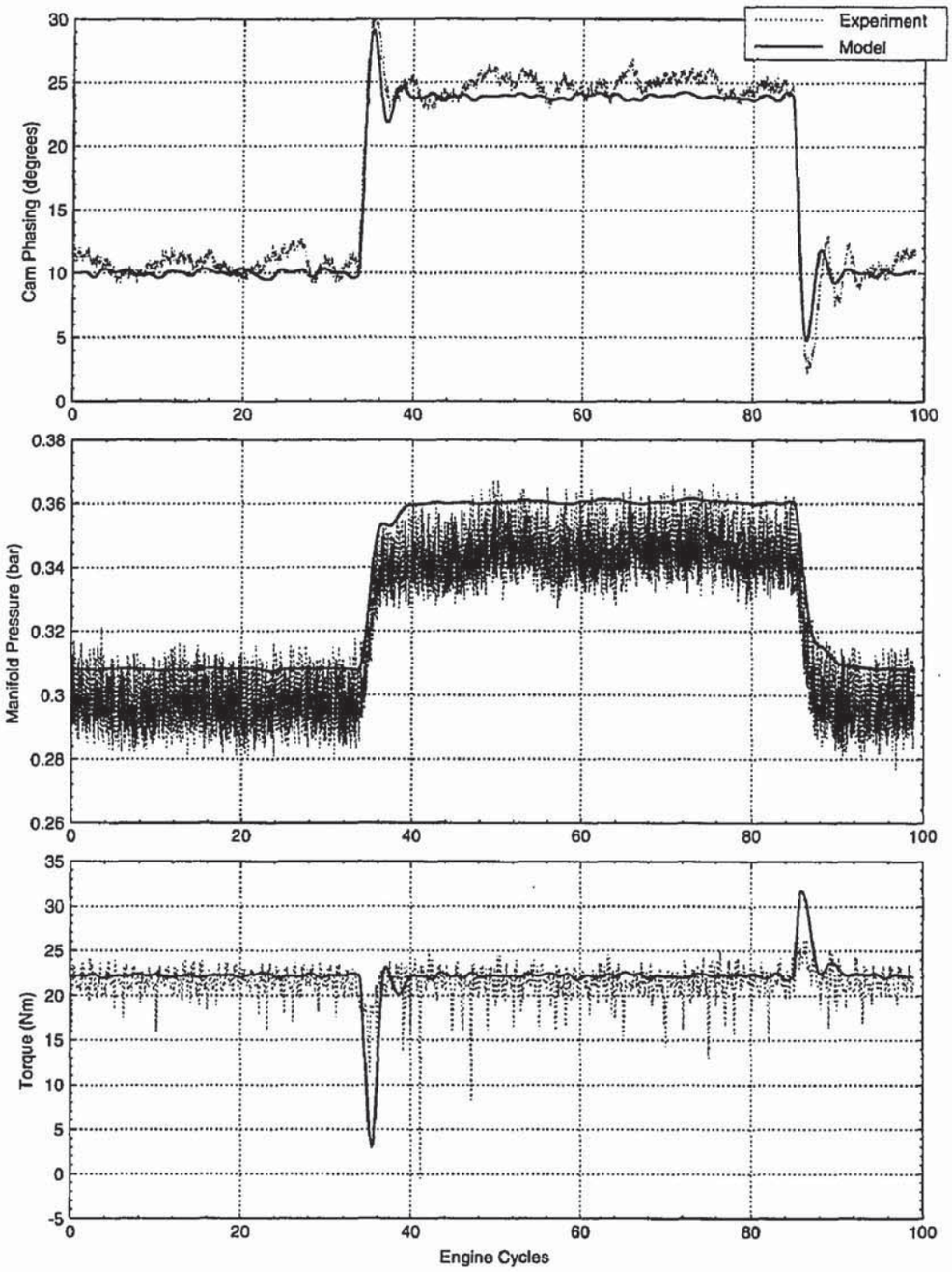


Figure 3.11: Model and engine actual dynamic response to cam phasing step command

PETITIONER'S EXHIBIT 1002
US PATENT NO. 6,557,540

CHAPTER 4

Control of Variable Cam Timing Engine.

4.1 Feedback Controller Structure.

The control oriented model developed has two actuators: the fuel injector pulse widths (F_c) and the cam position (CAM_c). The measured outputs are: air fuel ratio (A/F_{exh}) at the EGO sensor, the mass air flow (MAF), throttle position (θ_m), and cam phasing (CAM_m). The goal of the control design is to keep emissions as low as possible, by maintaining air fuel ratio (A/F) close to stoichiometry, and minimizing feedgas NO_x and HC emissions, while providing good driveability during rapid throttle movements.

Performance variables are tailpipe emissions, and the engine torque response during throttle changes. Tailpipe emissions depend on (i) the NO_x and HC feedgas emissions that the catalytic converter has to process, and (ii) the A/F signal that regulates the catalytic converter efficiency. Conventional automobiles are not equipped with sensors that can provide feedgas emissions and torque measurement. The control scheme studied will address the static torque and feedgas emissions performance requirements through nonlinear scheduling of the steady-state cam phasing. The structure of the feedback controller is shown in Fig. 4.1.

4.2 Performance Tradeoffs.

The purpose of this section is to explain the dynamics of the spark ignition engine equipped with a variable cam timing (VCT) mechanism, and how these affect the control design specifications. The dynamic and static interactions between the cam phasing and several subsystems of the engine are very important in the early phase of the control design process, because they lead to performance tradeoffs. Achievement of satisfactory overall engine performance requires judicious decisions about these performance tradeoffs. The following subsections describe the interaction between cam timing and engine torque response, and the interaction between the cam phasing and the A/F signal. The effects of these interactions on the engine performance, and how these are translated to control design specifications are explained.

PETITIONER'S EXHIBIT 1002
US PATENT NO. 6,557,540

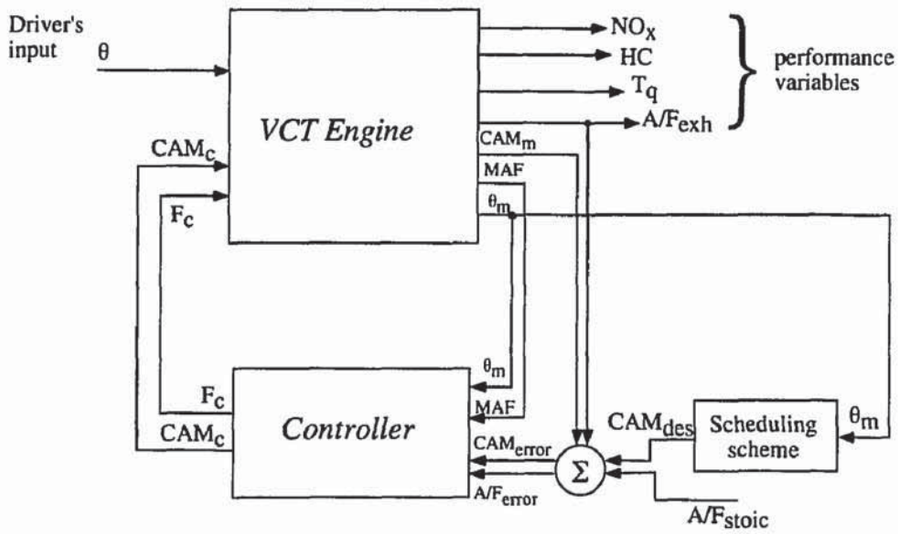


Figure 4.1: Diagrammatic representation of the feedback controller structure.

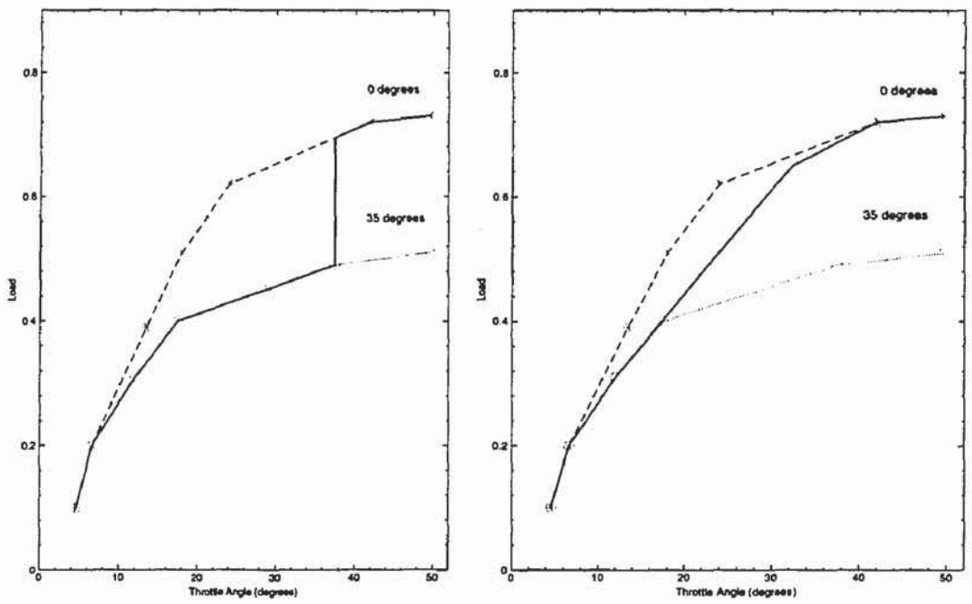
4.2.1 Engine Torque Response versus Feedgas Emissions.

Here we are considering the basic customer performance requirement: the torque response of the engine. Variable cam timing can alter the steady-state and the transient engine torque response, and the control scheme must carefully schedule the cam phasing. On the other hand, satisfying low NO_x and HC emissions is straightforward, as can be seen in Figs. 3.7 and 3.8, by using the maximum cam phasing whenever possible. The steady-state cam phasing that minimizes emissions is scheduled as follows: (1) near idle it is scheduled for idle stability which requires cam phasing equal to zero; (2) at mid-throttle it is scheduled for emissions which favors fully retarded cam phasing; and (3) at wide open throttle (WOT) it is scheduled for maximum torque which requires cam phasing to be advanced back to 0 degrees. Figure 4.2(a) shows the engine load response for the above cam phasing scheduling scheme and constant engine speed.

However, the above scheduling scheme cannot be implemented because it introduces torque discontinuities, which might entail drivability problems, and possibly introduces large A/F excursions, which, in turn, might affect adversely the tailpipe emissions. The designed cam scheduling scheme in Fig. 4.2(b) ensures reduction of feedgas emissions under the constraint of smooth steady-state torque response. Figure 4.3 shows the resulting steady-state cam phasing for engine speed equal to 2000 RPM.

This scheme satisfies smooth static torque requirements and low feedgas emissions. However, the transition of the cam phasing between set-points during rapid throttle changes is a crucial parameter in achieving good driveability. There is a dynamic interaction between the cam phasing and the torque response. Reduction of the feedgas emissions and good dynamic torque response cannot be achieved independently because good torque response

PETITIONER'S EXHIBIT 1002
US PATENT NO. 6,557,540



(a) (b)

Figure 4.2: Load response of an engine with variable cam timing mechanism and mechanical throttle for different scheduling schemes of cam phasing: (a) ideal schedule; (b) realizable scheme.

favors slow cam phasing to the new set points, but this might degrade the feedgas emissions which require fast cam transients. The following simulations illustrate a compromise between the torque response and emissions, and will be used to define the cam phasing control loop bandwidth.

Figures 4.4 and 4.5 illustrate cam phasing and torque response to step changes in throttle position at 750, and 2000 rpm. In all simulations, stoichiometric A/F and MBT spark timing were used. Therefore the torque response in Figs. 4.4 and 4.5 is only a function of air charge and internal exhaust gas recirculation (or cam phasing). The cam phasing controller dynamics are described by a low-pass filter between the desired and the commanded cam phasing. Figure 4.4 shows the cam phasing and torque response at 750 rpm for controllers with time constants between 0.5 and 1.5 engine cycles. Good torque response is a critical requirement at low engine speeds, and a time constant of 1 engine cycle was considered sufficient at this operating point. Figure 4.5 shows the cam phasing and torque response at 2000 rpm for various cam phasing controller dynamics. Here, the interaction between torque and cam phasing loop is considerably weaker than the interaction at lower engine speeds, and a time constant of 1 engine cycle is once again adequate for the cam phasing controller. Therefore, the bandwidth of the cam phasing controller has to be scheduled based on engine speed to correspond to one engine cycle in order to achieve good torque response over the entire operating regime.

PETITIONER'S EXHIBIT 1002
US PATENT NO. 6,557,540

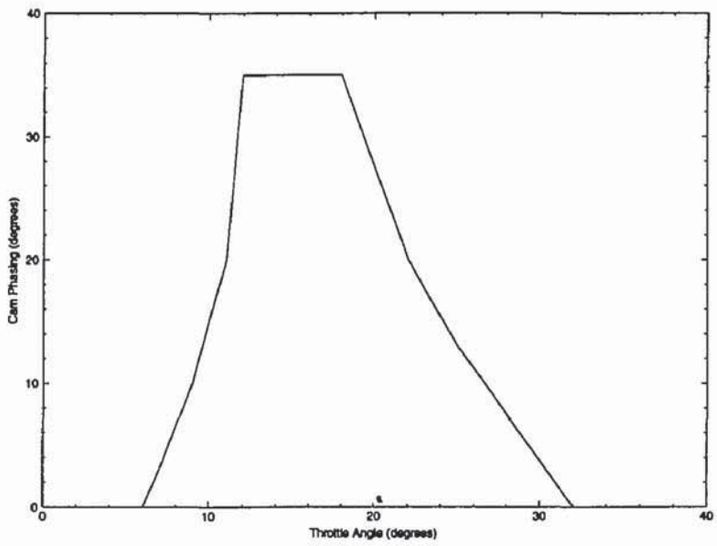


Figure 4.3: Steady state cam phasing

4.2.2 Nonlinear Breathing Process and Feedforward Fuel Control

In the VCT engine, changes in the throttle position are now followed by changes in the cam phasing based on the scheduling scheme shown in Fig. 4.3. The desired cam phasing reduces feedgas emissions by regulating the diluent in the cylinders. The contribution of this diluent to the mixture in the cylinder affects the breathing process, and consequently the mass charge in the cylinders, which in turn affects the air fuel ratio (A/F) in the cylinder mixture. This makes the A/F response highly coupled with the cam phasing activity.

It is important here to mention that variable cam timing does not affect the steady-state of the breathing process in the sonic regime. Note that in the breathing process, the cam phasing variable has the same topology as the secondary throttles from Section 2.3. In the subsonic regime, changes in cam phasing affect the dynamic and steady-state A/F response. Cam phasing is regulating feedgas emissions during changes in throttle position, but through its interaction with A/F, it affects the catalytic converter efficiency.

The structure of the electronic fuel control always consists of a feedback and a feedforward term. The feedback term regulates the fuel command based on the significantly delayed A/F signal from the EGO sensor, which inhibits good control. Due to these limitations, the feedforward term is important in adjusting the fuel command based on the measured mass air flow (MAF) and the measured cam position (CAM_m). The feedforward term is also necessary when the engine is cold and the A/F measurement is not available. The feedforward and feedback term in the fuel command result in a two degrees of freedom control topology, which gives more freedom in achieving the design goals during rapid throttle steps.

The feedforward term ($F_{c_{ff}}$) is based on the recent work in [27], and is modified to

PETITIONER'S EXHIBIT 1002
US PATENT NO. 6,557,540

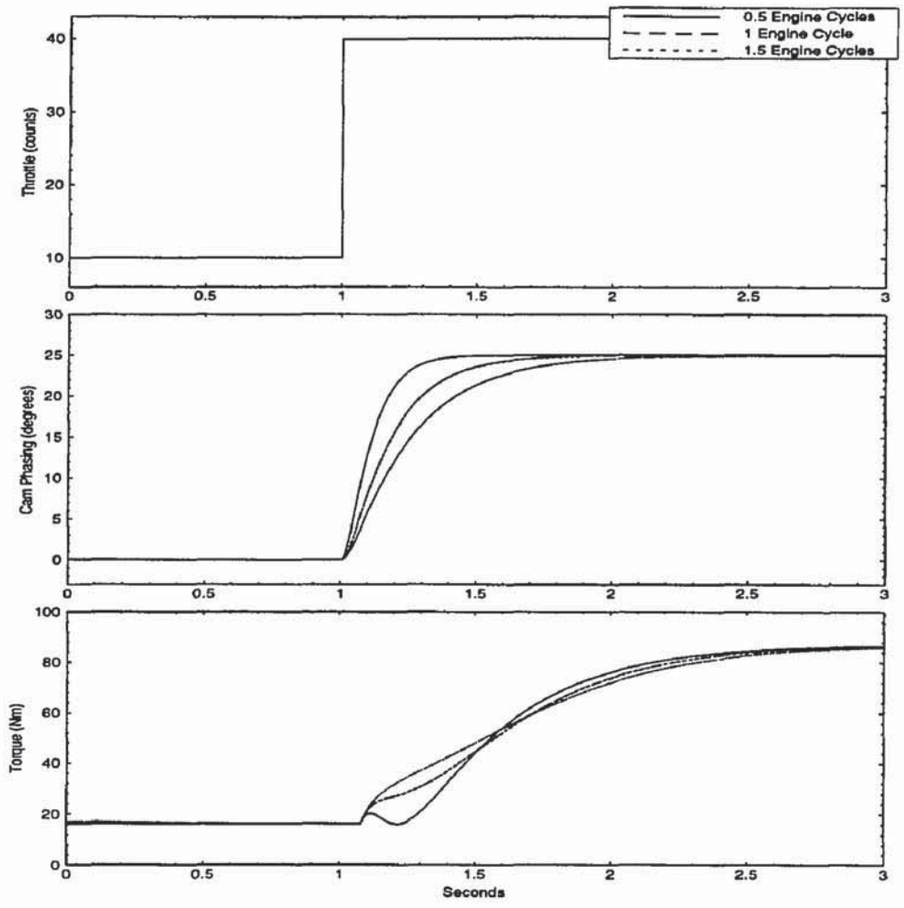


Figure 4.4: Torque response (at 750 rpm) using different low-pass filters in the cam phasing dynamics.

include the effects of variable cam timing on the cylinder air charge. The task involves the estimation of the cylinder pumping mass air flow rate ($\widehat{\dot{m}_{cyl}}$) from the measured cam phasing (CAM_m), the estimated manifold pressure ($\widehat{P_m}$), and the engine speed

$$\widehat{\dot{m}_{cyl}} = P(CAM_m, \widehat{P_m}, N) \tag{4.1}$$

The estimated manifold pressure ($\widehat{P_m}$) is calculated as (see also Equation 3.1)

$$\frac{d}{dt}\widehat{P_m} = K_m(\tau\frac{d}{dt}MAF + MAF - \widehat{\dot{m}_{cyl}}) \tag{4.2}$$

where we have used the dynamics of the mass air flow meter : $\tau\frac{d}{dt}MAF + MAF = \dot{m}_\theta$. To eliminate the derivative on the air flow measurement, we use the variable

PETITIONER'S EXHIBIT 1002
US PATENT NO. 6,557,540

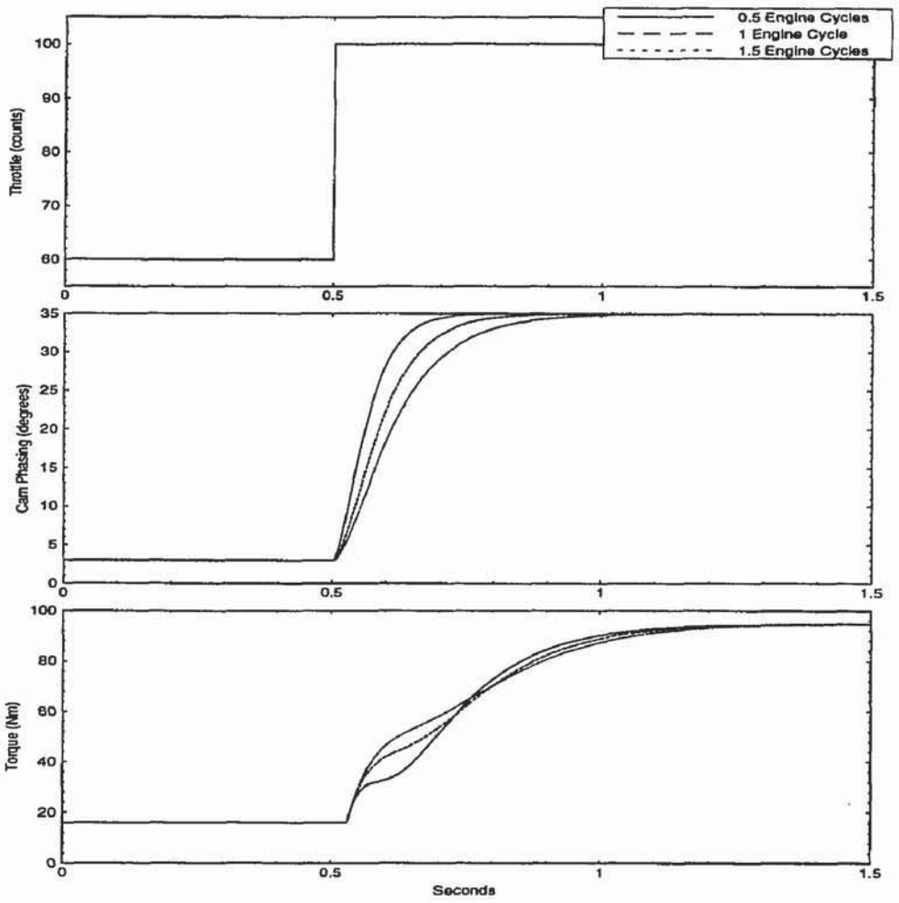


Figure 4.5: Torque response (at 2000 rpm) using different low-pass filters in the cam phasing dynamics.

$\chi = \widehat{P_m} - K_m \cdot \tau \cdot MAF$. This yields the estimated cylinder mass air flow rate :

$$\begin{aligned} \tfrac{d}{dt}\chi &= K_m(MAF - \widehat{\dot{m}_{cyl}}) \\ \widehat{P_m} &= \chi + K_m \cdot \tau \cdot MAF \\ \widehat{\dot{m}_{cyl}} &= P(CAM_m, \widehat{P_m}, N) \end{aligned} \tag{4.3}$$

For the estimation of the mass air charge into the cylinders ($\widehat{m_a}$) we assumed uniform flow during the intake event (ΔT, for the calculation of ΔT see 3.2.4) :

$$\widehat{m_a} = \widehat{\dot{m}_{cyl}} \cdot \Delta T = \widehat{\dot{m}_{cyl}} \cdot \frac{15}{N} \text{ where } N : \text{engine speed in rpm} \tag{4.4}$$

The feedforward fuel command ($F_{c_{fw}}$) is given by :

$$F_{c_{fw}} = \frac{\widehat{m_a}}{14.64}. \tag{4.5}$$

PETITIONER'S EXHIBIT 1002
US PATENT NO. 6,557,540

4.2.3 Catalytic Converter Efficiency versus Feedgas Emissions.

The feedforward term ensures decoupling of the cam phasing and the A/F in steady-state, but allows high frequency interaction. Reducing feedgas NO_x and HC emissions favors instantaneous change of the cam phasing to the scheduled set-point. Such cam phasing activity would cause a high frequency disturbance to the A/F loop. Unfortunately the long delay (810 degrees) in the A/F measurement associated with the combustion-exhaust stroke and the transport delay in the exhaust manifold imposes a bandwidth limitation on the A/F loop. If the disturbance to the A/F loop caused by the cam activity is at high frequency (i.e., beyond the achievable bandwidth of the A/F controller), then the disturbance cannot be rejected. In this case, it is a common technique to slow down the cam phasing signal, i.e., to de-tune the subsystem that causes the high frequency disturbance. This alternative, although consistent with current design practice, entails loss of the potential benefits of the VCT engine.

The dynamic performance tradeoff is between (a) the feedgas emissions that the catalytic converter must process and (b) the efficiency of the catalytic converter (which is a function of A/F excursions from stoichiometry). Due to the interaction between the cam timing loop and the A/F loop we cannot simultaneously minimize (a) and maximize (b); this is because, maximum catalytic efficiency requires that A/F be held perfectly at stoichiometry, which in turn rules out moving the cam rapidly to reduce feedgas emissions. A dynamic model of the catalytic converter efficiency could help specify a rigorous tradeoff between the two bandwidths, because, after all, the ultimate goal is to minimize tailpipe emissions. Since it is difficult to identify an accurate and simple dynamic model of the tailpipe emissions, we selected the bandwidth of the cam phasing loop based on indications taken from engine-dynamometer data and experimental vehicle tests. The tests suggest that cam transitions are to be achieved within one engine cycle (720 degrees), so that we can realize the benefits of variable cam phasing early in the transient period. This dictates the lower bound on the cam phasing bandwidth. On the other hand, we have found in the previous section that increasing the bandwidth beyond this lower bound results in unacceptable hesitation. For the above reasons we chose one engine cycle (720 degrees) to be the required time constant of the cam phasing dynamics.

4.3 Multivariable Feedback Control Design.

A multivariable controller was designed to track the desired cam phasing (value from the scheduling map) and maintain A/F at stoichiometry by controlling fuel and cam phasing command using the cam phasing position measurement, the A/F signal from the EGO sensor, and throttle position measurement. The VCT engine model does not incorporate fuel puddling dynamics. Also, there is a significant degradation of the cam phaser performance due to aging. For these two reasons the multivariable control design is based on

PETITIONER'S EXHIBIT 1002
US PATENT NO. 6,557,540

the LQG/LTR methodology to meet the necessary robustness properties and to meet the following performance requirements : (i) The required cam phasing dynamics are equal or faster than one engine cycle ($8\Delta T$), which, at 2000 rpm corresponds to a time constant equal or faster than 0.060 sec. (ii) Minimize A/F excursions.

We linearized the model at a throttle position equal to 9.33 degrees, cam phasing equal to 10 degrees, and engine speed equal to 2000 rpm. This operating point lies in the transition region on the cam phasing scheduling scheme shown in Fig. 4.3. The delays are represented by 1st and 2nd order Padé approximations. The linear model has 9 states and 2 integrator states. The state space representation of the linearized model is given by :

$$\dot{x}(t) = Ax(t) + Bu(t) + B_r r(t)$$
$$y(t) = Cx(t) + Du(t) \tag{4.6}$$

where

$$x = \begin{bmatrix} P_m \text{ (manifold pressure)} \\ A/F \text{ (at the UEGO sensor)} \\ X \text{ (air charge estimator state)} \\ MAF \text{ (mass air flow)} \\ CAM_m \text{ (measured cam phas.)} \\ CAM_a \text{ (actual cam phas.)} \\ F_{del} \text{ (delayed fuel)} \\ A/F \text{ (at the cat. conv.)} \\ A/F \text{ (at the cylinder)} \end{bmatrix}, \quad u = \begin{bmatrix} CAM_c \text{ (cam phas. command)} \\ F_c \text{ (fuel command)} \end{bmatrix}$$

$$r = \theta \text{ throttle position, and} \quad y = \begin{bmatrix} A/F_{exh} \text{ (A/F measurement)} \\ CAM_m \text{ (cam phas. measured)} \end{bmatrix}, \text{and}$$

$$A = \begin{bmatrix} -8.109 & 0 & 0 & 0 & 0.173 & 0 & 0 & 0 & 0 \\ 213.22 & -14.286 & 213.221 & 3.198 & 0 & -11.102 & -102649 & -44.404 & 0.056 \\ 0 & 0 & -8.109 & 0.434 & -0.173 & 0.422 & 0 & 0 & 0 \\ 0 & 0 & 0 & -37.037 & 0 & 0 & 0 & 0 & 0 \\ 0 & 0 & 0 & 0 & -26.958 & 0 & 0 & 0 & 0 \\ 0 & 0 & 0 & 0 & 109.288 & -133.333 & 0 & 0 & 0 \\ 0 & 0 & 0.554 & 0.008 & 0.012 & -0.029 & -133.333 & 0 & 0 \\ 852.886 & 0 & 852.886 & 12.793 & 0 & -44.408 & -410595 & -88.808 & -40.929 \\ 0 & 0 & 0 & 0 & 0 & 0 & 0 & 64 & 0 \end{bmatrix},$$

PETITIONER'S EXHIBIT 1002
US PATENT NO. 6,557,540

$$B = \begin{bmatrix} -0.000341 & 0 \\ 0 & 4 \\ 0.000341 & 0 \\ 0 & 0 \\ 4 & 0 \\ -0.215668 & 0 \\ 0 & 0.0103 \\ 0 & 16 \\ 0 & 0 \end{bmatrix}, \quad B_r = \begin{bmatrix} 0.04010 \\ 0 \\ 0 \\ 2.6734 \\ 0 \\ 0 \\ 0 \\ 0 \\ 0 \end{bmatrix},$$

$$C = \begin{bmatrix} 0 & 3.571 & 0 & 0 & 0 & 0 & 0 & 0 & 0 \\ 0 & 0 & 0 & 0 & -6.83 & 16.667 & 0 & 0 & 0 \end{bmatrix}, \text{ and } D = \begin{bmatrix} 0 & 0 \\ 0.0135 & 0 \end{bmatrix}.$$

During changes in throttle position, it is important to maintain A/F at stoichiometry and maintain zero tracking error in the cam timing. This is accomplished by augmenting the state vector with the integral of the error in the A/F ($\dot{q}_1 = A/F_{stoic} - A/F_{exh}$), and the integral of the error in the cam timing ($\dot{q}_2 = CAM_{des} - CAM_m$):

$$\dot{q} = y - \begin{bmatrix} A/F_{stoic} \\ CAM_{des} \end{bmatrix}. \tag{4.7}$$

We augmented the input and state vector to the VCT engine as followes :

$$\hat{r} = \begin{bmatrix} \theta \\ A/F_{stoic} \\ CAM_{des} \end{bmatrix}, \text{ and } \hat{x} = \begin{bmatrix} x \\ q \end{bmatrix}. \tag{4.8}$$

The resulting augmented system is :

$$\begin{bmatrix} \dot{x} \\ \dot{q} \end{bmatrix} = \underbrace{\begin{bmatrix} A & 0 \\ C & 0 \end{bmatrix}}_{\hat{A}} \begin{bmatrix} x \\ q \end{bmatrix} + \underbrace{\begin{bmatrix} B \\ D \end{bmatrix}}_{\hat{B}} u + \underbrace{\begin{bmatrix} B_r & 0 \\ 0 & -I \end{bmatrix}}_{\hat{B}_r} \hat{r},$$

$$y = \underbrace{\begin{bmatrix} C & 0 \end{bmatrix}}_{\hat{C}} \begin{bmatrix} x \\ q \end{bmatrix} + \underbrace{[D]}_{\hat{D}} u \tag{4.9}$$

or simpler

$$\begin{aligned} \dot{\hat{x}} &= \hat{A}\hat{x} + \hat{B}u + \hat{B}_r\hat{r} \\ \hat{y} &= \hat{C}\hat{x} + \hat{D}u. \end{aligned} \tag{4.10}$$

The controller feedback gain $u = -K\hat{x} = [-K_1 \; -K_2]\begin{bmatrix} x \\ q \end{bmatrix}$ is found by solving the LQR problem. The weighting matrices R_{xx} and R_{uu} used in the minimization of the cost function

PETITIONER'S EXHIBIT 1002
US PATENT NO. 6,557,540

$J = \int_0^\infty (x' R_{xx} x + u' R_{uu} u)\, dt$ are selected so that the closed loop requirements are satisfied. Their values are :

$$\begin{aligned} R_{xx} &= diag([0.364,\ 1500,\ 0.3,\ 18,\ 1000,\ 1000,\ 0.9,\ 1500,\ 1500,\ 70000,\ 5000]) \\ R_{uu} &= diag([1,\ 1]) \end{aligned} \tag{4.11}$$

The resulting K_1 and K_2 feedback gains are :

$$K_1 = \begin{bmatrix} -34.083 & -8.057 & -0.118 & -0.0018 & 33.653 & 13.503 & 8729.56 & -2.648 & -8.076 \\ -465.941 & -60.796 & 51.999 & 0.780 & 4.443 & -3.693 & 107225 & -15.396 & -54.205 \end{bmatrix}$$

$$K_2 = \begin{bmatrix} 35.096 & -70.086 \\ 262.237 & 9.380 \end{bmatrix}. \tag{4.12}$$

The only measurements available are the CAM timing measurement, and the A/F at the EGO sensor. Perfect measurements of the throttle angle (θ) are also assumed. For the complete controller design we need to estimate the states (x) using an observer. The observer gains are derived from a Kalman filter design by minimizing the covariance between the actual and the estimated values of the state. The real symmetric positive semi-definite matrix representing the intensities of the state noises Q_{xx}, and the real symmetric positive definite matrix representing the intensities of the measurement noises Q_{yy} are assumed diagonal. The Kalman filter gain is adjusted so that the LQG controller can asymptotically approach the robustness properties of the LQR design. Loop transfer recovery in the input is employed and the final values for the covariance matrices Q_{xx}, and Q_{yy} are :

$$\begin{aligned} Q_{xx} &= diag([0.001, 0.1, 0.001, 1, 0.1, 0.1, 0.0009, 0.1, 0.1]) \\ Q_{yy} &= 1000 \cdot diag([0.1, 0.1]). \end{aligned} \tag{4.13}$$

The resulting observer gain is :

$$L = \begin{bmatrix} 1.107894e-05 & 8.112784e-07 \\ 5.597648e-01 & -6.344560e-07 \\ -1.197880e-05 & 8.116791e-07 \\ -2.629355e-06 & -1.764878e-13 \\ -5.024201e-07 & 8.407023e-05 \\ -3.418612e-07 & 1.488718e-04 \\ -2.202050e-05 & -1.355407e-08 \\ -1.416589e-01 & 5.572409e-07 \\ 7.158249e-02 & -1.302364e-05 \end{bmatrix}. \tag{4.14}$$

The combined observer and controller state-space representation is described by the

PETITIONER'S EXHIBIT 1002
US PATENT NO. 6,557,540

following equations:

$$\begin{aligned}
\dot{x}_e &= Ax_e + Bu + B_r r_1 + L(y - y_e) \\
y_e &= Cx_e + Du + D_r r_1 \\
u &= -K_1 x_e - K_2 q \qquad (4.15) \\
\dot{q} &= -y + \begin{bmatrix} r_2 \\ r_3 \end{bmatrix} \quad \text{where } x_e \text{ is the estimated state,}
\end{aligned}$$

and finally

$$\begin{aligned}
\frac{d}{dt}\begin{bmatrix} x_e \\ q \end{bmatrix} &= \begin{bmatrix} A - LC - BK_1 + LDK_1 & LDK_2 - BK_2 \\ 0 & 0 \end{bmatrix}\begin{bmatrix} x_e \\ q \end{bmatrix} + \begin{bmatrix} L \\ -I \end{bmatrix} y + \begin{bmatrix} B - LD_r & 0 \\ 0 & I \end{bmatrix} \hat{r} \\
u &= \begin{bmatrix} -K_1 & -K_2 \end{bmatrix}\begin{bmatrix} x_e \\ q \end{bmatrix} . \qquad (4.16)
\end{aligned}$$

The controller design process involved testing the performance of the linear controller when applied to the nonlinear VCT engine model. Controllers with A/F bandwidth beyond 12 rad/sec result in worse A/F response due to the deleterious effects of the delay in the A/F measurements. Figure 4.6 shows the Bode gain plots of the resulting closed loop transfer functions.

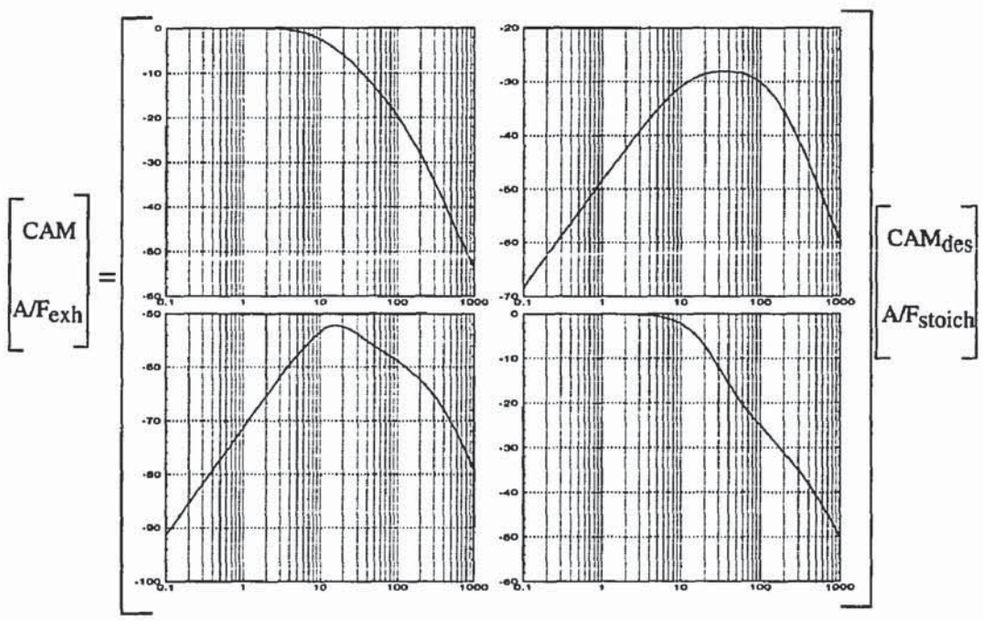


Figure 4.6: Bode gain plots of the closed loop transfer functions (frequency in rad/sec).

PETITIONER'S EXHIBIT 1002
US PATENT NO. 6,557,540

4.4 Nonlinear Simulation Example.

The purpose of this section is to illustrate some of the properties of the closed loop system for a conventional engine (fixed cam phasing) and the VCT engine. Figure 4.7 shows the simulated response of the conventional engine (fixed cam phasing) and the VCT engine to a square wave in commanded throttle at 2000 rpm. The sequence of throttle commands is 9.0 degrees (nominal) to 7.2 degrees to 12.0 degrees and back to 7.2 degrees and then to 9.0 degrees. The corresponding cam phasing set-points are 3 degrees to 10 degrees to 35 degrees (maximum) and back to 3 degrees and then to 10 degrees. The conventional engine scheme has fixed cam at 0 degrees.

The resulting torque response of the VCT engine is kept as responsive as the conventional engine in acceleration. During the abrupt deceleration at the 5th second of the simulation, the torque response of the VCT engine has an abrupt transient behavior which might entail drivability problems. The transient A/F response of the VCT engine is slightly worse than the A/F response of the conventional engine.

The advantage of the VCT engine over the conventional scheme is demonstrated at the feedgas NO_x and HC emissions. Using the integrated area defined by the NO_x and HC emission curves as a crude measurement of engine emissions, we can estimate a possible reduction of 10% in NO_x and 20% in HC during that period. Moreover, the engine operates in higher manifold pressure, which may reduce the pumping losses and provide an improvement in fuel economy.

4.5 PI Feedback Control Design.

In this section we investigate a simpler controller architecture for the previous feedback problem. It consists of (i) a classical, time-invariant, single-input single-output (SISO) PI controller that, based on the A/F measurement at the EGO sensor and the feedforward term (Equation 4.3), adjusts the fuel command; and (ii) a lowpass filter that regulates the cam phasing dynamic behavior. This control structure is easy to develop, implement and calibrate, and it is identical to the existing control architecture in conventional automobiles, with the addition of the cam phasing low pass filter. Investigation of simpler controller architectures is very important to the implementation stage of any controller development. Here, the motivation arises from the fact that if the simpler control structure results in satisfactory performance, then addition of the variable cam timing mechanism to a conventional automotive engine does not require completely new software development, but merely involves calibration of (i) the PI gains in the A/F loop and (ii) the time constant of the cam phasing dynamics. Figure 4.8 shows the different control architectures for the MIMO and the PI scheme.

In Sections 4.2.1 and 4.2.3 we discussed the importance of the cam transient behavior to the torque response and the A/F loop excitation. This interaction imposed bandwidth

PETITIONER'S EXHIBIT 1002
US PATENT NO. 6,557,540

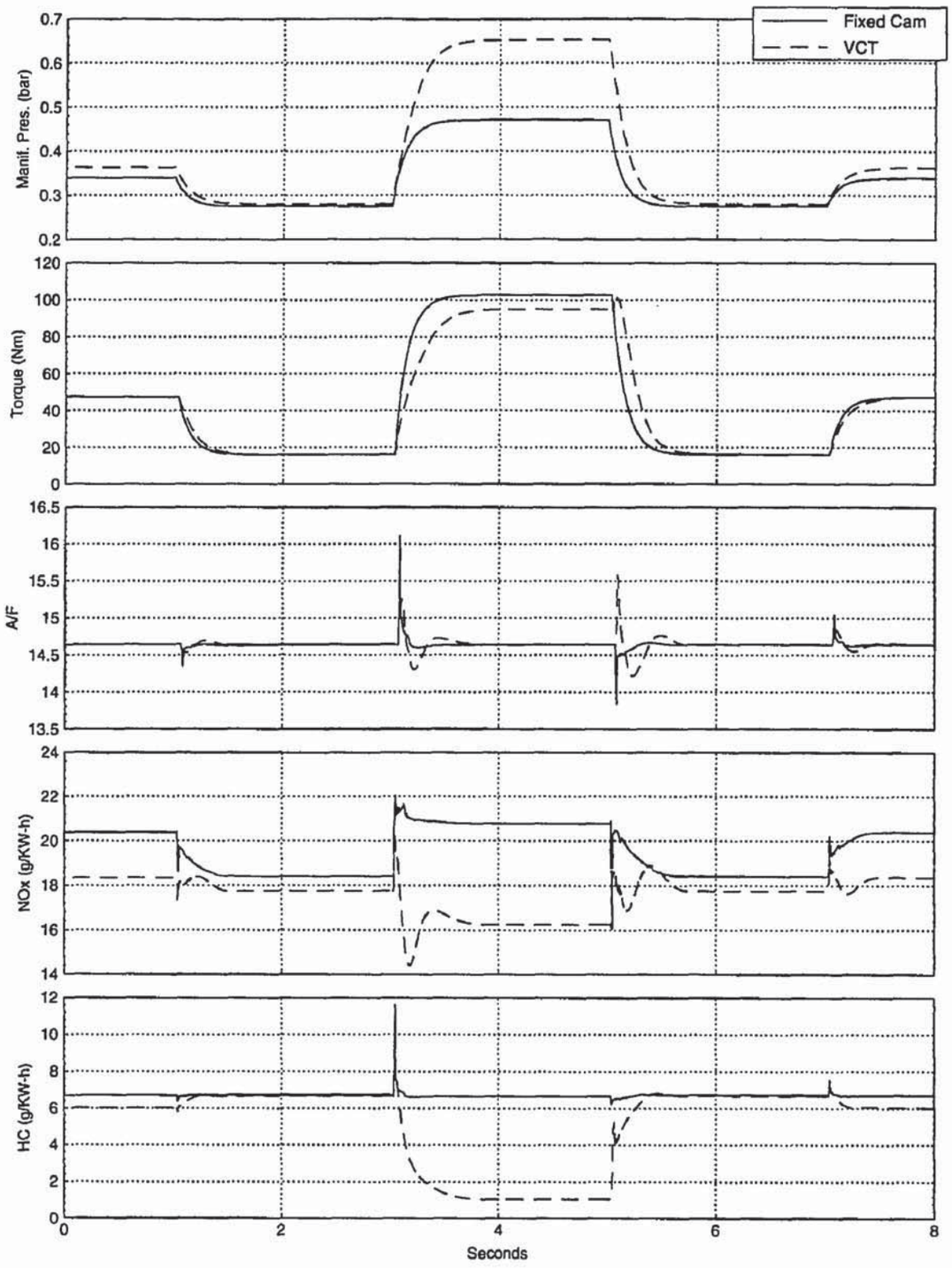


Figure 4.7: Simulation response of the conventional and the VCT engine.

PETITIONER'S EXHIBIT 1002
US PATENT NO. 6,557,540

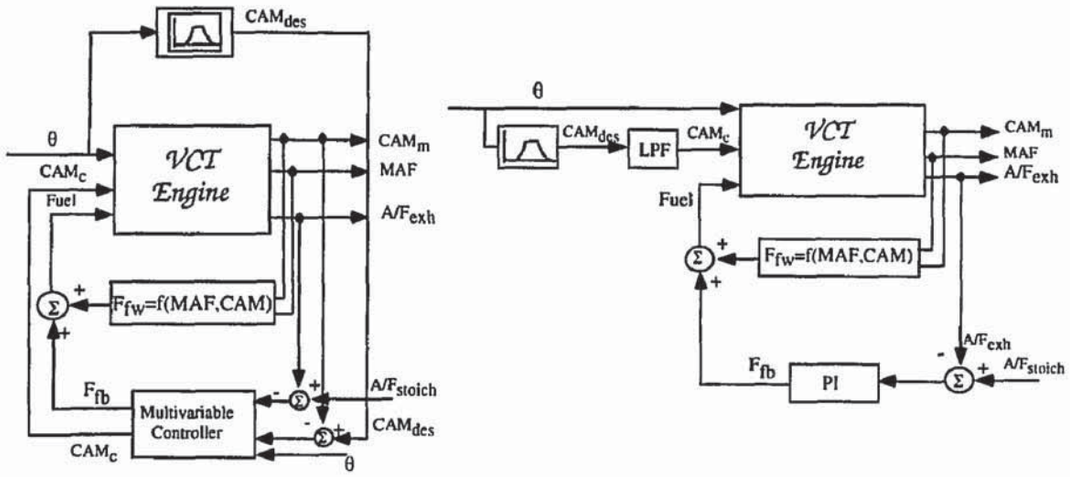


Figure 4.8: Diagrams of the MIMO control scheme, and the "PI-lowpass filter" control scheme.

limitations to the cam phasing dynamics, which corresponded to a time constant of one engine cycle. The lowpass filter designed has a time constant of 0.060 sec which corresponds to one engine cycle at 2000 rpm:

$$CAM_c = \frac{1}{0.060s + 1} CAM_{des} \ . \tag{4.17}$$

Tuning the PI gains in the A/F loop, we achieved the closed loop shown in the right plot of Fig. 4.9 (dashed line). The transfer function of the PI controller is :

$$F_c = \frac{0.57045s + 5.7045}{s} A/F_{error} \ . \tag{4.18}$$

For the comparison of the two control schemes, Figure 4.9 shows the Bode gain plots of the two resulting closed loops for the MIMO and simple PI scheme. The Bode gain plots of the closed loop transfer function between the desired and measured cam phasing for the two control schemes is shown at the left plot of Fig. 4.9. The Bode gain plot of the closed loop transfer function from the desired stoichiometric A/F (A/F_{stoic}) to the A/F at the EGO sensor (A/F_{exh}) for the two control schemes is shown at the right plot of Fig. 4.9.

Figure 4.10 compares the two schemes in a nonlinear simulation : MIMO controller versus PI controller. Similarity in the cam phasing dynamics is maintained, and the engine torque responses are almost identical. The NO_x and HC emissions in both cases are equivalent. However, the MIMO controller that coordinates the cam phasing and fuel command results in a small improvement in the nonlinear A/F simulation response. Comparison of the MIMO and the simpler controller architecture merits more investigation, since a degradation in A/F performance might cause an increase in the tailpipe emissions due to the sensitive performance of the three-way-catalytic (TWC) converter as a function of A/F. To capture the main features of the two control designs we concentrate on the linear engine

PETITIONER'S EXHIBIT 1002
US PATENT NO. 6,557,540

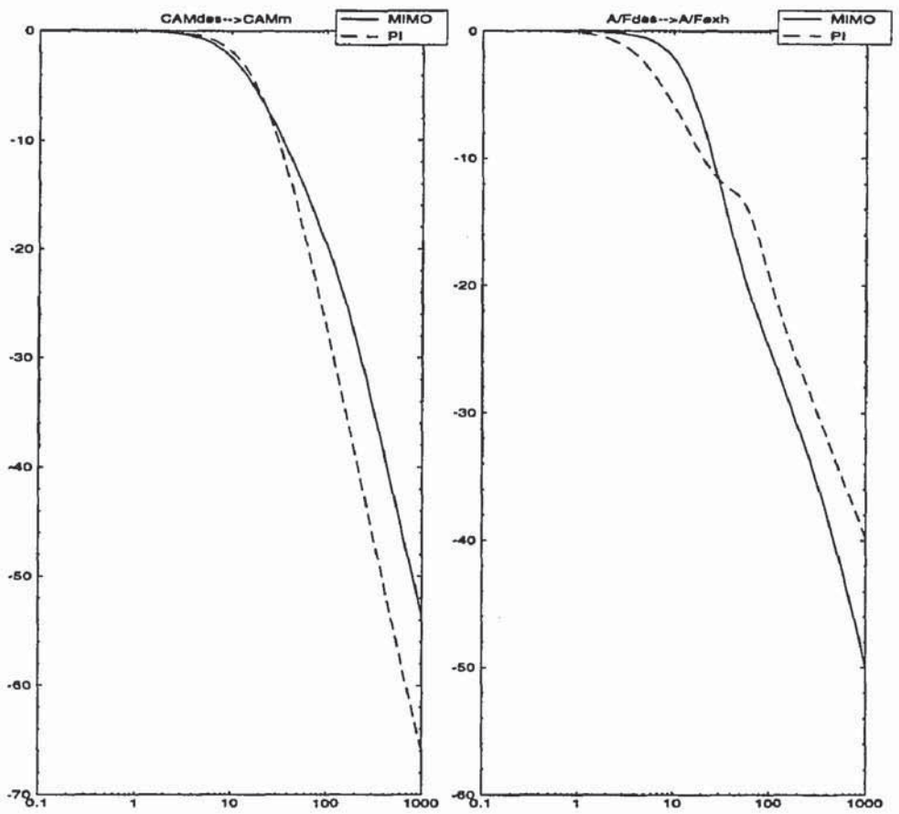


Figure 4.9: Bode gain plots of closed loop transfer functions with the MIMO and the "PI-lowpass filter" feedback controllers (frequency in rad/sec).

model and the linear closed loop response corresponding to the controller architectures. By eliminating the effects of the nonlinear engine model on the dynamic response, one can study the effects of the multivariable and the decentralized controller architecture on the dynamic response of the VCT engine.

PETITIONER'S EXHIBIT 1002
US PATENT NO. 6,557,540



Figure 4.10: Simulation response of the multivariable and the PI control scheme.

PETITIONER'S EXHIBIT 1002
US PATENT NO. 6,557,540

CHAPTER 5

Consequences of Modular Controller Development for the VCT Engine.

A modular architecture refers to a software organization consisting of a collection of independent program components with well-defined interfaces specifying the information flow across module boundaries. Such an architecture has many benefits: improved productivity through module reuse, seamless integration of new features, transparent removal of obsolete features, and module sharing across powertrain platforms. Additionally, maintainability is substantially enhanced in that modules can be modified independently of other parts of the powertrain control strategy. That is, one might remove and replace the EGR or fuel control module without affecting the rest of the strategy.

Because of these advantages, modular controller architectures have largely been used in automotive industry leading to the conventional decentralized control design. Conventional control design practice has been to assume independence of the powertrain subsystems, and apply classical control techniques to individual engine and powertrain subsystems. During the calibration process the feedback gains for each control loop are tuned with the other loop in manual (open loop). Often the overall performance is unsatisfactory when the other loops are placed in automatic (closed loop) due to the interaction between the different loops, thus further calibration is required. Dynamic interactions are minimized by de-tuning or calibrating a subsystem controller to avoid the unintentional excitations. This process often results in suboptimal performance which might not be sufficient for the increasingly demanding requirements in transient engine performance. Moreover, the advanced technology engines have strongly coupled subsystems. These interactions impose performance tradeoffs and require laborious tuning process of the multiple SISO-loops (decentralized controller).

Applying modern control techniques to design a multivariable controller is the natural approach to the problem. Designing a multivariable controller, however, is a complicated task and requires the development of a complete dynamic model of the system studied. Furthermore, MIMO controllers are difficult to tune, modify, and recover after component failure. It is hard to implement MIMO controllers because they require large memory space and execution time. Due to their complexity, MIMO controllers are rare in the automotive

PETITIONER'S EXHIBIT 1002
US PATENT NO. 6,557,540

industry. In the next sections we show that the multivariable controller designed in the previous chapter can be simplified without detrimental consequences in the engine dynamic response.

5.1 Decentralized Control of Multivariable Plants.

The simplest approach in controlling a MIMO plant is to ignore the multivariable nature of the plant and design a set of SISO feedback systems. However, designing a set of SISO systems to satisfy individual closed loop performance (e.g. speed of response and disturbance rejection) does not imply that the whole multivariable system will inherit these properties. Closing some loops might have deleterious effects on the behavior of the remaining loops. When high loop gain is not available, the only means to reduce the interaction is to de-tune the previous loops, and therefore impose performance tradeoffs. Using decentralized controllers in MIMO plants with strong interactions imposes performance limitations that have been explored and identified as early as the 1960s in [6]. In the process control literature, there are a significant number of studies on the interactions of subprocesses in MIMO plants and their significance on the closed loop performance ([50, 70] and references therein).

One way of reducing the interaction between subsystems is to design decouplers, i.e. feedforward compensators that maximize diagonal dominance at the frequency where the subsystem interaction is strong and the loop gains are not sufficient to attenuate this interaction [38, 44]. Analysis and synthesis of robust decentralized controllers (robust decouplers and decentralized controllers) have been studied in [87], and tested through simulations in automotive control applications in [67]. Another way of reducing interactions in MIMO plants is the design of multivariable controllers. In [42] it is mentioned that multivariable design techniques reduce the interaction between subsystems even without having taken explicit steps to do so. It is also well known [50, 25] that multivariable controllers manage design tradeoffs inherent to MIMO plants more successfully than decentralized controllers.

Despite many studies in the area of multivariable feedback control, there are no well accepted guidelines in defining an acceptable tradeoff between control design complexity and system performance in highly interactive multivariable systems. Investigation of these issues in the application of the VCT engine will aid in better understanding the underlying issues of a design methodology and its portability to other systems. The VCT engine has significant interaction between the dynamics of the variable cam mechanism and those of the air-fuel ratio subsystem.

5.2 Multivariable and Decentralized Controller: Design.

In a decentralized design, one could think of controlling cam phasing to minimize feedgas emissions (cam phasing loop), and regulating fuel pulse-width duration to minimize A/F

PETITIONER'S EXHIBIT 1002
US PATENT NO. 6,557,540

excursions (fuel loop). This leads to two single-input single-output (SISO) control systems, which is the decentralized control approach. This approach initially ignores the interaction between cam phasing and A/F that makes the two loops (cam loop and A/F loop) dynamically coupled over a large bandwidth. Figure 5.1 shows the Bode gain plots of the plant linearized at 2000 RPM. Cam phasing is measured in degrees, A/F is dimensionless, and the fuel command is scaled so that a unit deviation in fuel causes a unit deviation in the A/F signal.

The plant has a lower triangular form because the fuel command affects the system downstream of the breathing process. Therefore, there is no interaction between the fuel command and the cam phasing loop ($p_{12}(s) = 0$). In Fig. 5.1 we can see the interaction term (p_{21}) between the cam phasing control signal and A/F measurement. Through the term (p_{21}) the cam control command acts as an output disturbance in the A/F subsystem (see Fig. 5.2).

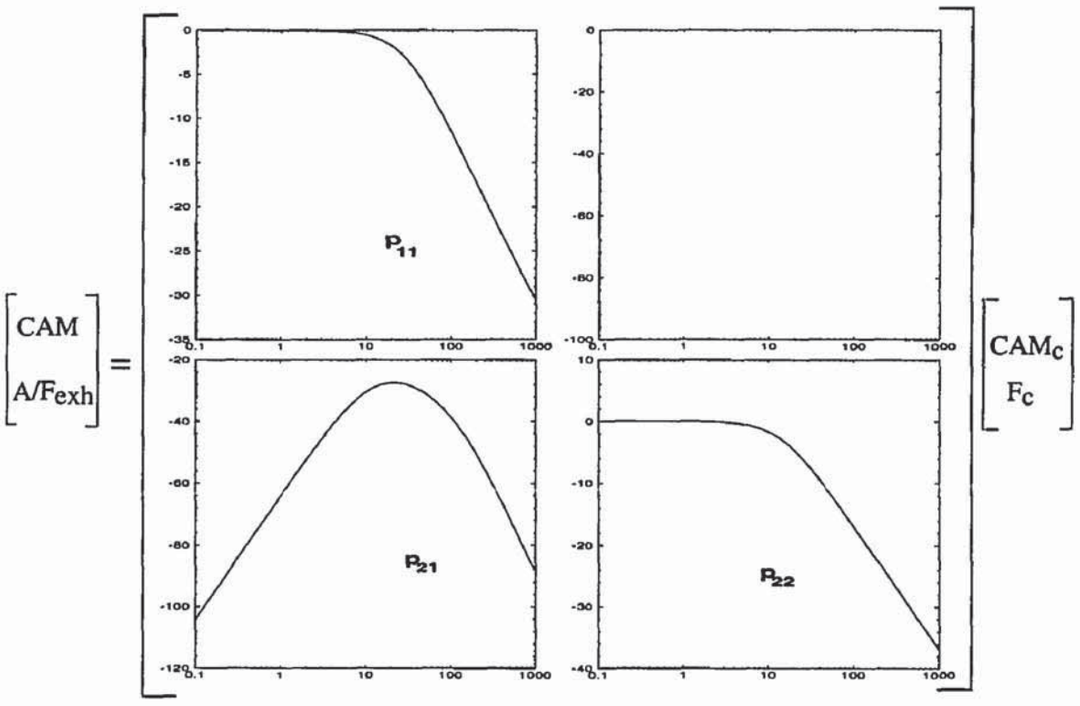


Figure 5.1: Bode gain plots of the linearized plant (frequency in rad/sec).

We repeat here the controller design considerations: (a) There is a 810 degrees of delay in the A/F process (see Fig. 5.2). At 2000 rpm, this translates into a time delay of 0.0675 sec. Due to this delay, the A/F bandwidth should not exceed 12 rad/sec (Section 4.3). (b) The required time constant for the cam phasing dynamics is 720 degrees (1 engine cycle). At 2000 rpm this corresponds to a time constant equal to 0.06 sec, which translates into a cam phasing closed loop bandwidth equal to 17 rad/sec. The peak of the interaction

PETITIONER'S EXHIBIT 1002
US PATENT NO. 6,557,540

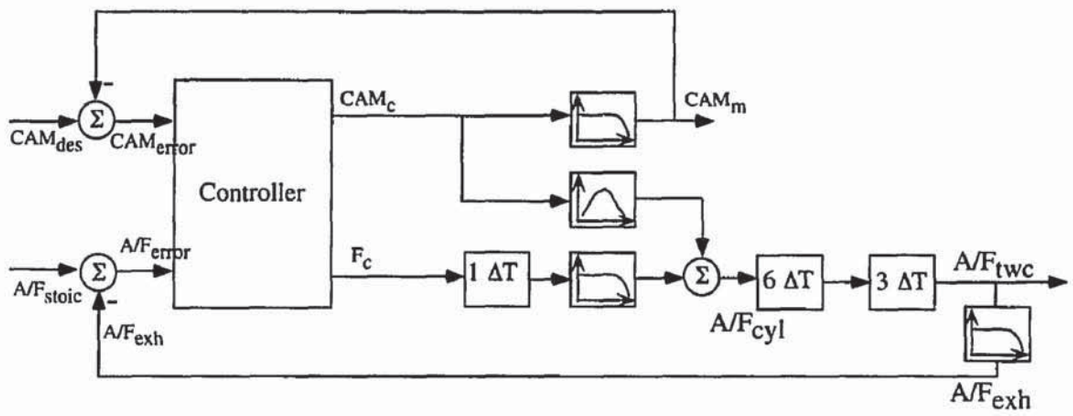


Figure 5.2: Block diagram of the linearized plant.

term (p_{21}) occurs at 20 rad/sec while we require the cam phasing activity to roll off after 17 rad/sec. Therefore, the control signal generated to force the cam phasing to track a command input will also produce a transient response in the A/F loop; in effect, the cam loop acts as a disturbance to the A/F loop. We thus see that we are faced with a difficult design problem.

The decentralized control design involves defining the two single-input single-output feedback loops that satisfy the design specifications. The transfer function describing the dynamics in the cam phasing loop (p_{11} term) is given by :

$$CAM = \underbrace{\frac{-0.01348(s-2000)}{s+26.96}}_{p_{11}(s)} CAM_c \ . \tag{5.1}$$

The transfer function describing the dynamics in the A/F loop (p_{22} term) is given by :

$$A/F_{exh} = \underbrace{\frac{(s-133.34)(s^2-88.8081s+2633.67)}{(s+14.286)(s+133.33)(s^2+88.8081s+2619.44)}}_{p_{22}(s)} F_c \ . \tag{5.2}$$

To meet the design specifications on the cam phasing loop the controller was chosen to be :

$$CAM_c = \underbrace{\frac{0.3425(s+26.96)}{s}}_{c_{11}(s)} CAM_{error} \ . \tag{5.3}$$

A few design iterations resulted the following controller in the A/F feedback loop :

$$F_c = \underbrace{\frac{0.57(s+10)}{s}}_{c_{22}(s)} A/F_{error} \ . \tag{5.4}$$

The Bode gain plots of the MIMO controller designed in 4.3 (solid line) and the decentralized controller (dashed line) are illustrated in Fig. 5.3. Both controller designs achieve

PETITIONER'S EXHIBIT 1002
US PATENT NO. 6,557,540

the bandwidth requirement in the cam phasing loop, and provide adequate speed of response in the A/F loop. The bandwidth specifications for the two loops essentially fix the band-

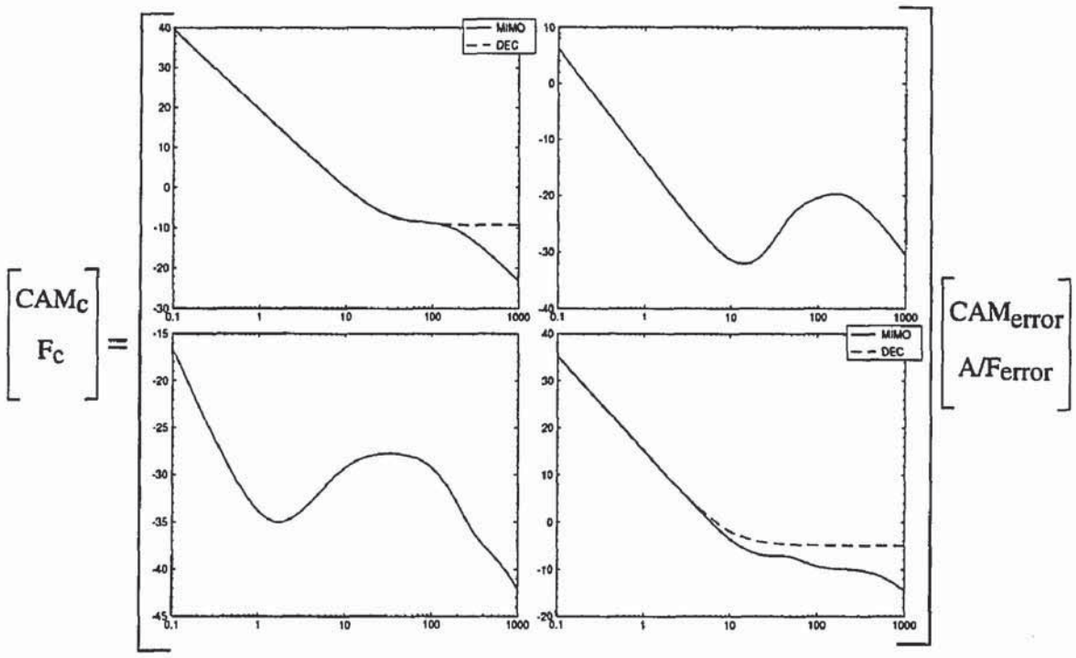


Figure 5.3: Bode gain plots of the MIMO controller and the decentralized controller (frequency in rad/sec).

widths of the diagonal elements of the controller independently of the controller structure. As a result, the diagonal elements of the two controllers are approximately identical.

Comparisons between the system response with the previously selected diagonal controller (see Fig. 5.3), and the system response with a decentralized controller consisting of the diagonal elements of the multivariable controller, showed only negligible differences. Hence, for the rest of this study, we will simply compare and discuss the decentralized controller obtained by using the diagonal elements of the multivariable controller and the fully multivariable controller.

Figure 5.3 shows linear simulations of the output and control signals during various cam phasing step commands for the two different controller architectures. The A/F deviations for the multivariable control scheme are significantly better than those corresponding to the decentralized control scheme.

Implementing the multivariable controller thus seems to be beneficial, but there are several questions we must address before we justify implementation of the multivariable strategy on a vehicle: How did the multivariable controller manage to reject the A/F disturbance faster than the decentralized controller? In which way did the multivariable controller reduce the interaction between the two loops? In the next section we identify the mechanism by which the multivariable controller achieves smaller A/F excursions during

PETITIONER'S EXHIBIT 1002
US PATENT NO. 6,557,540

Figure 5.4: Simulation using the linearized VCT engine model during cam phasing commands.

cam phasing transients.

5.3 Multivariable and Decentralized Controller: Analysis.

We begin by describing a design limitation present with decentralized control. Consider the decentralized control system in Fig. 5.5. Topologically, the CAM loop acts as an output disturbance to the A/F loop. As noted in Section 5.2 there is no interaction from the A/F loop to the CAM loop.

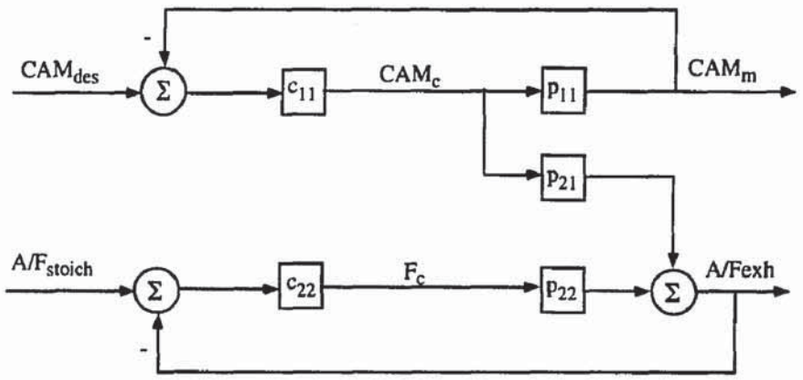


Figure 5.5: Block diagram of the decentralized control scheme.

Denote the sensitivity and complementary sensitivity functions for each loop by $s_{ii}(s) = (1 + p_{ii}(s)c_{ii}(s))^{-1}$ and $t_{ii}(s) = 1 - s_{ii}(s)$, $i = 1, 2$. Then the transfer function describing the closed loop A/F response is given by

$$A/F_{exh}(s) = t_{22}(s)A/F_{stoic}(s) + s_{22}(s)p_{21}(s)\underline{c_{11}(s)s_{11}(s)CAM_{des}(s)} \tag{5.5}$$

The term underlined in Equation 5.5 is equal to $CAM_c(s)$, the control signal in the CAM loop generated in response to a CAM command (CAM_{des}). As we have seen, the plant interaction (quantified by the transfer function $p_{21}(s)$), causes this signal to act as a disturbance to the A/F loop.

Suppose that this closed loop interaction results in unacceptable A/F transients. With a decentralized controller structure, there are two alternate approaches to reducing the interaction:

(i) Increase the bandwidth of the A/F loop, thus obtaining smaller sensitivity ($\mid s_{22}(j\omega) \mid \ll 1$), and greater disturbance attenuation, over a wider frequency range. This alternative is not feasible in the present problem, because of the time delay that limits the speed of response in the A/F loop (see Fig. 5.2).

(ii) Decrease the bandwidth of the CAM loop to obtain less control activity ($\mid c_{11}(j\omega)s_{11}(j\omega) \mid \ll 1$) at the frequencies of the problematic interaction. This alternative has been ruled out because it entails loss of potential benefits of the variable cam

PETITIONER'S EXHIBIT 1002
US PATENT NO. 6,557,540

timing engine, as argued in Section 4.2.3.

The preceding analysis implies the existence of a tradeoff between CAM and A/F responses. Specifically, to reduce the undesirable effects of interaction from CAM command to A/F response, it is necessary to either reduce the bandwidth in the CAM loop, and/or increase the bandwidth in the A/F loop. Increasing the speed of the A/F response is not feasible due to the time delay; hence, the tradeoff is resolved by sacrificing CAM performance in favor of the A/F loop.

We have seen that a decentralized controller structure imposes a tradeoff between achieving the bandwidth specifications in the two loops. Let us now consider two mechanisms by which a MIMO controller can (potentially) mitigate such a tradeoff.

(1) Let the CAM control signal depend upon errors in both cam and A/F loops (the term (c_{12}) in Fig. 5.6). Essentially, this strategy allows the controller for the CAM loop to achieve a compromise between regulating errors in the two loops and is an elegant alternative to the de-tuning practice (ii), that we mentioned above. In the present case, the delay in the A/F loop prevents this method from being useful because it is present in the response of A/F to both actuators. The significantly delayed A/F measurement cannot contribute information through the term (c_{12}) sufficient rapidly to slow the cam activity. Indeed, in Fig. 5.2 we can observe the nearly identical cam phasing control signals issued by the two controllers. We verified that the MIMO controller does not make effective use of the A/F error in computing the CAM control signal by zeroing the term (c_{12}) of the MIMO controller and noting that closed loop performance is virtually unchanged.

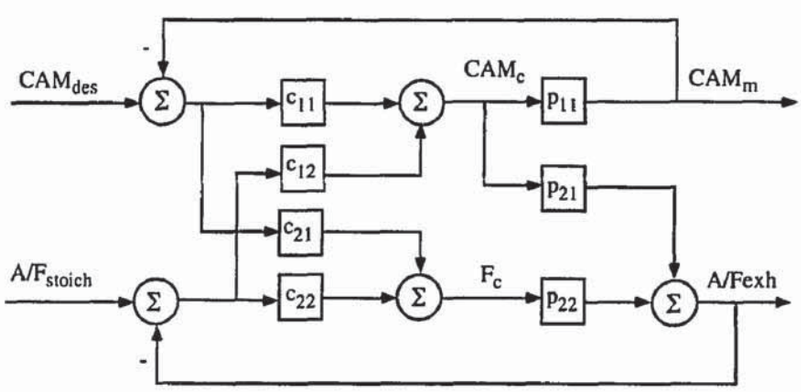


Figure 5.6: Block diagram of the fully multivariable scheme.

(2) Let the fuel signal depend upon the error in both CAM and A/F loops (the term (c_{21}) in Fig. 5.6). As depicted in Fig. 5.7, this control strategy results in a feedforward path from the cam phasing error to the fuel command used to control A/F. The feedforward term (c_{21}) sends information to the fuel command about the cam phasing error, and this allows faster response during cam phasing transients. The disturbance imposed on the A/F

PETITIONER'S EXHIBIT 1002
US PATENT NO. 6,557,540

loop by a command issued to cam phasing loop is shown at the following equation :

$$A/F_{exh}(s) = (p_{21}(s)c_{11}(s) + p_{22}(s)c_{21}(s))CAM_{error}(s) \tag{5.6}$$

Note here, that the same disturbance for the decentralized controller (see Fig. 5.5) is given by :

$$A/F_{exh} = p_{21}(s)c_{11}(s)CAM_{error}(s) \tag{5.7}$$

The multivariable controller can potentially reduce the coupling between the two subsystems by choosing the term (c_{21}) such that

$$\mid p_{21}(j\omega)c_{11}(j\omega) + p_{22}(j\omega)c_{21}(j\omega) \mid < \mid p_{21}(j\omega)c_{11}(j\omega) \mid \tag{5.8}$$

In Fig. 5.8, we see that MIMO control reduces the peak in the closed loop response from CAM commands to A/F measurements.

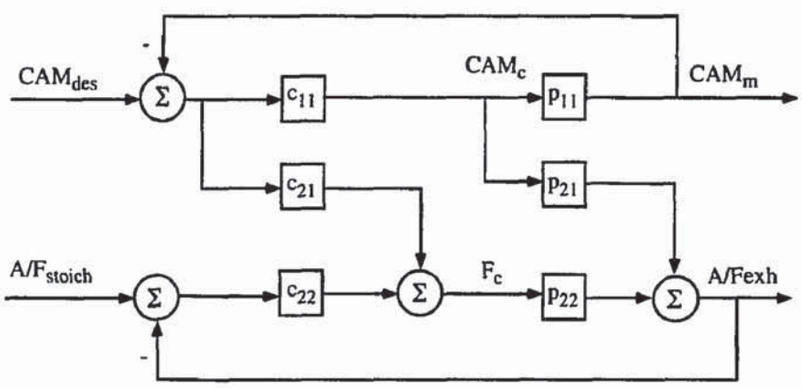


Figure 5.7: Block diagram of the simplified multivariable control scheme.

It is possible to interpret the action of the MIMO controller as partially decoupling the A/F response from the CAM loop. Indeed, setting the feedforward term equal to

$$c_{21}(s) = \frac{-c_{11}(s)p_{21}(s)}{p_{22}(s)} \tag{5.9}$$

achieves zero closed loop interaction from CAM to A/F. An alternate representation of the perfect decoupler is depicted in Fig. 5.9. With this topology, the CAM and A/F loops become completely decoupled, and the two remaining controller parameters, c_{11} and c_{22}, may be chosen independently. This controller design may be prone to robustness problems, since the term (c_{21}) is cancelling the undesired disturbance by inverting the signal along the path of the plant interaction.

In practice, there is no need to achieve perfect decoupling. Indeed, at lower frequencies, the integral action in the A/F loop achieves zero steady state error despite the interaction with the CAM loop. At higher frequencies, on the other hand, the CAM loop rolls off and thus does not produce a response in A/F.

PETITIONER'S EXHIBIT 1002
US PATENT NO. 6,557,540

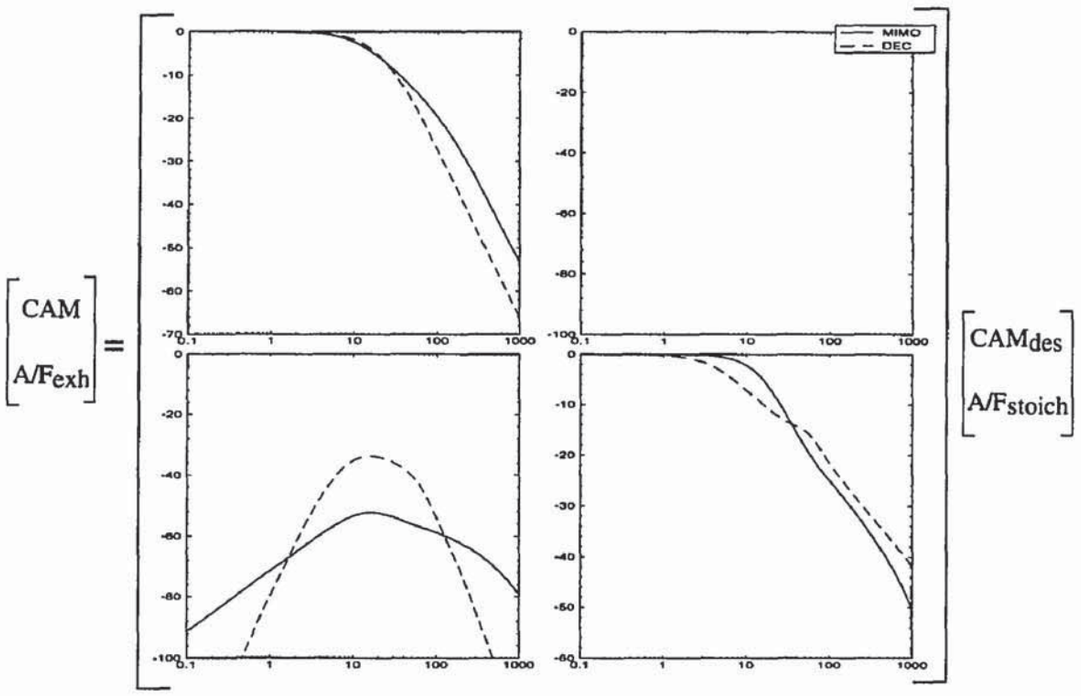


Figure 5.8: Bode gain plots of the closed loop transfer function (frequency in rad/sec).

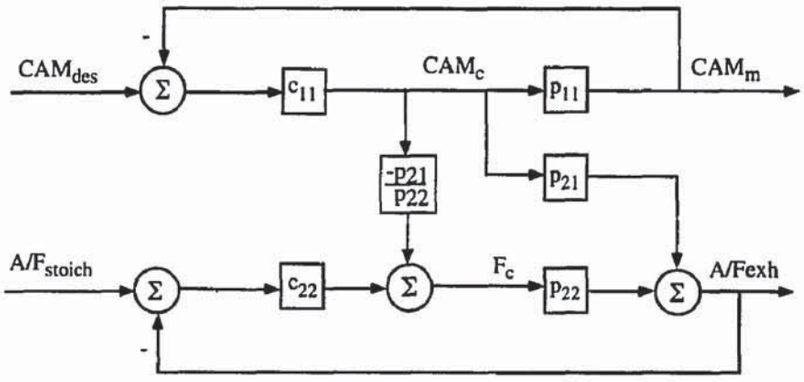


Figure 5.9: Block diagram of the decoupling controller.

As we see in Fig. 5.8, the MIMO controller merely reduces the peak due to the interaction, thus attenuating the effect of the CAM loop upon A/F without achieving total decoupling.

A potential difficulty with implementing the MIMO controller is that the feedforward term in the controller depends upon the plant; hence the performance improvements associated with MIMO control are sensitive to plant modeling errors. Indeed, the bandwidth limitation that precludes feedback from being used to reduce the effect of the CAM distur-

PETITIONER'S EXHIBIT 1002
US PATENT NO. 6,557,540

bance upon the A/F loop also prevents feedback from being used to reduce the effects of modeling uncertainty upon A/F.

5.4 Conclusions.

The potential benefits of multivariable control for an engine equipped with variable cam timing are demonstrated here. By designing and analyzing a multivariable controller for the cam phasing and A/F loops, we showed that coordinated control for these two loops resulted in better A/F transient performance without detuning the cam phasing loop. A complete design, including a study of robustness and scheduling, remains to be completed.

PETITIONER'S EXHIBIT 1002
US PATENT NO. 6,557,540

CHAPTER 6

Conclusions and Directions for Future Work.

In this dissertation we have studied control design issues for two advanced technology automotive engines. Both engine configurations were multivariable and nonlinear, thus imposing challenging control problems associated with control authority, long sensor delays, and strongly coupled subsystems. We have developed and validated dynamic engine models, studied the subsystem interactions, identified performance tradeoffs, and have applied classical and modern control techniques to improve engine performance. Moreover, we have studied the impact of modular controller architecture on the engine dynamic response, and demonstrated that even if the controller is eventually implemented in independent software modules, coordinating the design and analysis allows for a better assessment of the tradeoffs between the dynamic performance of different subsystems. In particular, the effects of subsystem interactions emerge at an earlier phase of the design process. This will reduce the calibration effort, and will result in advanced powertrain systems that can meet future performance requirements.

There are a number of directions in which the engine control applications that we have addressed in this dissertation can be extended.

Engine with secondary throttles : The control design for the engine with the secondary throttles was a preliminary assessment of the benefits of the new actuator, and there are several issues that merit further investigation. In particular, it would be valuable to experimentally validate the model of the engine with the secondary throttles. The model of the breathing process has been substantiated from the experimental data collected for the VCT engine. The secondary throttles and the variable cam timing affect the breathing process in a similar way, and it was shown that the proposed model captures the VCT engine dynamics accurately. It would be useful to extend the model to capture the nonlinear behavior of air flow through the secondary throttles and the ram air charging effects. The resulting system will provide an extremely powerful tool for the analysis and design of dynamically controlled camless engines.

We should investigate the issues arising from the assumptions made in the dissertation,

PETITIONER'S EXHIBIT 1002
US PATENT NO. 6,557,540

namely, the availability of good torque and throttle position measurements. Finally, it will be valuable to schedule the linear controller designed in this dissertation, and to develop an adaptive algorithm that upgrades the demand map.

Variable cam timing engine : The feedback controller designed for the VCT engine is based on a linearized engine model at one operating point. A scheduling scheme of a series of linear controllers or a completely nonlinear controller has to be designed to ensure operation over a wide range of engine speed and load conditions. This scheme has to address difficulties that arise from the event-based delays, the hybrid (continuous- and discrete-time) engine behavior, and the nonlinearities of physical processes and sensors. Furthermore, new emission mandates require emission control over an extended region (wide open throttle, cold start, etc.). Thus, modeling and control of the VCT engine, or any other conventional engine over these regions, will be imperative and challenging since no prior systematic studies in these regimes are available.

A possible way to improve the engine transient response is to coordinate the design of the feedforward (steady-state cam phasing) and the feedback terms of the variable cam timing controller. A methodology that addresses the design of feedforward and feedback controllers will assist in developing and maintaining integrated powertrain control systems.

Another significant study that remains to be completed is assessing the robustness properties of the multivariable versus the decentralized controller. The closed loop performance is affected by uncertainty in the cam actuator and/or uncertainty in the fuel puddling dynamics, and will be valuable to assess the nominal performance and the performance under uncertainty.

To address the complete powertrain control problem, it is necessary to incorporate the transmission and driveline into the existing VCT engine model. In the resulting VCT powertrain model, variable cam timing, fuel command, and gear ratio should be dynamically scheduled to improve the overall powertrain performance. A significant result of this systematic investigation will be the development of an integrated powertrain controller architecture. Implementation issues of modular controller architecture, addressed in the last chapter of this dissertation, will emerge and require a rigorous methodology of achieving a tradeoff between controller complexity and engine performance. This work is viewed as a combination of research in the area of engine modeling and multivariable control: (i) by developing dynamical models for the highly multivariable powertrain and identifying the important subsystem interactions that impose performance tradeoffs in the control design, and (ii) by translating the level of interaction in terms of design specifications for different subsystems.

It is our conclusion that the development of advanced technology powertrains requires

PETITIONER'S EXHIBIT 1002
US PATENT NO. 6,557,540

systematic modeling and control techniques to achieve the stringent performance requirements which are compelling their design. Moreover, there is a strong need for a systematic approach that can integrate the design phase with the implementation phase of the complete powertrain controller development on the vehicle. In this dissertation, we have demonstrated the advantages of such an integrated approach, and laid the foundations for a rigorous methodology of developing automotive powertrain control systems.

PETITIONER'S EXHIBIT 1002
US PATENT NO. 6,557,540

APPENDICES

PETITIONER'S EXHIBIT 1002
US PATENT NO. 6,557,540

APPENDIX A

Engine Mapping

The engine static mapping data, specification of the region of interest, and the set of experiments performed to obtain the nonlinear static model of the VCT engine are explained in this appendix.

A.1 Set of experiments

The goal in controlling the VCT in this dissertation is to reduce emissions and satisfy drivability, mostly in the region defined by the Federal Procedure Test (FTP) cycles, and centered in the part-throttle part-load operating regime. The static engine mapping data for the $4.6L$ $V8$ experimental VCT engine spans the region between 0.15-0.65 Load (normalized torque) and 750-2000 RPM.

The independent variables for the VCT engine model are :

- Engine Speed : Experiments were performed at 750 rpm, 1000 rpm, 1500 rpm and 2000 rpm constant engine speed.
- Throttle position : The necessary throttle position (in counts=degrees*8.33) to span the region of 0.15-0.65 Load (important for the FTP cycles) was identified by cranking the engine at constant engine speed. For this reason throttle positions are different for each engine speed (see Table A1-A4).
- CAM phasing : Experiments were performed at cam phasing equal to 0, 5, 12, 19, 28, and 37 degrees for each engine speed and for each throttle position.
- A/F : Experiments were performed at A/F equal to 12.2, 13.9, 14.6, 15.2, and 16.0 for each engine speed, each throttle position, and each cam phasing.

PETITIONER'S EXHIBIT 1002
US PATENT NO. 6,557,540

750 rpm

		CAM phase in degrees					
Load	TPrel	0	5	12	19	28	37
0.18	18	12.2	12.2	12.2	12.2	12.2	12.2
		13.9	13.9	13.9	13.9	13.9	13.9
		14.6	14.6	14.6	14.6	14.6	14.6
		15.2	15.2	15.2	15.2	15.2	15.2
		16.0	16.0	16.0	16.0	16.0	16.0
0.20	27	12.2	12.2	12.2	12.2	12.2	12.2
		13.9	13.9	13.9	13.9	13.9	13.9
		14.6	14.6	14.6	14.6	14.6	14.6
		15.2	15.2	15.2	15.2	15.2	15.2
		16.0	16.0	16.0	16.0	16.0	16.0
0.30	49	12.2	12.2	12.2	12.2	12.2	12.2
		13.9	13.9	13.9	13.9	13.9	13.9
		14.6	14.6	14.6	14.6	14.6	14.6
		15.2	15.2	15.2	15.2	15.2	15.2
		16.0	16.0	16.0	16.0	16.0	16.0
0.40	63	12.2	12.2	12.2	12.2	12.2	12.2
		13.9	13.9	13.9	13.9	13.9	13.9
		14.6	14.6	14.6	14.6	14.6	14.6
		15.2	15.2	15.2	15.2	15.2	15.2
		16.0	16.0	16.0	16.0	16.0	16.0

Table A.1: The 120 steady-state experiments performed at 750 rpm and the associated input variables.

PETITIONER'S EXHIBIT 1002
US PATENT NO. 6,557,540

1000 rpm

		CAM phase in degrees					
Load	TPrel	0	5	12	19	28	37
0.15	24	12.2	12.2	12.2	12.2	12.2	12.2
		13.9	13.9	13.9	13.9	13.9	13.9
		14.6	14.6	14.6	14.6	14.6	14.6
		15.2	15.2	15.2	15.2	15.2	15.2
		16.0	16.0	16.0	16.0	16.0	16.0
0.20	41	12.2	12.2	12.2	12.2	12.2	12.2
		13.9	13.9	13.9	13.9	13.9	13.9
		14.6	14.6	14.6	14.6	14.6	14.6
		15.2	15.2	15.2	15.2	15.2	15.2
		16.0	16.0	16.0	16.0	16.0	16.0
0.30	63	12.2	12.2	12.2	12.2	12.2	12.2
		13.9	13.9	13.9	13.9	13.9	13.9
		14.6	14.6	14.6	14.6	14.6	14.6
		15.2	15.2	15.2	15.2	15.2	15.2
		16.0	16.0	16.0	16.0	16.0	16.0
0.40	77	12.2	12.2	12.2	12.2	12.2	12.2
		13.9	13.9	13.9	13.9	13.9	13.9
		14.6	14.6	14.6	14.6	14.6	14.6
		15.2	15.2	15.2	15.2	15.2	15.2
		16.0	16.0	16.0	16.0	16.0	16.0
0.50	99	12.2	12.2	12.2	12.2	12.2	12.2
		13.9	13.9	13.9	13.9	13.9	13.9
		14.6	14.6	14.6	14.6	14.6	14.6
		15.2	15.2	15.2	15.2	15.2	15.2
		16.0	16.0	16.0	16.0	16.0	16.0

Table A.2: The 150 steady-state experiments performed at 1000 rpm and the associated input variables.

PETITIONER'S EXHIBIT 1002
US PATENT NO. 6,557,540